Carbon Nanofiller Reinforced Epoxy Nanocomposites

by

Cihan Uzunpinar

A dissertation submitted to the Graduate Faculty of
Auburn University
in partial fulfillment of the
requirements for the Degree of
Doctor of Philosophy

Auburn, Alabama
August 6, 2011

Keywords: epoxy nanocomposites, carbon nanotubes, functionalization, dispersion, phase separation, partitioning, damping

Approved by

Maria L. Auad, Chair, Professor of Polymer and Fiber Engineering
Peter Schwartz, Professor Polymer and Fiber Engineering
Xinyu Zhang, Professor of Polymer and Fiber Engineering
Hareesh Tippur, Professor of Mechanical Engineering

Abstract

Nanocomposites are unique materials with unique physical, mechanical and chemical properties that can find use in a wide range of applications. Nanocomposites are made of at least one nanosize material with polymeric systems or other materials.

The incorporation of carbon nanotubes (CNTs) and nanofibers (CNFs) has led to countless possibilities for structural polymer nanocomposites with superior specific modulus, strength, and toughness. These materials have gained enormous attention in fabricating next-generation advanced structural materials with added thermal, mechanical, optical and electrical advantages. However, questions concerning the filler dispersion, effect of the nanofillers on the interface and the final properties of nanocomposites remain partially addressed.

During this work, CNTs and CNFs were modified with covalent functionalization. This was achieved by adding carboxyl, ester and epoxy groups as well as monofunctional polyhedral oligomeric silsesquioxanes (POSS) molecules. The effects of these functionalization methods, as well as concentration of nanofillers on the quality of dispersion in epoxy matrix were explained. It was observed that functionalization of carbon nanotube helps to provide a better dispersion of carbon nanofillers. It was also detected that carbon nanotubes create a network structure after a critical threshold concentration that is called as percolation threshold. By using acidified SWCNTs, it was found that the percolation threshold value was 0.47 wt%.

Grafting monofunctional POSS molecules onto SWCNTs creates a phase separation phenomenon in epoxy/diamine systems. Whether this phase separation process provides a better dispersion of SWCNTs was discussed through rheological, calorimetric and visual analysis. It was found that phase separation creates POSS-rich domains that can help nanotubes create some kind of ordered arrays. This system did not show an improvement in storage modulus of epoxy/diamine system; however, the glass transition temperature of the system kept its value after incorporation of POSS functionalized SWCNTs.

Changes in the structure of interface by incorporation of unmodified and modified CNTs and CNFs and the effects of these fillers on the thermo-mechanical behavior of epoxy system were studied. The observed alterations in the structure of epoxy nanocomposites were explained with partitioning and phase separation phenomena. It was found that systems with acidified SWCNT, MWCNT and CNF showed two relaxation peaks in nanocomposites assigned to a partitioning of monomers at the carbon interface. This produced a significant decrease of the glass transition temperature. However, esterification led to a single relaxation peak close to the one for the neat epoxy, for the three types of nanofillers without any penalty in the glassy and rubbery elastic moduli.

Finally, the damping properties of epoxy elastomers reinforced with CNTs were analyzed. Results showed that epoxy nanocomposites with SWCNTs and MWCNTs have high damping capacity at high temperatures. The aid of CNTs incorporation on damping level at elevated temperatures was explained by “stick-slip” mechanism.

Acknowledgments

This dissertation is the account of four years of dedicated work in the field of carbon nanofiller reinforced polymer nanocomposites at the Polymer and Fiber Engineering Department of Auburn University, Auburn, Alabama which would not have been completed without the help of many.

To begin, I would like to thank deeply my advisor Dr. Maria L. Auad for her help and wide perspective in my research and also in my academic career. I wish to thank her for who she is a professor, an advisor, and a friend. This work would not be completed without her endless support, feedback and encouragement through all stages of my Ph.D. work.

Secondly, I wish to acknowledge and thank to my graduate committee members, Prof. Peter Schwartz, Prof. Hareesh Tippur and Prof. Xinyu Zhang, for their help and guidance during this project. In addition, I would like to express my gratitude to Dr. Leonardo De La Fuente for his time evaluating my thesis. I also would like to thank Dr. Mirna Mosiewicki, Dr. Roberto J.J. Williams, and Dr. Mike Miller for their help through my research.

Additional thanks to Samantha Bird for her time finding my mistakes in my presentations and papers and making me one-step closer to perfection. I also would like to thank Dr. Tara Richardson, Dr. Hasan Kocer, Ozgur Ozmen, Volkan Barim, Volkan Oktem, Alper Yavuz and Kemal Solakyildirim for their help and guidance. There are many people that I could not write their name that I would like to thank.

Of course, this work would not be completed without Auburn University Polymer and Fiber Engineering Department. I wish to thank every person in this department for being a family away from home and support me all these years. Moreover, this research would not have been possible without funding from the Department of Commerce. I also would like to express my acknowledgement to Educational Ministry of Turkey for their support.

Specifically, I would like to thank to my parents, Satiye and Mehmet Uzunpinar. My work would not be completed without their love, support, prayers and encouragement. I owe them much of what I become. I also would like to thank my mom to cut the phone conversations short because of my studies even though she wanted to talk more. I also owe my dad for the fact that he raised me to value honesty, courage and gratefulness. I cannot forget whole his efforts for learning new topics for helping me when I was in high school. I am sure he would do more if he would have the same major in college. Last but not least, I would like to thank Alina Braun for her endless unconditional love, support and encouragement. I am lucky to have been blessed by her wonderful companion, and constant source of motivation. She always stood by my side like a solid rock against all the difficulties. I cannot say enough words to explain my appreciation to her for all the meals she cooked when I was working. Finally, I would like to express my thankfulness to God for providing me skills and ability to think.

Table of Contents

List of Tables

158

List of Figures

List of Abbreviations

SWCNT	Single Wall Carbon Nanotube
MWCNT	Multi Wall Carbon Nanotube
CNF	Carbon Nanofiber
POSS	Polyhedral oligomeric silsesquioxanes
DGEBA	Diepoxide based on diglycidylether of bisphenol A
MDEA	4,4′-methylenebis (2,6-diethylaniline)
DSC	Differential Scanning Calorimetry
TGA	Thermal Gravimetric Analysis
FTIR	Fourier Transform Infrared
SEM	Scanning Electron Microscopy
DMA	Dynamic Mechanical Analysis
G’	Shear storage modulus
G”	Shear loss modulus
E’	Storage modulus
E’’	Loss modulus
T_g	Glass transition temperature

CHAPTER 1

LITERATURE REVIEW

1.1 POLYMER NANOCOMPOSITES

In recent years, nano-scale filled polymer composites have created many opportunities to overcome the limitations of traditional micrometer scale polymer composites. While some of the main properties such as toughness, stiffness or optical clarity have been sacrificed in traditional composites, nanocomposites created opportunity to have materials, which can possess optical clarity in addition to being tough as well as stiff (Schadler L.S., 2003).

Research and development in polymer nanocomposites have been increased dramatically in recent years because there have been extraordinary combinations of properties in some polymer nanocomposite systems. For instance, 4 vol% mica-type silicates (MTS) in epoxy increase the modulus 58% in the glassy stage and 450% in the rubbery region (Messersmith et al., 1994). In another study, Yano et al. showed a 50% decrease in water permeability of polyimides with reinforced 2 wt% of MTS and they also showed that these nanocomposites are optically transparent and optically active (K. Yano et al., 1995).

Another reason for the large increase in research and development is the discovery of carbon nanotubes. Iijima reported carbon nanotubes in 1991 and since then these materials have been

investigating as possible reinforcement filler for polymer matrices (S. Iijima, 1991). Because of their unique structure, which exhibits extreme combination of mechanical, electrical and thermal properties, they have been considered as one of the most important candidates in polymer nanocomposite applications. Moreover, low percolation thresholds and high aspect ratios provide the nanotubes additional advantage over spherical fillers to obtain high performance composites. For instance, Fidelus et al. reported 70% increase in tensile impact strength for 0.5 wt% multiwall carbon nanotubes (MWCNT)/epoxy system (Fidelus et al. 2005).

In another study Ounaies et al. studied the electrical properties of single wall carbon nanotubes (SWCNT)/ polyimide system as a function of SWCNT concentration. The conductivity of the pristine polyimide was reported as 6.3×10^{-18} S/cm. A sharp increase of conductivity value was obtained at relatively low percolation threshold value of 0.07 vol% where the conductivity changed from 3×10^{-17} S/cm to 1.6×10^{-8} S/cm (Ounaies et al. 2005).

Another significant advantage of nanocomposites is the unprecedented control over the morphology of such materials. The small size of the nanofillers creates an exceptionally large interfacial area in the composite and, thus, the surface area increases dramatically when the filler size is below 100 nm. Thus, nanofillers have created endless abilities in controlling the interface region between the matrix and the filler. This interface region begins at the point in the fiber at which the properties differ from those of the bulk filler and ends at the point in the matrix at which the properties become similar or same to those of the bulk matrix. At this region, chemistry, polymer chain mobility, degree of cure and crystallinity can change. The interface

controls the degree of interaction between the filler and the matrix, which also affects the final properties. Even if the interfacial region is small, the entire polymer matrix has different behavior than the bulk. By extending the size of the interfacial region by increasing the surface area of the filler, the polymer matrix behavior can be altered at much smaller loadings (P.M Ajayan, 2003).

In this chapter, several aspects of the polymer nanocomposites are reviewed. First of all, the properties and applications of nanofillers such as carbon nanotubes, carbon nanofibers that used during this thesis are explained. The challenges during the polymer nanocomposite preparation and some of the available solutions such as functionalization are mentioned. Furthermore, mechanical properties and energy dissipation in polymer nanocomposites are described. Finally, the available application areas are explained.

1.2 NANOFILLERS

1.2.1 Carbon Nanotubes

Carbon tubes (micro-meter size) were first found in 1960 by Roger Bacon. They had similar structure as recently discovered multi-wall nanotubes however the dimensions were different. In 1991, Sumio Iijima discovered nano-meter size tubes (nanotubes) while he was investigating the surface of carbon electrodes used in an electric arc-discharge apparatus that had been used to produce fullerenes. The first nanotubes observed by Iijima were multi-wall carbon nanotubes (MWCNTs), which consists two or more cylindrical shells of graphene sheets arranged around a central hollow core. The general diameter range for MWCNTs is between 2nm to 100nm and the

separation distance between each layer is around 0.34 nm. After two years, in 1993, Iijima, Ichihashi and Bethune achieved to synthesize single-wall carbon nanotubes (SWCNTs) by use of metal catalysts in the arc-discharge method. SWCNTs have a single layer of graphite cylinder and have a diameter range between 1nm-2nm (Figure 1.1). After their first discovery, carbon nanotubes have been synthesized with various methods such as laser-ablation (Smalley et al., 1995) and catalytic growth of nanotubes by the chemical vapor decomposition (Yacaman et al., 1993).

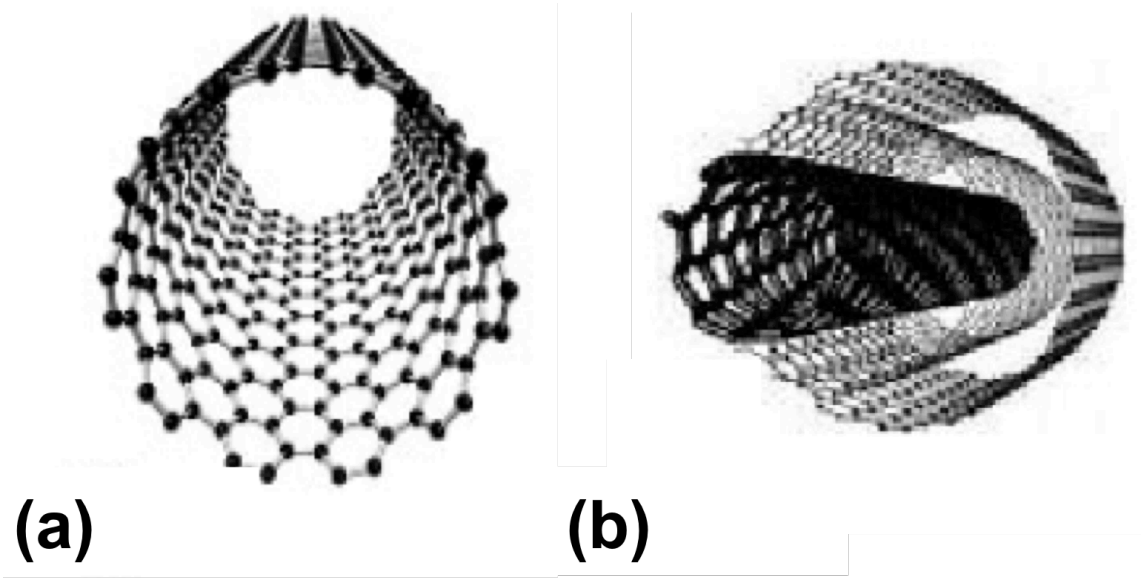

Figure 1.1. Schematic of a) SWCNT b) MWCNT (reproduced from http://www.wtec.org/loyola/nano/04_03.htm)

Carbon nanotubes have a molecular structure identical to the graphene sheet. Similarly, the repeating unit for nanotubes is the hexagonal mesh of sp^2 hybridized carbon atoms. SWCNTs are basically the roll-up form of the graphene sheets. The angle at which the graphene sheet is rolled, determines the chirality of nanotubes, which separates nanotubes into the two groups; semi-conductor and metal. The chirality angle can also be shown as (n, m) index where n and m

describe the number of the repeat units contained in the chiral vector. If nanotubes have the index of n=m (i.e. (n, n)), they are called metallic " armchair" SWCNTs and if they have index of m=0 (i.e. (n, 0)), then they are semiconductor "zigzag" SWCNTs.

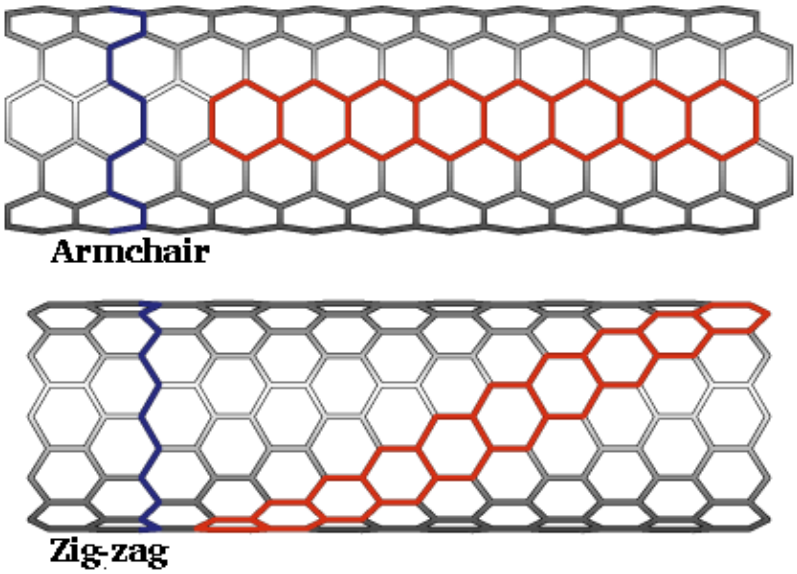

Figure 1.2. Schematic of chirality of nanotubes
(http://mailhost.ccs.uky.edu/~ernst/carbontubes/structure.html)

The properties of carbon nanotubes are unique and redundant compared to the traditional carbon fibers, which have been used industrially for several decades. Carbon nanotubes represent the ideal and perfect structure in the atomic level. Because of perfect carbon-carbon bond observed in nanotubes, which is one of the strongest in nature, carbon nanotubes are excellent candidates for the stiffest and strongest material ever synthesized. The Young's modulus of SWCNTs and MWCNTs were reported in the range of 1 TPa and 500 GPa, respectively (Krishman et al.1998). Thermal conductivity of single wall carbon nanotubes was reported as 6000 W/(mK) while the thermal conductivity of diamond is around 3320 W/(mK). The electrical current carrying

capability is estimated to be 1×109 amp/cm^2 whereas copper wires burn out at about 1×106 amp/cm^2. The main properties of carbon nanotubes are summarized in Table 1.1.

Table 1.1. Measured properties of carbon nanotubes (Schadler L.S., 2003)

Property	Nanotubes
Lattice Structure	(Cylindrical) hexagonal lattice helicity Nanotubes: ropes, tubes arranged in triangular lattice with lattice parameters of a= 1.7nm, tube-tube distance 0.315
Specific gravity	0.8-1.8 g/cc (theoretical)
Elastic modulus	~ 1TPA for SWCNT ~ 500GPa for MWCNT
Strength	50-500GPa for SWCNT 10-60GPa for MWCNT
Electric current carrying capacity	1× 10^9 amp/ cm^2
Thermal conductivity	3000 W/(mK) (theoretical)
Thermal expansion	Negligible
Oxidation	> 700 °C in air > 2800 °C in vacuum

Since their discovery in 1991, carbon nanotubes have gained a great interest by various industries due to their wide application areas such as composite reinforcement material, hydrogen containers, field emission sources, super-capacitors, molecular sensors and scanning probe tips (R.H. Baughman et al., 2002). Some of these applications have been already realized in products. For instance Entropy Sports, Amroy Europe Ltd. and Bayer Material created surfboards that incorporate carbon nanotubes. The result was tougher and more durable surfboards than standard epoxy system surfboards (Composite manufacturing, winter 2009).

1.2.2 Vapor Grown Carbon Nanofibers

Vapor grown carbon nanofibers (VGCNFs) are hollow cored fibers with diameters 70-200 nm and the lengths of a few to 50-200 microns (Figure 1.3). The fibers can be arranged in a single

layer or double layer and includes graphite planes stacked parallel or at angle to the axis. VGCNFs are manufactured by the deposition of carbon on metal catalysts such as iron (Fe) or nickel (Ni) by pyrolysis of carbon containing gases like methane or acetylene at ~1000° C. A further annealing at higher temperatures, ~2500° C, takes place in order to crystallize the layers of tubes and form a fiber with ring concentric cylinder morphology. The diameter of nanofibers depends on the catalyst size (De Jong, K.P, 2000). Moreover, the diameter of nanofibers affects the mechanical properties of these fibers. High tensile strength, 12-30 GPa, and high modulus, 75-100 GPa, were reported for VGCNFs. These values also depend on the existence of a good adhesion between the graphitic planes of VGCNFs. Beside their high mechanical properties; VGCNFs also possess high electrical conductivity, corrosion resistance and high thermal conductivity (Potschke et al., 2004).

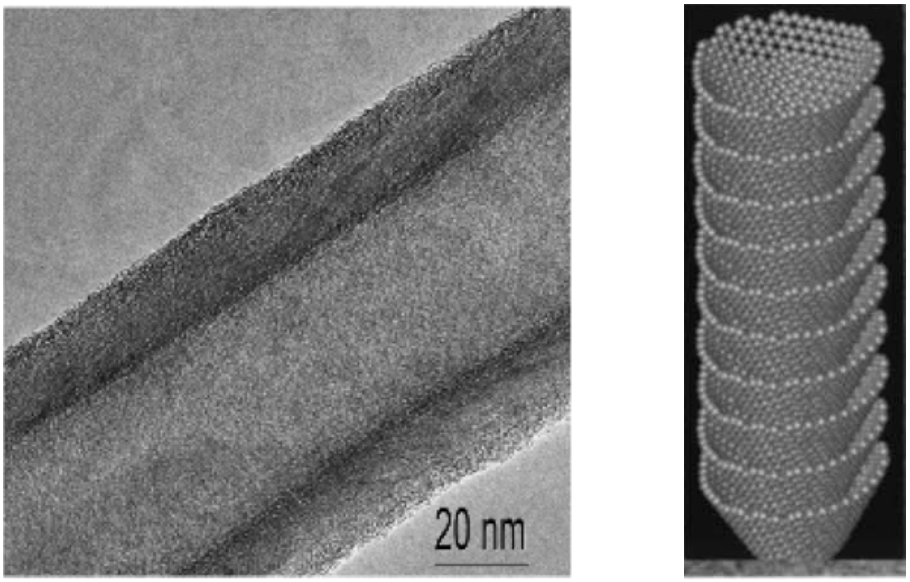

Figure 1.3. TEM image of VGCNF with the cylindrical hollow core at the center (left) and the molecular model (right) (G.G. Tibbets et al. 2007)

Vapor-grown carbon nanofibers have occasioned so much interest in composite applications. Nouranian et al. (2010) showed that 0.5 wt% of carbon nanofibers increased the storage modulus 20% of vinyl ester composites (Nouranian et. al., 2010). Lafdi and Matzuk reported that tensile strength and modulus of epoxy composites improved 35% and 140%, respectively, as 4 wt% oxidized VGCNFs added into the system (Lafdi et al., 2003). Zeng et al. (2004) extruded polymethyl methacrylate reinforced with VGCNFs and achieved 80% improvement in modulus with a 5 wt% loading of VGCNFs, however when the concentration was increased to 10 wt%, a decrease in tensile modulus was observed because of the poor dispersion of VGCNFs.

Beside their reinforcement role in composites, VGCNFs also found a huge interest in electrical applications. For instance, Finegan and Tibbets (2001) reported 3 vol% percolation threshold in VGCNFs/ polypropylene and nylon composites and resistivity values reached as low as 0.15 Ω cm at 20 vol% loading. In another study, Xu et al. (2004) reported 2-3 wt% percolation thresholds, however at higher loadings resistivity was above 10 Ωcm, probably due to the imperfect dispersion of nanofibers.

On the other hand, Lafdi and Matzek studied the thermal conductivity of VGCNF/epoxy composites. They observed that the thermal conductivity increased from 0.2 W/ (m K) for epoxy matrix to 2.8 W/ (m K) for a 20 wt% fiber loading.

Even though there have been many challenges such as bonding to matrix, dispersion, and orientation of VGCNFs, the above results show that carbon nanofibers have the potential for applications such as aerospace, automotive, construction industry where high performance materials are required.

1.3 CHALLENGES

In spite of their superior properties compared to the traditional fillers, nanofillers have various challenges. These challenges make nanofillers not easy to process. For instance, because of their smooth, non-reactive surface, carbon nanotubes bonds polymers through physical interactions rather than chemical interactions. This weak physical interaction causes poor adhesion between the polymer and the nanotubes that limits the efficient load transfer. In this case, nanotubes are typically pulled out from the matrix rather than fractured and play limited reinforcement role (Lourie et al., 1998).

Another main challenge is that carbon nanotubes are not easy to disperse individually in the polymers because they create bundles and clusters due to the strong interaction energy between each individual tubes. Thus, bad dispersion of carbon nanotubes that create large bundles initiate cracks in the composites rather than reinforcing them. Furthermore, carbon nanotube bundles decrease the available surface area that prevents providing more energy dissipation.

In order to disperse the CNTs in the polymer homogeneously, the entanglement of CNTs produced by the synthesis and agglomerates of the CNTs caused by the intermolecular van der Waals force must be broken for homogenization. MWCNTs are generally entangled in the form

of curved agglomerates and SWCNTs are produced as bundles.

The origin of the attractive forces between nanotubes is due to the extended π electron system that these systems are highly polarizable, and thus subject to large attractive van der Waals forces. These forces causes secondary bonding that holds nanotubes together and lead to agglomeration. Extended structures are also formed side-by-side between the aggregated nanotubes.

Another reason makes the dispersion of nanotubes a challenge is that attractive force between suspended nanotubes in a polymer arises due to pure entropic factors. There is a depletion of polymer in the corona region of the colloidal filler that causes osmotic pressure forcing the nanotubes together by limiting the mobility of the roughly half of polymer chains configurations (Bechinger et al., 1999). Furthermore, the linear structure of carbon nanotubes increases attraction forces because rods interact along a line.

The ability of control dispersion of carbon nanotubes in polymer matrix is the key challenge for polymer nanocomposite applications. Even though some of the applications do not desire to have perfect dispersion, in particular for electrical conductivity and mechanical reinforcement, controlling the dispersion is key for proper function of the nanocomposite in its intended application. A lot of methods have been reported to solve the problem dispersions such as functionalization of carbon nanotubes, using strong acids or certain solvents and applying mechanical techniques (high-shear mixing, ultra-sonication, centrifugation).

Functionalization of CNTs provides better dispersion and stronger interfacial bonding between the CNT-matrix. Functionalization involves the covalent and noncovalent attachment of various functional groups to either to nanotube end-caps or sidewalls.

1.3.1 Covalent Functionalization of Carbon Nanotubes

Covalent functionalization consists in chemically grafting functional groups on the CNTs. This may lead to an alternation of CNT structure in the case of high levels of functionalization. Covalent (chemical) functionalization of carbon nanotubes relies on the transformation of sp^2 to sp^3 hybridized of carbon atoms, which is associated with a change from a trigonal-planar local bonding geometry to a tetrahedral geometry (Moniruzzaman et al., 2006). This reaction is more favorable at the nanotube caps due to the two dimensional curvature. Similarly, the curvature on the sidewall of nanotubes makes them more reactive than a planar graphene sheet. Covalent functionalization of nanotubes can improve nanotube dispersion in solvents and polymers. For example, the pristine SWCNT is completely insoluble in chloroform whereas covalently functionalized SWCNTs with pyrrolidine show a solubility of 50 mg/mL in chloroform, even without aid of sonication (Georgakilas et al., 2002).

Covalent functionalization of nanotubes also leads to the creation of novel composite materials and elastomers. For example, the interfacial adhesion could be modified through covalent interactions between the functional group on the nanotube and the polymer matrix to maximize load transfer. A notable drawback of covalent functionalization is the disruption of the extended conjugation in nanotubes. This may have limited impact on thermal and mechanical properties.

Additionally, the electrical properties are affected by covalent functionalization since each covalent functionalization site scatters electrons (Dyke et al., 2004).

The discovery of the oxidation process of CNTs led to improve the surface chemistry of CNTs. The end-caps of CNTs can be opened by oxidation and terminated with oxygenated functionalities including carboxylic (—COOH), carbonyl (—CO) and hydroxyl (—OH) groups. Oxidized nanotubes are expected to form well-dispersed electrostatically stabilized colloids in water and ethanol (Shaffer et al., 1998). The carboxylic acid groups can be used to attach thionyl chloride ($SOCl_2$), long chains amines (—NH) or ester groups (—COOR). Furthermore, carboxylic acid groups can undergo esterification reactions with epoxy (Figure 1.4). Some cross-linking may also take place because both the surface and ends of nanotubes are expected to carry more than one carboxylic acid group (Riggs et al., 2000).

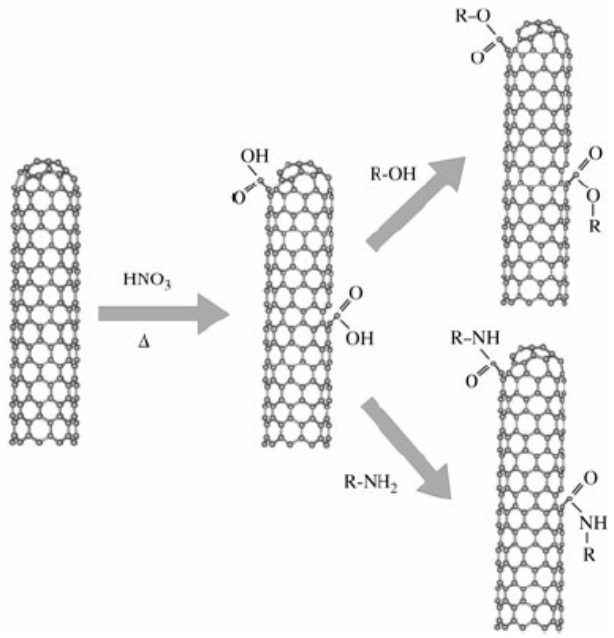

Figure 1.4. CNT functionalization through oxidation followed by esterification or amidization of carboxyl groups (Balasubramanian et al., 2007)

There have been many researchers who have reported improved thermal, mechanical and electrical properties of polymer carbon nanotube composites through chemical functionalization. For example Velasco et al. reported that at 1 wt% loading, the oxidated MWCNT/PMMA (Poly-methyl methacrylate) composite showed 66% increase in storage modulus and 41% improvement in tensile strength compared to the matrix at 40°C. (Velasco-Santos et al., 2003). Zhu et al. reported fluorination of acidified MWCNTs/epoxy system and showed 30% increase in Young's modulus and 18% increase in tensile strength compared to the epoxy matrix. The reason for combination of acid treatment and fluorination is that while acid treatment results in shortened nanotubes with carboxyl acid groups mainly on the end tips and reduction in the nanotube bundles diameter, fluorination improves the solubility due to interaction of the solvent and the fluorine atoms on the surface of nanotubes. The fluorine atoms in fluorinated carbon nanotubes can be replaced simply through nucleophilic substitution reactions thus opening a flexible approach for providing the sidewalls with various types of functional groups (Figure 1.5). It is known that the epoxy groups can directly react with the carboxylic acid functionalities to form esters. In the presence of tertiary amines, the epoxy groups are also capable of reacting with the hydroxyl function to form an ether linkage. On the other hand fluoro nanotubes may also react in situ with the amine groups of the hardener during the high temperature curing process, which means that an efficient interfacial bonding will occur by an epoxy/amine reaction (Zhu et al., 2003).

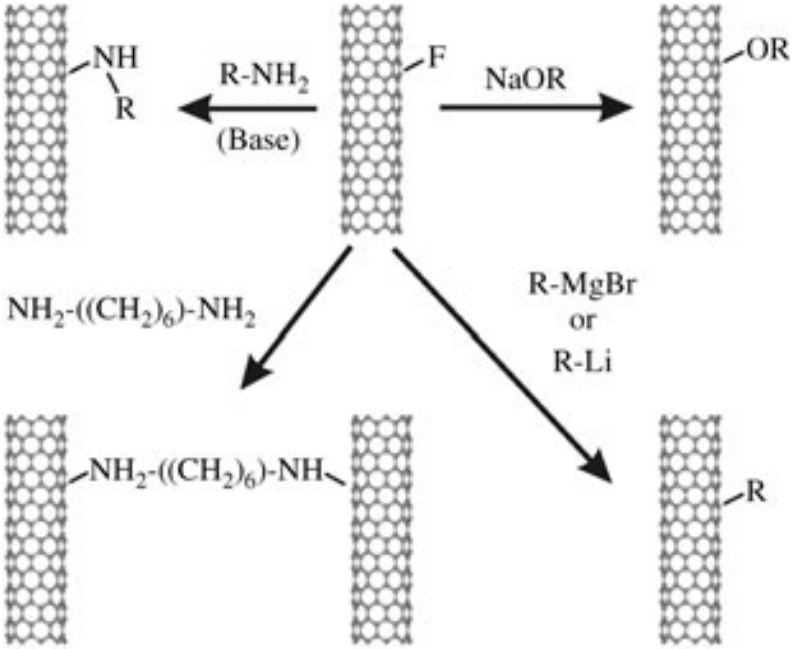

Figure 1.5. Functionalization of CNT sidewall through nucleophilic substitution reactions after fluorination of CNTs (Balasubramanian et al.2007)

Gojyn et al. reported the effect of amino functionalized MWCNTs on the thermo-mechanical behavior of nanocomposites. They found that the addition of both types of 0.05 wt% MWCNTs (non-functionalized and amino functionalized) did not show a considerable increase in storage modulus at room temperature, however a strong increase at the elastic properties was seen at the higher temperatures (rubbery region). They also observed an increase in glass transition temperature from 65°C to 77°C at 0.05 wt% loading of MWCNTs due to reducing matrix mobility by the covalent bonds between the epoxy matrix and amino-functions on the surface of MWCNTs (Gojny et al., 2004).

Polymer chains can also be attached to the surface of nanotubes through two general approaches: “grafting from” and “grafting to”. The “grafting to” approach is based on the attachment of pre-

formed end-functionalized polymer molecules to functional groups on the nanotube surface via chemical reactions. Sun et al. investigated the maximum reinforcement effect of the SWCNT in the epoxy without compromising processability. The SWCNTs were functionalized via oxidation, followed by grafting with polyamidoamine generation (PAMAM-0) dendrimers to chemically bridge between SWCNTs and epoxy. A strong bond is expected to occur, because the amine groups on PAMAM-0 can react with both the carboxylic acid groups on the oxidized SWCNT surfaces and epoxy monomers. The results show that PAMAM-0 functionalized SWCNTs improved modulus and strength by 27% and 17%, respectively (Sun et al., 2008).

On the other hand the "grafting from" approach is based on the initial attachment of the initiators onto the nanotube surface, which is followed by polymerization of appropriate monomers with the formation of the polymer molecules bound to the nanotube. Vigolo et al. (2009) developed PMMA-SWCNT composites by using the "grafting from" procedure and they reported that the interfacial adhesion between the SWCNTs and the matrix was improved compared to the non-functionalized SWCNTs.

In another study, Yan et al. reported single-walled carbon nanotubes (SWCNTs) with 1-vinylimidazole species, which were covalently attached to their sidewalls and end caps, have been prepared by ultraviolet (UV) irradiation in 1-vinylimidazole monomer. This process can be greatly assisted by argon (Ar) plasma pretreatment, and as a result of Ar plasma pretreatment, some defects were generated such as oxygen-containing species including peroxidic, alcoholic, and carboxylic species at the tube ends and sidewalls acting as the active sites for the subsequent

UV grafting of 1-vinylimidazole molecules. The estimated functionalization degree by x-ray photoelectron spectroscopy (XPS) measurement was as high as around 26 wt% 1-vinylimidazole molecules grafted onto the nanotubes. It was also mentioned that other vinyl monomers, such as vinylpyridine, acrylic acid, acrylate, acrylonitrile and even styrene, might be employable as functional groups (Yan et al., 2007).

1.3.2 Non-Covalent Functionalization of Carbon Nanotubes

Non-covalent functionalization consists of surfactant molecules or wrapping polymers. They are physically absorbed onto the CNTs, which have the advantage of not damaging the CNT surface, however their presence in the final materials may cause a negative effect on composite properties such as decreasing the interaction between the CNTs and the polymer matrix (Vigolo et al., 2009).

Non-covalent functionalization of nanotubes is widely used because this physical process leaves the nanotube structure undamaged and maintains the intrinsic properties of the nanotube. Non-covalent (physical) treatments, such as application of surfactants and polymer coating followed by surfactant treatment do not disturb the inherent π- bonds of CNTs and thus the electrical properties. These approaches are based on interactions of the hydrophobic part of the adsorbed molecules with nanotubes sidewalls through van der Waals, π-π, CH-π, and other interactions, and hydrophilic part of the molecules provides aqueous solubility. In the last few years, the non-covalent functionalization of CNTs with surfactants and polymers has been widely used in the dispersion of high weight fraction of CNTs in both aqueous and organic solutions (Vaisman et al., 2006).

Surfactant molecules have both polar and non-polar groups. These groups are adsorbed at the interface between immiscible bulk phases such as oil and water, air and water, particles and solution (in our case nanotubes and the polymer) and reduce the surface tension. After the surfactant has been adsorbed on the nanotube surface, ultra-sonication may help a surfactant de-bundle nanotubes by steric and electrostatic repulsions and thus, the surfactant-treated CNTs can overcome van der Waals attraction by electrostatic/steric repulsive forces promoted by the surfactant addition. This physical adsorption of surfactant on the CNT surface prevents the formation of aggregates.

The effect of surfactant on dispersibility and other property changes of CNTs have been studied by many researchers. Generally, CNTs are dispersed in aqueous solutions of ionic surfactants, whereas, non-ionic surfactants are preferable when organic solvents have to be used. The adsorption of surfactants onto inorganic and organic surfaces usually depends on the chemical characteristics of particles, surfactant molecules and the type of solvent. Thus, the driving force for the adsorption of ionic surfactants on charged surfaces is the Coulombic attractions, which are formed between surfactant's positively charged head group and the negatively charged solid surface or vice versa. On the other hand, non-ionic surfactant's treatment is based on a strong hydrophobic attraction between the solid surface and the surfactant's hydrophobic tail. Once the surfactant is adsorbed onto the filler surface, the surfactant molecules are self-organized into micelles above a critical micelle concentration (CMC). The charge of ionic surfactants leads to electrostatic repulsion between the surfactant molecules, and this stabilizes the nanotube colloids, whereas, the non-ionic surfactants stabilize the nanotubes in solution primarily by steric and not electrostatic interactions. Therefore, bulky hydrophilic groups were reported to have an

advantage in the case of nanotubes suspended with nonionic surfactants due to the enhanced steric stabilization provided by longer polymeric groups (Moore et al., 2003).

There have been many studies included non-ionic surfactants such as polyoxyethylene 8 lauryl ($CH_3(CH_2)_{11}(OCH_2CH_2)_7OCH_2CH_3$), polyoxyethylene octyl phenyl ether (Triton X-100) (Vaisman et al., 2006) anionic surfactants such as sodium dodecyl sulfate (SDS); cationic surfactants dodecyl tri-methyl ammoniumbromide (DTAB) (Whitsitt et al., 2003).

Geng et al. reported the use of a non-ionic surfactant Triton X-100 to treat CNT surface for epoxy nanocomposite fabrication. They highlighted from this study that after treating CNTs by surfactant no structural defects were created according to Raman results. They also reported 60% improvement in toughness compared to the matrix and similar electrical conductivities with 0.25 wt% non-surfactant treated CNTs system (Geng et al., 2008). In another study, Gong et al. used polyoxyethylene 8 lauryl ($C_{12}EO_8$) with 1 wt% carbon nanotubes in epoxy matrix. They observed increase in the glass transition temperature from 63°C to 88°C and the elastic modulus increased more than 30% (Gong et al. 2000). Jiang et al. studied the dispersion of MWCNTs under the optimum composition of 0.5 wt% MWCNTs and 2.0 wt% SDS relative to water. They obtained homogeneous dispersion of MWCNTs because of the higher negative surface charge and a steric repulsion through the interaction between CNTs and hydrophobic segment of SDS (Jiang et al., 2002).

The interaction of surfactant molecules and carbon nanotubes surface has already been extensively studied, however the arrangement of the surfactant molecules on the CNTs surface is

still unclear. Three main approaches have been considered: structureless random adsorption on the CNTs walls without any preferential arrangement of the head and tail (Yurekli et al., 2004), hemi-micellar adsorption on the CNTs surface (Richard et al., 2003), and encapsulation of the CNTs in a cylindrical surfactant micelle (Mattarredona et al., 2003). However, it is mostly accepted that the organization of surfactant molecules on CNT walls is structure-less random configuration (Hu et al. 2009).

Another challenge for preparation homogenous and stable CNTs suspensions is that the choice of the concentration of the both CNTs and surfactants. If the amount of surfactant is too low, then the total amount of surfactant molecules adsorbed onto the total CNTs surface is not enough and, thus, only a fraction of CNTs are effectively dispersed but many CNTs bundles remain. If the amount of surfactant is too large respect to the number of CNTs, then attractive depletion-type interactions between the CNTs are induced by presence of surfactant micelles. That causes the formation of clusters of aggregated CNTs (Vigolo et al., 2002).

Other type of non-covalent functionalization is polymer wrapping. O'Connell et al. improved the solubility of SWCNTs in water with polyvinyl pyrrolidone (PVP) and polystyrene sulfonate (PSS). PVP is a polymer with a hydrophobic alkyl backbone and hydrophilic pendant groups. These groups can be formed to coil around the nanotube so that its backbone is in contact with the nanotube surface and pyrrolidone groups are exposed to water (O'Connell et al., 2001). In another study, Tan S. et al. successfully functionalized MWCNTs with water-soluble poly (2-ethyl-2-oxazoline)(PEOX) through the polymer wrapping process. The non-functionalized MWCNTs gave a stable dispersion in water and as well as other organic solvents such as ethanol

and N,N-dimethylformamide (DMF) (Tan S et al., 2007).

1.3.3 Phase Separation Induced Dispersion

The initially homogeneous solution of a non-reactive component (rubber, thermoplastic polymer, liquid crystal, etc.) in reactive monomers, phase separation will occur in the course of polymerization, which is known as polymerization-induced phase separation (PIPS). The origin of phase separation is the increase in the molar mass of reacting system during the pre-gel stage that produces a decrease in the contribution of the entropy and the increase in cross-link density. This generates elastic contribution during the gel state, which limits the amount of the modifier in the swollen network (Elicabe et al., 1997).

In this study, Polyhedral oligomeric silsesquioxanes (POSS) which are nanosized cage structures with a formula $(RSiO_{1.5})n$ (n=6,8,10…), where R indicates an organic group, are used as a modifier (i.e. non-reactive component). The typical POSS monomers have the structure of cube-octameric frameworks with eight organic corner groups, one or more of which is reactive or polymerizable. POSS molecules with non-reactive organic substituents or organic functional groups are emerging as a chemical technology for the nano-reinforced organic-inorganic hybrids. The hybrid structure of POSS molecules provides advantage over inorganic and organic materials, since inorganic materials are very strong and chemically stable, but can be difficult to process, especially when used as additives in polymers. On the other hand, organic materials are compatible with polymers and can often ease processing, but can damage mechanical properties. POSS molecules provide properties of organic and inorganic materials.

"The ideal structure consisting in pendent POSS cages homogenously dispersed in the network is frequently not achieved in practice due to the lack of compatibility of POSS with organic network. In this sense, monofunctional POSS are not different from different types of rubbers, thermoplastics, or liquid crystals used to modify polymer networks (Zucchi et al., 2006)." Thus, by using monofunctional POSS structures, a phase separation can occur in the course of polymerization and by controlling the functional group and the nature of the inert organic groups on the phase separation, either amorphous or crystalline POSS aggregates can be generated.

Functionalized POSS cages can also be attached on CNTs as the modification agents to prepare the nanocomposites combining the two types of nano-reinforcement agents. If phase separation occurs by using POSS functionalized CNTs in the course of polymerization of a reactive solvent, then some kind of ordered arrays can be prevented in the polymer that may improve the dispersion.

Chen et al. grafted multiwall carbon with POSS and prepared dispersion in poly (L-lactide) matrix. MWCNTs were functionalized with POSS via amide linkages. MWCNTs were oxidized and then MWCNT-COOH was converted to the acyl chloride functionalized MWCNTs (MWCNT-COCl) by treating them with thionyl chloride ($SOCl_2$). MWCNT-COCl was reacted with aminopropylissooctyl-POSS to prepare POSS modified MWCNTs. The resulting POSS modified MWCNTs were dispersed in PLLA matrix uniformly through a solvent casting method and a simple melt compounding. They reported that the fractured surface of the composites showed not only a uniform dispersion of MWCNTs but also a strong interfacial adhesion with the matrix. Scanning electron microscopy (SEM) images showed many broken but strongly

embedded MWCNTs in the matrix in the absence of debonding of MWCNTs from the matrix. They also reported an increase of 40% in Young's modulus compared to the epoxy matrix (Chen et al., 2008).

Monitoring the quality of CNTs dispersion in polymers

Monitoring the quality of dispersion is a critical step for nanocomposites. The quality of dispersion cannot be explained with the naked eye. There are direct microscopic observations and indirect estimative methods. Direct microscopic observations include optical microscopy (OM), scanning electron microscopy (SEM), atomic force microscopy (AFM), transmission electron microscopy (TEM) and so on. Because of the limited magnification capacity, optical microscopy cannot observe individual CNTs. SEM and AFM show only cross-section of the specimen. AFM is used to determine average bundle size in solvent-dispersed nanotubes, however, this method will only image tubes at a surface for a polymer. Even though TEM has ability to determine bundle distribution statistics, it is also difficult to observe CNTs by using TEM because CNTs have extreme differences between radial and axial dimensions and very thin samples are required for observation.

Another characterization method is to analyze the intensity of a UV-absorbance band, which gives a measurement that is at least proportional, if not equivalent, to the bundle fraction for SWCNTs. Haddon et al. and Tan et al., reported the dispersion of SWCNTs by using very similar methods. In these methods, they reported that the intensity of a UV-absorbance band (or multiple bands) can be used to monitor the relative concentration of individually dispersed tubes in water since only individual tubes will have the relatively narrow diameter distribution. A

higher fraction of individual nanotubes in the suspension gives better-resolved spectral features. The sharpness of the spectral features relative to the background can be qualified by two parameters. The first one is the resonance ratio where is the ratio of the resonant band area to its non-resonant background area (B.P Grady, 2010). The second parameter is the normalized width where is the ration of the width of the band at half-height to the peak height on a spectrum that has been normalized at 900 nm. The peak height can be used as a measure of exfoliation, since the incremental effect on the non-resonant background by adding another tube to a bundle is much less than that on the resonant band by adding an individual tube (Tan et al. 2005, Haddon et al. 2004).

Dynamic rheological measurement provides information about the dispersion state of CNTs. Different behaviors of storage modulus and complex viscosity are expected for different dispersion qualities. Well-dispersed suspensions are expected to exhibit a plateau at low frequencies for storage modulus, which suggests the formation of network of nanotubes in the suspension. However, there are some researchers who found that a better dispersion decreases G' and did not plateau at low frequencies (Song et al., 2005). These two different observations can be explained by the presence of different dispersion microstructures in the different systems. The quality of dispersion determines how uniformly nanotubes are distributed in the suspension. A good dispersion of the tubes is particularly important for final properties. On the other hand, bad dispersion causes a phase separation due to the strong surface interactions between the tubes. After an effective dispersion technique, the fillers become better dispersed in the matrix. The entire nanotube interfacial area becomes effective transferring load between the filler and the matrix. Both of these CNT network structures exhibit distinct viscoelastic behavior, which can

be observed as a Newtonian plateau of the storage modulus (G') developed at low frequencies during frequency sweep tests and considerable higher values of G' for the well dispersed sample (Figure 1.6).

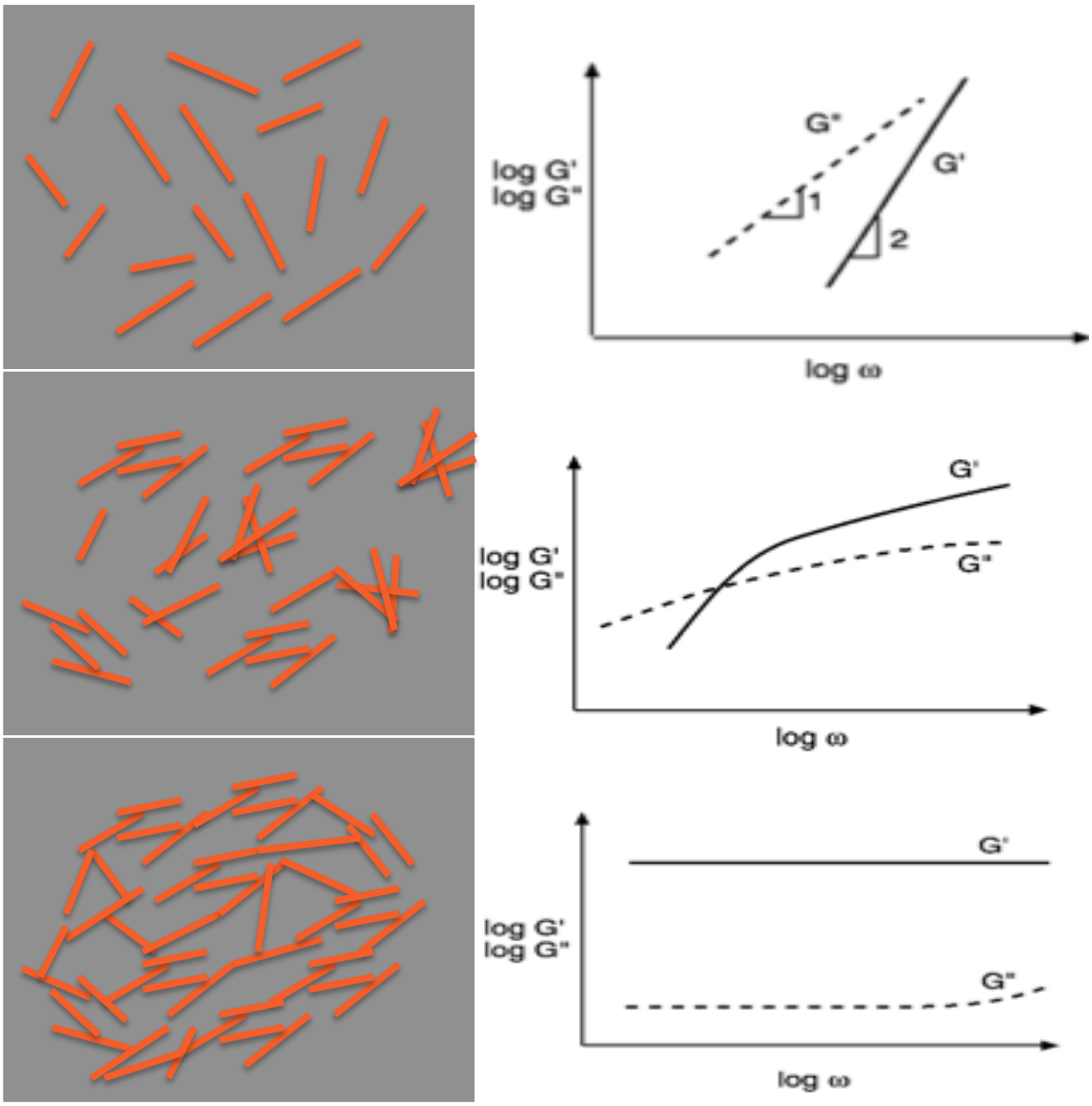

Figure 1.6. Changes in rheological behavior at different dispersion states

1.4 MECHANICAL PROPERTIES OF POLYMER NANOCOMPOSITES

The use of nanotubes improves the mechanical properties of polymers. However, experimental results have not been close enough to theoretical findings. The load transfer between nanotubes

and matrix needs to be improved in order to increase the efficiency of reinforcement. If load can be effectively transferred to the nanotubes, then the modulus of the composite should be similar to that of randomly oriented short fiber composite containing fibers of extremely high modulus and strength. In addition, the high surface area of nanotubes creates a large interfacial region, which can have properties different from the bulk (Villoria et al., 2007).

Load transfer depends on the interfacial shear stress between the fiber and the matrix. A high interfacial shear stress will transfer the applied load to the fiber over a short distance, and a low interfacial shear stress will require a long distance. There are three main mechanisms of load transfer from the matrix to the filler. The first is micromechanical inter-locking; this could be difficult in nanotube composites due to their atomically smooth surface. The second is chemical bonding between the nanotubes and the matrix that can be improved through functionalization. The third mechanism is a weak van der Waals bonding between the fiber and the matrix. Improved dispersion of nanofillers creates more available surface area to interact with the matrix. (Ajayan et al., 2000, Moniruzzaman et al., 2006).

Zhu et al. prepared two different SWCNT/epoxy systems. SWCNTs were functionalized through fluorination and oxidation. As it is expected, after functionalization, SWCNTs were dispersed more uniformly than non-functionalized SWCNTs. Mechanical properties of these two different systems were also studied and it was also reported that functionalization increased the Young's modulus over 30% compared to the neat epoxy. The tensile strength of the functionalized SWCNT epoxy system increased while non-functionalized SWCNTs epoxy system showed a decrease of tensile strength compared to the matrix. This can be explained by inefficient

reinforcement of epoxy with non-functionalized SWCNTs. On the other hand, homogenous dispersion created larger surface area available for interaction with the matrix. Through covalent bonds between the matrix and the filler, more effective load transfer to the epoxy matrix was obtained (Zhu et al. 2003).

Allaoui et al. (2003) investigated the influence of MWCNTs in a rubbery epoxy and they found that the addition of MWCNTs up to 1 wt% could lead to a 100 and 200% increase in strength and Young's modulus, respectively. They also reported 400% improvement in Young's modulus at 4 wt% loading. Zhu et al. (2003) made a significant progress in improving the CNTs dispersion and matrix adhesion by adding 1 wt% alkylamino-functionalized SWCNTs to the epoxy. They showed an increased of 18% in strength and 30% in Young's modulus.

Guo et al. fabricated well-dispersed MWCNTs in epoxy matrix by using ultrasonication and cast molding method. They used modified MWCNTs by mixing acids at high concentrations. The combination of chemical functionalization of MWCNTs and high-energy sonication were reported as useful approach to improve the dispersion state of the CNT and the interfacial adhesion to the epoxy matrix. They observed 12% increase of strength and 128% increase of fracture strain at break with acidified MWCNTs with 8 wt% content (Guo et al., 2007).

Schadler et al. (1998) reported two different Young's modulus values for compression and tensile loadings. In tensile loading, the reason may be either the poor bonding between the matrix

and the outermost nanotube layer; or the outermost nanotube is loaded, but because of the relatively weak bonding between the nanotube layers, load is not transferred to the inner layers. Instead the inner tubes may slip with respect to the outer tubes. In compression, the load transfer occurs to the inner layers of the MWNT through easy buckling and through the bent sections of the nanotubes. Slippage of nanotube layers in compression is prevented because of the seamless structure of the tubes and the geometrical constraint the outer layers impose on the inner ones.

Ci et al. evaluated the mechanical properties of SWCNTs/epoxy nanocomposites with different rigidity degrees. In the soft and ductile composite, carbon nanotubes show a significant reinforcement because of the possible accelerated curing process and the better interface adjoining. The interface interaction is poor due to complete cross-link of the polymer molecules surrounding carbon nanotubes in the stiff composite. Thus, when the epoxy is adequately cured, the gain in rigidity with addition of SWCNTs is much lower. While the increase in Young's modulus and strength were 200 and 140%, respectively for 9 wt% hardener and 48 h. curing time, the increase in modulus and strength dropped till 23% for 13 wt% hardener and 48 h. curing (Ci et al., 2006).

Loos et al. (2008) showed an increase in tensile and compression modulus and strength in 0.25 wt% SWCNT/epoxy system. Regarding tensile properties, there is an increasing trend in strength (up to 8%) and Young's modulus (up to 7%) for the nanocomposites and regarding compression tests, the compression strength of the pure epoxy was 57.8 MPa, whereas the nanocomposites presented 8% higher value. They reported that the elongation at break and flexural properties were virtually unaffected by SWCNTs loading.

In general, the tensile modulus and strength of polymer nanocomposites are found to increase with nanotube loading, better dispersion and alignment in the matrix. However, the results at low nanotube loadings typically stand far behind the idealized theoretical predictions from the rule of mixture and the Halpin-Tsai model. For example, Haggen-mueller found that the tensile modulus of PE fiber was improved 200% with the addition of 5 wt% SWCNT. However, Halpin-Tsai model predicts the modulus to be 16 times higher than experimental result (Haggenmueller et al. 2003). At higher nanotube loadings, the high viscosity of the composite and the resulting void defects might limit the extent of improvement properties.

The gap between the predictions and experimental results arises from imperfect dispersion and poor load transfer. Nanotube agglomeration impacts the diameter and length distributions of the filler. Agglomerated nanotubes act like large spherical particles in the matrix and likely decreases the aspect ratio. In addition, nanotube agglomeration reduces the modulus of the filler relative to that of isolated nanotubes because there are only weak dispersive forces between nanotubes. As conclusion, the improvement in dispersion and alignment of CNTs in polymer matrix provide very effective reinforcement in the material.

1.5 ENERGY DISSIPATION IN CNT NANOCOMPOSITES

Vibrations and noise are usually undesirable in engineering structures. Reduced vibration alleviates dynamic stresses and enhances system performance, safety, and reliability. Structural damping can take the vibration and noise under control in a variety of dynamic components. Thus, the demand for high-performance damping material is rapidly growing in a variety of applications if aerospace, mechanical and civil systems. For these applications manufacturers

need to design materials that will be lightweight, cost effective and reliable vibration-absorbing materials. For instance, the most important parameters that affect the vibration damping in aerospace-related structures are huge temperature changes (from -140°C to 600°C and higher), rotational speed (up to 10,000 rpm in turbine engines), frequency and amplitude of vibrations. Thus, the new materials, which can be designed for damping application, need to meet all these needs.

Many researchers have reported the capability of nanotechnology to develop materials that enhance strength/damping behavior and reduce noise of engineering structures through dissipating the vibrational energy. Composites with nanofillers (such as carbon nanotubes) have the potential to provide significant energy dissipation with minimal weight penalty because of the combination of extremely large interfacial contact area and low mass density. Furthermore, the nanoscale fillers can be integrated into the composite system without sacrificing mechanical properties or structural integrity.

The ability of materials to damp vibrations can be characterized by dynamic mechanical analysis. The storage modulus (E') represents the energy stored through elastic behavior and the loss modulus (E'') is the energy lost through conversion to heat via molecular friction. When a polymer is in its viscoelastic region, which the transition between the hard glassy state and the soft rubbery state, it exhibits the highest level of damping. In the glass transition region, there is a distribution of phases. When the material is forced to vibrate, some molecules exhibit viscous flow while the others remain rigid. Thus, the friction among the molecules increases which results in heat buildup and a decreased amount of transmitted energy. When vibration-damping

polymers are formulated, it is desirable to maximize E''. However, maximizing E'' causes a lower elastic response and, therefore, poor physical and mechanical properties may occur (Rajoria et al., 2005, Suhr et al., 2006).

The mechanism for the observed damping increase in nanocomposite can be explained by "stick-slip" mechanism. In this mechanism, when a tensile stress is applied to a composite, it starts elongating. As a result of the applied stress, the matrix resin starts applying a shear stress on the nanotubes; thereby causing the load to be transferred to the nanotubes and normal strain starts to appear in the nanotube fillers. Then, the matrix and filler start elongating accordingly. When the applied stress is small, the nanotube remains bonded to the matrix (sticking phase) and both the matrix and the nanotubes deform together during this phase. As the applied load is increased, the interfacial shear stress on the nanotubes further increases; this results in more elongation of both matrix and the nanotubes. At a critical threshold stress, the nanotubes debond from the matrix resin. With further increase in stress, the maximum strain in nanotubes is reached and remains constant, while the strain in matrix increases and causes slippage (slipping phase). This results in energy dissipation due to slippage between the matrix and the nanotube causing the material structural damping to increase (Zhou et al., 2004, Suhr et al., 2008).

Koratkar et al. studied energy dissipation in SWCNT/polycarbonate composites. The polycarbonate composite beams were fabricated by a solution mixing process. They reported >1000% increase in loss modulus of the polycarbonate system with the addition of 2 wt% oxidized SWCNTs at 1% strain at room temperature compared to the polycarbonate matrix. The increase in damping was reported as a result of frictional sliding at the nanotube-polymer

interfaces. Furthermore, the functionalization of SWCNTs created larger available interfacial area that generates high damping efficiency and also better reinforcement (Koratkar et al., 2005).

In another study, Wang et al. (2004) investigated the dynamic mechanical properties of SWCNT buckypaper/epoxy nanocomposites. In their system, SWCNTs were dispersed in water-based suspension with the aid of surfactant and sonication. Through a filtration process, SWCNTs were fabricated into thin membranes called buckpapers to form networks of SWCNT ropes. A hot press molding process was used for curing to produce the final nanocomposites of multiple layer buckypapers with high SWCNT loading (up to 39 wt%). The dynamic mechanical analysis showed that the storage modulus increased 429 % and improved damping properties.

Suhr et al. (2006) studied the effect of temperature on interfacial friction damping in SWCNT/polycarbonate composites. They showed that interfacial slip at the tube-polymer interfaces could be activated at relatively low dynamic strain levels (~0.35%) by raising temperature. They reported that loss modulus increased ~85% when the temperature increased from 30 °C to 90 °C.

In another study, Auad et al. (2009) reported high damping capacity in rubbery SWCNT/epoxy nanocomposites at high temperatures. They showed that the increase in loss modulus was ~1400% at room temperature with 3 wt% oxidized SWCNTs. When the temperature increased up to 140°C, the loss modulus of the nanocomposites was almost constant while the epoxy matrix dropped to a negligible value.

1.6 APPLICATIONS

Nanocomposites present many benefits such as increased mechanical properties, high thermal and chemical stability, etc. However, the usage of nanocomposites in industry is not as high as expected, but the number of application areas has been growing in recent years. There are possible applications such as aerospace structural panels, sporting goods, and ultra-lightweight thin-walled space structures (Mallick 1993,Thostenson et al., 2005).

The automotive sector is one of the leading application areas for nanocomposite materials. Nanocomposites may be potentially utilized as mirror housings on various vehicle types, door handles, engine covers and intake manifolds and timing belt covers. Additionally, safety issues and environmental policies push manufacturers to find new materials that meet expectations. CNT-based nanocomposites are now available for different car models. For example Audi, Evobus and Diamler Chrysler automobiles have nano-coatings on their car's parts. Moreover, fuel cells, porous filters and energy conversion components are other popular applications. Additionally, lightweight bodies made of polymer-based nanocomposites are another significant area for the car industry.

Other application areas are microelectronics, dental applications, optical devices, composite membranes for gas separation applications, abrasion resistant coatings, beverage container applications, power tool housing, mobile phones, food packaging applications, etc.

1.7 CONCLUSION

In this review, an overview of the research in carbon nanotube/polymer composites and factors that will ultimately control their properties are explained. There have been many research groups that are interested in this area and thus different systems have been studied in this last decade. To summarize the main conclusions of these researches, the following points have been mentioned.

The properties of nanofiller/polymer composites strongly depend on the type (SWCNT, MWCNT, CNF), the amount of the nanotubes, the functionalization methods, dispersion state and alignment of nanofillers in the polymer matrix and the interfacial adhesion between the nanotube and the polymer matrix. Functionalization of nanofillers helps to improve dispersion and modify the interfacial properties that may improve the nanocomposite properties, especially mechanical properties. Evaluation of nanofillers dispersion in polymers and solvents is another challenging problem because it involves a range of length scales and requires multiple test methods. Nanofillers have also clearly demonstrated their capability in mechanical properties and conductive polymers.

In this work, carbon nanofibers will be modified with covalent functionalization and the degree of functionalization will be evaluated in the next chapter. Chapter 3 will include the evaluation of the dispersion quality of carbon nanofillers in epoxy system. Fourth chapter will be about the dispersion induced by the phase separation in the presence of monofunctional POSS molecules. Chapter 5 will cover the effect of incorporation of functionalized carbon nanofillers on the interphase of epoxy matrix. Finally, fifth chapter will include damping characteristics of elastomeric epoxy nanocomposites at elevated temperatures.

Research Objectives

The overall goal of this dissertation is to evaluate the achievability and advantages of carbon nanotubes and carbon nanofibers for polymer nanocomposites. By so doing, nanoreinforced epoxy based composites were prepared and enhanced properties enabling new properties were evaluated.

Our approach to this complex problem consists of two basic stages. First nanotubes were modified to achieve the desired compatibility in the target polymer matrix. During this task we developed and optimized the nanocomposite preparation to ensure adequate dispersion of the nanofillers; dispersion was characterized based on rheological and morphological properties. Second, we evaluated the effects of surface treatments and chemical modifications on the final properties of polymer nanocomposites such as mechanical, thermal and damping properties. Different amounts of the selected nanofillers were used.

This work will broaden and integrate the knowledge of the behavior of CNT epoxy nanocomposites through the development of synthesis-structure-properties relationships. The following section highlights the objectives of this research:

Objective 1: To obtain a basic understanding and comprehension of the various covalent functionalization methods of carbon nanotubes (i.e. oxidation, esterification, POSS) and analyze the effectiveness of the functionalization procedure.

Objective 2: To control and evaluate the quality of dispersion of nanotubes epoxy suspensions.

Objective 3: To evaluate whether phase separation process helps to improve the dispersion quality of SWCNTs in the epoxy/diamine systems.

Objective 4: To study the effect of interphase on the thermo-mechanical properties of nanotube epoxy nanocomposites

Objective 5: To understand the correlation between the novel nanostructures, the morphology and the thermal, mechanical and damping properties in the final nanocomposites.

REFERENCES

1. Ajayan P.M., Schadler L.S., Giannaris C., Rubio A., "Single-Walled Carbon Nanotube-Polymer Composites: Strength and Weakness", Adv Matter, 12, 10, 2000

2. Allaoui A., Bai S., Cheng HM, Bai JB., "Mechanical and electrical properties of a MWNT/Epoxy composite", Compos Science and Technology, 62;1993-1998, 2003

3. Auad M.L, Mosiewicki M.A., Uzunpinar C., Williams R.J.J., "Single-wall carbon nanotubes/epoxy elastomers exhibiting high damping capacity in an extended temperature range", Composites Science and Technology, 69, 1088–1092, 2009

4. B. Vigolo, V. Mamane, F. Valsaque, T.N. Ha Le, J. Thabit, J. Ghanbaja, L. Aranda, Y. Fort, E. McRae., "Evidence of sidewall covalent functionalization of single-walled carbon nanotubes and its advantages for composite processing", Carbon 47, 411-419, 2009

5. Balasubramanian, K. and Burghard, M., "Chemically Functionalized Carbon Nanotubes", *Small* 1 (2), 180-192, 2005

6. Bechinger C., Rudhart D., Leiderer P., Roth R., Dietrich S., "Understanding Depletion Forces beyond Entropy", Physical Review Letters, 83, 3960-3963, 1999

7. Brian P. Grady, "Recent Developments Concerning the Dispersion of Carbon Nanotubes in Polymers", Macromol. Rapid Commun. 31, 247-257, 2010

8. C. Velasco-Santos, A.L. Martinez-Hernandez, F. T Fisher, R. Ruoff, V.M. Castano, "Improvement of Thermal and Mechanical Properties of Carbon Nanotube Composites through Chemical Functionalization", Chem. Mater. 15, 4470, 2003

9. Chen G.X, Shimizu H., "Multiwalled carbon nanotubes grafted with polyhedral oligomeric silsesquioxane and its dispersion in poly(l-lactide) matrix", Polymer 49, 943-951, 2008

10. Ci LJ, Bai JC., "The reinforcement role of carbon nanotubes in epoxy composites with different matrix stiffnes", Composites Science and Technology, 66, 599-603, 2006

11. De Jong, K.P., "Carbon nanofibers: catalytic synthesis and applications", Catalysis Reviews, Vol. 42, No. 4, pp.308–311, 2000

12. Du F.M., R.C. Scogna, W. Zhou, S. Brand, J.E. Fischer, K.I. Winey, "Nanotube networks in polymer nanocomposites: rheology and electrical conductivity", Macromolecules, 37, 9048-9055, 2004

13. Dyke A.C, Tour M.J., "Covalent Functionalization of Single-Walled Carbon Nanotubes for Materials Applications", J. Physc. Chem. A, 108, 51, 2004

14. Elicabe G.E, Larrondo H.A., Williams R.J.J., "Polymerization-induced phase separation- A maximum in the intensity of scattered-light associated with a nucleation-growth mechanism", Macromolecules, 30, 6550-6555, 1997

15. F.H. Gojny, K. Schulte, "Carbon nanotube-reinforced epoxy-composites: enhanced stiffness and fracture toughness at low nanotube content", Composites Science and Technology, 64, 2303-2308, 2004

16. Fidelus J.D., Wiesel E., Gojyn F.H., Schulte K., Wagner H.D., "Thermo-mechanical properties of randomly oriented carbon/epoxy nanocomposites", Compos Part A 336, 1555, 61, 2005

17. Finegan I.C., Tibbetts G.G., "Electrical conductivity of vapor-grown carbon fiber/thermoplastic composites", J Mater Res, 16(6), 1668–74, 2001

18. Gary G. Tibbetts, Max L. Lake, Karla L. Strong, Brian P. Rice, "A review of the fabrication and properties of vapor-grown carbon nanofiber/polymer composites", Composites Science and Technology 67, 1709–1718, 2007

19. Geng Y., Liu M.Y., Li J., Shi X.M., Kim J.K., "Effects of surfactant treatment on mechanical and electrical properties of CNT/epoxy nanocomposites", Composites: Part A 39, 1876-1883, 2008

20. Georgiakilas V., Kordatos K., Prato M., Guldi D.M., Holzinger M., Hirsch A., "Organic functionalization of carbon nanotubes", J Am. Chem. Soc. 124,760-761, 2002

21. Gong X, Liu J. ,Baskaran S., Voise R.D., Young J.S., "Surfactant assisted processing of carbon nanotube/polymer composites", Chem. Mater., Vol 12, 4, 2000

22. Guo P., Chen X., Gao X., Song H., Shen H., "Fabrication and mechanical properties of well-dispersed multiwalled carbon nanotubes/epoxy composites", Composites Science and Technology, 67, 3331-3337, 2007

23. Guzman R. de Villoria, Miravete A., "Mechanical model to evaluate the effect of the dispersion in nanocomposites", Acta Materialia, 55, 3025-3031, 2007

24. Haddon R.C., Sippel J., Rinzler A.G., Papadimitrakopoulos F., "Purification and separation of carbon nanotubes", MRS Bulletin 29, 252, 2004

25. Haggenmueller R., Zhou W., Fischer J.E., Winey K. I., "Production and characterization of polymer nanocomposites with highly aligned single-walled carbon nanotubes", J. Nanosci. Nanotechnol, 3, 105-110, 2003

26. Hammel, E., Tang, X., Trampert, M., Schmitt, T., Mauthner, K., Eder, A. and Pötschke, P., "Carbon nanofibers for composite applications", Carbon, Vol. 42, No. 5–6, pp.1153–1158, 2004

27. Huang, J.-M., Huang, H.-J., Wang, Y.-X., Chen, W.-Y. and Chang, F.-C., "Preparation and characterization of epoxy/polyhedral oligomeric silsesquioxane hybrid nanocomposites". Journal of Polymer Science Part B: Polymer Physics, 47: 1927–1934., 2009

28. I. K. Jones, Y. X. Zhou, S. Jeelani, J. M. Mabry, "Effect of polyhedral-oligomeric-silsesquioxanes on thermal and mechanical behavior of SC-15 epoxy", eXPRESS Polymer Letters Vol.2, No.7, 494–501, 2008

29. J.Zhu, J. Kim, H. Peng, J.L Margrave, V.N. Khabashesku, E. Barrera, "Improving the dispersion and integration of single-walled carbon nanotubes in epoxy composites through functionalization", Nanoletters Vol. 3, No. 8, 1107-1113, 2003

30. Jiang, L. Q., Gao L., Sun J., "Production of aqueous colloidal dispersions of carbon nanotubes", J. Colloid. Interface. Sci., 260, 89, 2003

31. K. Yano, A. Usuki, A. Okada, T. Kuraychi, O. Kamigaito, "Synthesis and Properties of Polyimide-Clay Hybrid", J. Polym. Sci., Part A: Polymer Chem., 33, 1047, 1995

32. Koratkar N.A., Suhr J., Joshi A., Kane R.S., Schadler L.S., Ajayan P.M., Bartolucci S., "Characterizing energy dissipation in single-walled carbon nanotube composites", Phys., Lett. , 87, 6, 063102, 2005

33. Krishman A., Dujardin E., Ebbesen T.W., Yianilos P.N., Treacy M.M.J., "Young's modulus of single-walled nanotubes", Phys Rev B, 58:4013, 1998

34. L. S. Schadler, S. C. Giannaris, and P. M. Ajayan, "Load transfer in carbon nanotube epoxy composites", App Physc Letter Vol., 73, 26, 1998

35. L. Sun, G.L Warren, J.Y O'Reilly, W.N. Everett, S.M. Lee, D. Davis, D. Lagoudas, H.J Sue, "Mechanical properties of surface-functionalized epoxy/SWCNT nanocomposites", Carbon, 46, 320-328, 2008

36. Lafdi K., Matzek M., "Carbon nanofibers as a nano-reinforcement for polymeric nanocomposites", In: 48th international SAMPE symposium proceedings, Long Beach, USA, 2003

37. Lourie O, Wagner H.D., "Transmission electron microscopy observations of fracture of single-wall carbon nanotubes under axial tension", Appl. Physc. Lett., 73, 3527, 1998

38. M. Moniruzzaman, K.I. Winey, "Polymer nanocomposites containing carbon nanotubes", Macromolecules, 39, 5194-5205, 2006

39. M.R. Loos, L.A.F. Coelho, S.H. Pezzin, S.C Amico, "The effect of acetone addition on the properties of epoxy", Material Research, Vol 11, 2, 347-352, 2008

40. Mallick, P. K. “Fiber-reinforced composites”, Marcel Dekker, New York, 1993

41. Messersmith P.B., Giannelis E.P. “Synthesis and characterization of layered silicate-epoxy nanocomposites”, Chem. Mater. 6, 1719, 1994

42. Moore V., Strano M. S., Haroz E. H., Hauge R. H., Smalley R. E., Schmidt J. Talmon, Y., "Individually suspended single-walled carbon nanotubes in various surfactants”, Nano. Lett., 3, 1379, 2003

43. O’Connell M. J., Boul P., Ericson L. M., Huffman C., Wang Y.H., Haroz E., Kuper C., Tour J., Ausman K., Smalley R. E., “Reversible water-solubilization of single-walled carbon nanotubes by polymer wrapping”, Chem. Phys. Lett., 342, 265, 2001

44. Ounaies Z., Park C., Wise K.E., Siochi E.J., Harrison J.S., “Electrical properties of single wall carbon nanotube reinforced polyimide composites”, Composites Science Technology, 63:1637-46, 2003

45. Potschke P., Fornes T.G.D., Paul D.R., “Rheological behavior of multiwall carbon nanotube/ polycarbonate composites”, Polymer; 43, 3247-55, 2002

46. Rajoria H., Jalili N., “Passive Vibration Damping Enhancement Using Carbon Nanotube-Epoxy Reinforced Composites”, Composites Sciences and Technology, 65, 2079-2093, 2005

47. Ray H. Baughman, Anvar A. Zakhidov, Walt A. de Heer, “Carbon nanotubes-the route toward applications” Science, Vol. 297, 2002

48. Riggs J. E., Guo Z., Caroll D.L., Sun Y.P., ”Strong luminescence of solubilized carbon nanotubes”, J. Am. Chem. Soc, 122, 5879, 2000

49. S. Iijima, “Helical microtubules of graphitic carbon”, Nature, 354, 56-8, 1991

50. Sasan Nouranian, Hossein Toghiani, Thomas E. Lacy, Charles U. Pittman, Jr and Janice Dubien, “Dynamic mechanical analysis and optimization of vapor-grown carbon nanofiber/vinyl ester nanocomposites using design of experiments”, Journal of Composite Materials doi: 10.1177/0021998310385027, 2010

51. Shaffer M. S. P., Fan X., Windle A. H.,” Dispersion and packing of carbon nanotubes”, Carbon, 36, 1603, 1998

52. Shaffer MSP, Fan X, Windle AH. Macromolecules; 32:6864-6,1999

53. Suhr J., Zhang W., Ajayan P.M., Koratkar N.A., “Temperature activated interfacial friction damping in carbon nanotube polymer composites”, Nano Lett., 6 (2), pp 219–223, 2006

54. T. Guo, P. Nikolaev, A. Thess, D.T. Colbert and R.E. Smalley, “Catalytic growth of single-walled manotubes by laser vaporization”, Chemical Physics Letters, Volume 243, Issues 1-2,

49-54, 1995

55. Tan Y, D.E Resasco, “Dispersion of single-walled carbon nanotubes of narrow diameter distribution”, J.Phys. Chem. B, 109, 14454-14460, 109, 2005

56. Tan, S. H.; Goak, J. C., Lee, N.; Kim, J. Y.; Hong, S. C., ”Functionalization of multi-walled carbon nanotubes with Poly(2-ethyl-2-oxazoline)” Macromol. Symp., 249-250, 270, 2007

57. Thostenson ET, Ren Z, Chou TW, “Advances in the science and technology of carbon nanotubes and their composites: a review”, Composite science and technology 61 (13), 1899-1912, 2001

58. Vaisman l. Wagner HD, Marom G., “Dispersions of surface modified carbon nanotubes in water-soluble and –insoluble polymers”, Adv Funct Mater; 16(3), 357-63, 2006

59. Vaisman l. Wagner HD, Marom G., “The role of surfactants in dispersion of carbon nanotubes”, Adv. Colloid Interface Sci, 128-130, 37-46, 2006

60. Vigolo B., Mamane V.,Valsaque F.,Le. Ha T.N, Thabit J, Ghanbaja J., Aranda L, Fort Y. McRae E., “Evidence of sidewall covalent functionalization of single-walled carbon nanotubes and its advantages for composite processing” Carbon 47, 411-419, 2009

61. Vigolo, B., Poulin, P., Lucas, M., Launois, P., Bernier, P., “Improved structure and properties of single-wall carbon nanotube spun fibers”, Appl. Phys. Lett., 81, 1210, 2002

62. Wang A., Liang Z., Wang B., Zhang C., Kramer L., Processing and property investigation of single-walled carbon nanotube (SWNT) buckypaper/epoxy resin matrix nanocomposites”, Composites: Part A 35, 1225-1232, 2004

63. Whitsitt E.A., Barron A.R., “Silica coated single walled nanotubes”, NanoLett, 3(6):775-8,2003

64. Xu J., Donahoe J.P., Pittman Jr C.U., “Preparation, electrical, and mechanical properties of vapor grown carbon fiber (VGCF)/vinyl ester composites”, Composites: Part A; 35, 693–701, 2004

65. Y.S. Song, J.R. Youn, “Influence of dispersion states of carbon nanotubes on physical properties of epoxy nanocomposites”, Carbon 43, 1378-1385, 2005

66. Yacaman M.J., Yoshida M.M., Rendon L., Santiesteban J.G., “Catalytic growth of carbon microtubules with fullerene structure”, Appl. Phys. Lett. 62, 202–204, 1993

67. Yan Y. H., Cui J., Chan-Park M. B., Wang X., Wu Q. Y., “Systematic studies of covalent functionalization of carbon nanotubes via argon plasma-assisted UV grafting”, Nanotechnology 18, 115712, 2007

68. Zeng J, Saltysiak B, Johnson WS, Schiraldi DA, Kumar S., “Processing and properties of poly (methyl methacrylate)/carbon nanofiber composites”, Composites: Part B, 35, 173–8, 2004

69. Zhu J., Kim J.D., Peng H., Margrave J.L., Khabashesku V.N., Barrera E.V., “Improving the Dispersion and Integration of Single-Walled Carbon Nanotubes in Epoxy Composites through Functionalization”, Nano Lett 3, 1107, 2003

70. Zucchi I.A., Galante M.J., Williams R.J.J., Franchini E., Galy J., Gerard J.F., “Monofunctional epoxy-POSS dispersed in epoxy−amine networks: Effect of a prereaction on the morphology and crystallinity of POSS domains”, Macromolecules 40, 1274-1282, 2007

71. Zucchi I.A., Hoppe C.E., Galante M.J., Williams R.J.J., Lopez-Quintela M.A., Matejka L., Slouf M., Plestil J., “Self-Assembly of Gold Nanoparticles as Colloidal Crystals Induced by Polymerization of Amphiphilic Monomers”, Macromolecules 41, 4895-4903, 2008

CHAPTER 2

FUNCTIONALIZATION OF CARBON NANOTUBES AND CARBON NANOFIBERS

2.1 INTRODUCTION

The performance of carbon nanofiller/polymer nanocomposites depends on the dispersion of fillers in the polymer and the interfacial interaction between the matrix and the nano particles. The type, aspect ratio and the physical and chemical structure of these nano particles affect the interfacial interaction between the matrix and the nano particles. In this study, single and multi-wall carbon nanotubes and carbon nanofibers were used as the reinforcing nanoparticles.

Carbon nanotubes have chemically stable carbon atoms with sp^2 bonds. Therefore, CNTs are inert and cannot provide a strong chemical interaction with the matrix. Instead of a strong chemical interaction carbon nanotubes build physical interactions through Van der Waals forces (Avouris et al., 1998, Pogorelov et al. 2008). These interactions are unable to provide a sufficient load transfer from the matrix to CNTs that usually reduce the performance of nanocomposites. Therefore, the chemical modification of carbon nanotubes has become a new developing area in the research of nanotubes-based materials (Hirsch et al., 2002).

There have been several research groups that have reported successful functionalization reactions for carbon nanotubes. These reactions may roughly be divided into two categories: covalent functionalization and non-covalent functionalization.

Non-covalent functionalization includes surfactant adsorption (i.e; physical adsorption of molecules onto the wall of the tubes), polymer wrapping (i.e; through Van der Waals force), and endohedral method (i.e; capillary effect) (Balasubramanian et al., 2005, Tasis et al., 2006). This technique is a widely used modification because this physical process leaves the nanotube structure undamaged and with the same intrinsic properties. The non-covalent (physical) treatments, such as the application of surfactants and polymer coating followed by surfactant treatment, do not disturb the inherent π- bonds of CNTs and thus the electrical properties. This approach is based on the interactions of the hydrophobic part of the adsorbed surfactant molecule with the nanotube sidewalls through Van der Waals, π-π, CH-π, and other interactions, while the hydrophilic part of the molecule provides aqueous solubility. This physical adsorption of the surfactant on the CNT surface prevents the formation of aggregates. In the last few years, the non-covalent functionalization of CNTs with surfactants and polymers has been widely used in the dispersion of high weight fraction of CNTs in both aqueous and organic solutions (Vaisman et al. 2006, Moore et al. 2003).

Covalent functionalization relies on the transformation of sp^2 to sp^3 hybridized of carbon atoms, which is associated with a change from a trigonal-planar local bonding geometry to a tetrahedral geometry (Moniruzzaman et al.2006). This reaction is more favorable at the nanotube caps due

to the two dimensional curvature. Similarly, the curvature on the sidewall of nanotubes makes them more reactive than a planar graphene sheet.

Covalent functionalization of nanotubes can improve nanotube dispersion in solvents and polymers. For example, the pristine SWCNT is completely insoluble in chloroform whereas covalently functionalized SWCNTs with pyrrolidine show a solubility of 50 mg/mL in chloroform, even without aid of sonication (Georgakilas et al., 2002).

Covalent functionalization of nanotubes also leads to the creation of novel composite materials and elastomers. For instance, the interfacial adhesion could be modified through covalent interactions between the functional group on the nanotube and the polymer matrix to maximize load transfer. A notable drawback of covalent functionalization is the disruption of the extended conjugation in nanotubes. This may have limited impact on thermal and mechanical properties. Additionally, the electrical properties are affected by covalent functionalization since each covalent functionalization site scatters electrons (Dyke et al., 2004).

There are basically two types of covalent functionalization. It can be occurred at the sidewall or at the defects of CNTs. Sidewall covalent functionalization is associated with a change of hybridization from sp^2 to sp^3 and a simultaneous loss of π-conjugation system on graphene layer. Highly chemical reactive atoms such as fluorine can activate this change of hybridization. Mickelson et al. (1998) showed that the fluorination of purified SWCNTs occurs at temperatures

up to 325°C and Kelly et al. (1999) showed that the fluorinated CNTs have C-F bonds that are weaker than those in alky fluorides and thus providing substitution sites for additional functionalization. Successful replacements of the fluorine atoms by amino, alkyl and hydroxyl groups have been achieved (Touhara et al., 2002).

Defect functionalization can be defined as the transformation of defects site on the CNTs open ends and/or holes in the sidewalls. These defects can be created on the CNTs by processing with strong acids such nitric acid (HNO_3), sulfuric acid (H_2SO_4) or mixtures of them, or strong oxidants such potassium manganite (VII) ($KMnO_4$), ozone or reactive plasma (Esumi et al., 1996).

Bonding with carboxylic acid (-COOH) or hydroxyl (-OH) groups can terminate the defects on CNTs created by oxidants. The carboxylic acid groups can be used to attach thionyl chloride ($SOCl_2$), long chains amines (—NH) or ester groups (—COOR). Furthermore, carboxylic acid groups can undergo esterification reactions with epoxy. Some cross-linking may also take place because the surface and ends of nanotubes are expected to carry more than one carboxylic acid group (Sun et al., 2002).

Carboxylic acid groups can also change the solubility characteristic of CNTs. They can change the hydrophobic nature of the CNTs to hydrophilic one due to attachment of polar groups. Thus, oxidized CNTs are soluble in many organic solvents such as water, chloroform, methanol,

tetrohydrofuran (THF) and dimethylformamide (DMF) (Rai et al., 2007). For instance, oxidized nanotubes are expected to form well-dispersed electrostatically stabilized colloids in water and ethanol (Shaffer et al., 1998). Moreover, the defect functionalization of CNTs creates an opportunity to build strong interfacial bonds with many polymers. This increases the compatibility of nanotubes with the matrix for high-quality polymeric carbon nanocomposite materials.

In this chapter, covalent functionalization technique was used to attach organic functional groups onto the structure of carbon nanotubes and carbon nanofibers. Acid groups (-COOH), ester groups (-PGE) and epoxy groups (-EPON) were attached on defect sites in order to increase the compatibility with epoxy resins. In addition, glycidyloxypropyl-heptaisobutyl polyhedral oligomeric silsesquioxane (iBu-Gly-POSS) molecules were attached on CNTs defects sides. Furthermore, surfactant adsorption was also used in order to distinguish the effects of covalent and non-covalent functionalization methods.

2.2 EXPERIMENTAL

2.2.1 Materials

MWCNTs and SWCNTs used in this research were purchased from Shenzhen Nanotech Port Co. Ltd., China). The MWCNTs' diameter range was 40-60 nm, the length range was 5-15 μm, and purity was ≥ 95%. The SWCNTs diameter range was < 2 nm, the length range was 5-15 μm and purity was ≥ 90%. The CNFs (Pyrograf III Carbon Fiber, PS Grade) were provided from Pyrograf Products,Inc. Their diameter was ~ 0.2 μm, apparent density was 2 to 20 lb/ft. The purity of the CNFs was > 98wt%.

Two epoxy monomers were selected for this study, the monoepoxide phenyl glycidil ether (PGE, Aldrich) and the diepoxide based on diglycidylether of bisphenol A (DGEBA, EPON 828, Miller-Stephenson) (Figure 2.1 a, b). Triphenylphosphine (TPP, Aldrich) was used as a catalyst of the esterification reactions to attach PGE and DGEBA to the surface of the acidified nanoparticles and tetrahydrofuran (THF) was used as solvent. The POSS structure that was used in this study is shown below (Figure 2.1 c). POSS is a crystalline powder with a molar mass of 931.6 g/mol.

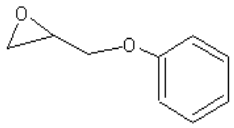

(a)

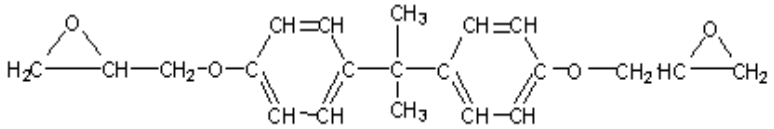

(b)

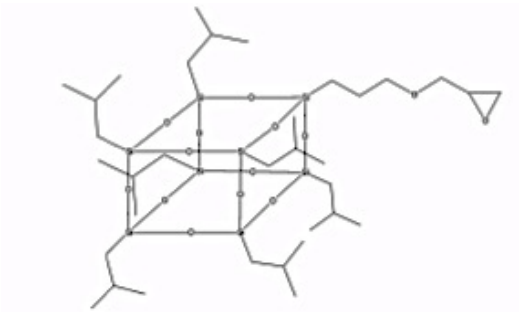

(c)

Figure 2.1. Structure of (a) PGE, (b) Epon and (c) Glycidyloxypropyl-heptaisobutyl Polyhedral Oligomeric Silsesquioxane (iBu-Gly-POSS)

2.1.2 Sample Preparation

Oxidation Procedure

1 gram of nanofiller was dispersed in 250 ml of concentrated 3:1 sulfuric acid and nitric acid (H_2SO_4 (98%) / HNO_3 (70%)). Different sonication and stirring conditions were used to achieve moderate oxidation and maintain a high aspect ratio. After the acid treatment, hydrochloric acid (HCl) was added to the acid mixture to facilitate the terminations of opened ends of the CNTs and CNFs with carboxylic acid groups (-COOH), rather than carboxylate ($-COO^-$) (Chen et al., 1998). The fillers were exhaustively washed with deionized water until constant pH. The acid-treated nanoparticles, denoted SWCNT-COOH, MWCNT-COOH and CNF-COOH were dried overnight in a vacuum oven at 90°C.

Esterification Procedure

After the acid treatment, the nanofiller were esterified following the procedure below. The reactions are illustrated in Figure 2.2. Triphenylphosphine (TPP) (0.2 mole per mole of epoxy groups) was employed as a catalyst to attach functional groups PGE and DGEBA onto the acidified fillers. Oxidized nanotubes or nanofibers (1 g), PGE (molar ratio PGE/COOH = 3) and TPP were dispersed in 200 ml THF. The esterification reaction was refluxed in an oil bath heated to 90°C for 96 hours. After the treatment, the fillers were thoroughly washed with THF, centrifuged and dried in a vacuum oven at 90ºC for 24 hours. These esterified fillers were denoted as the PGE plus type of filler and DGEBA plus the type of filler respectively. The same procedure was applied to attach the POSS molecules onto the acidified CNTs.

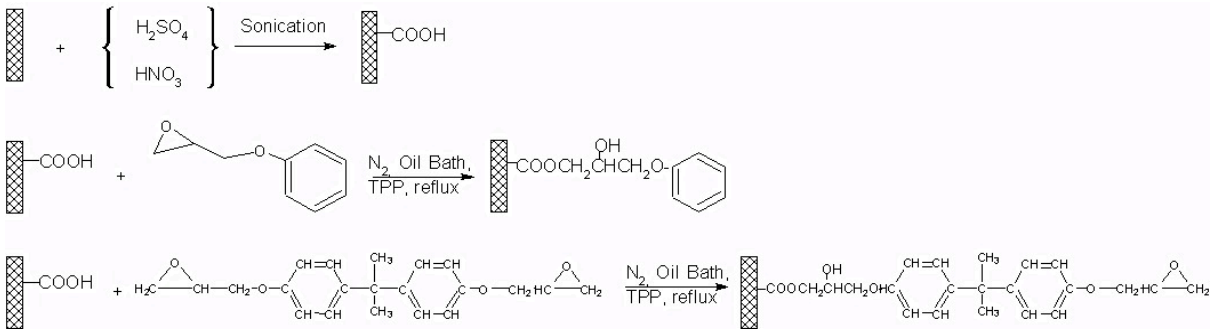

Figure 2.2. Schematic illustration of covalent functionalization of single, multi-wall carbon nanotubes and carbon nanofibers

2.1.3 Characterization

To verify that carbon nanotubes and carbon nanofibers were functionalized successfully, various techniques have been used such as thermal gravemetric analysis (TGA), Raman spectrum and Fourier transform infrared (FTIR).

Thermal gravimetric analysis (TGA Q500, TA Instruments) was employed to quantify the weight percentage (wt %) of the organic component grafted onto the nanofiller. A small sample (~10 mg) was heated from room temperature to 800°C at 10°C /min under nitrogen.

Raman spectroscopy was carried out using a Renishaw (Hoffman Estates, IL) InVia Raman Spectrometer with 514 nm laser. A Leica 50x N-Plan objective (NA 0.75) was used to image the samples and resulting laser spot size was 0.84 μm for the 517 nm laser. Samples for Raman spectroscopy were prepared by holding the dried nanotubes to microscope slides using double sided tape.

Attenuated total reflectance (ATR) infrared spectroscopy (ATR-FTIR, Nicolet 4700) was employed to assess the presence of the organic groups in functionalized SWCNT, MWCNT, and CNF.

2.3 RESULTS AND DISCUSSION

2.3.1 TGA Analysis

Thermal degradation results for pure and functionalized SWCNTs, MWCNTs, CNFs are shown in Figure 2.3, 2.4, 2.5, respectively. The amount of the functional groups attached on the nanotubes and nanofibers was calculated by using the weight loses during the heating process. Most of the functional groups are changeable or decompose upon heating in an inert media, whereas CNTs are stable up to high temperatures (1200 °C). Therefore, any weight loss before 800 °C can be used to determine the functionalization ratio of functionalized SWCNTs, MWCNTs and CNFs. In this study, the mass fraction of the organic groups eliminated at 600ºC was calculated.

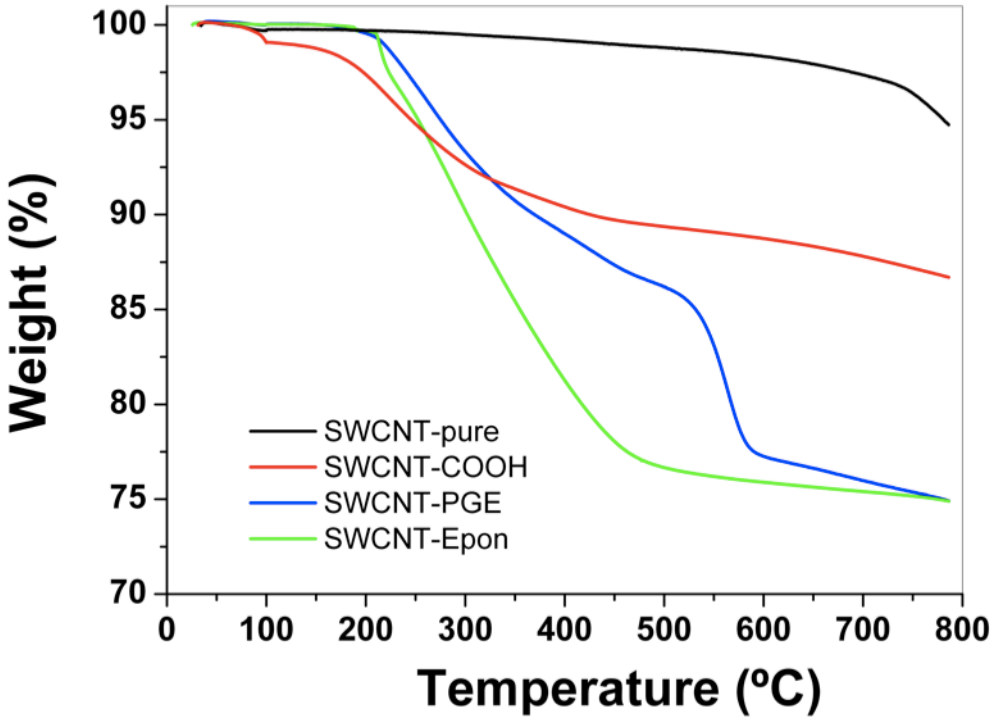

Figure 2.3. Thermal gravimetric analysis (TGA) of pure and functionalized SWCNTs

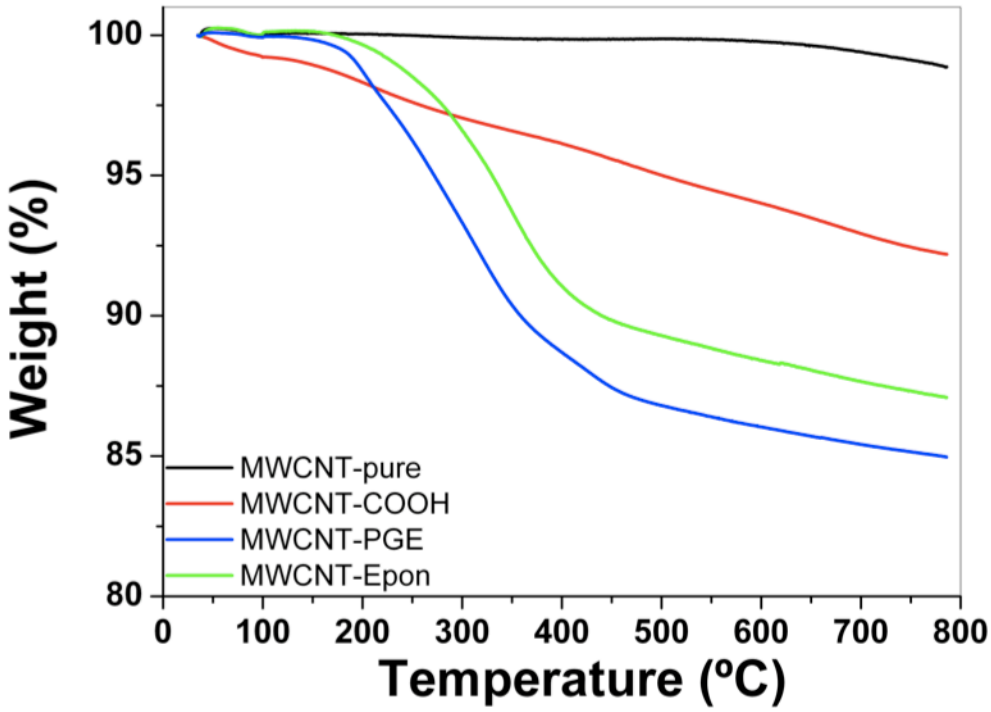

Figure 2.4. Thermal gravimetric analysis (TGA) of pure and functionalized MWCNTs

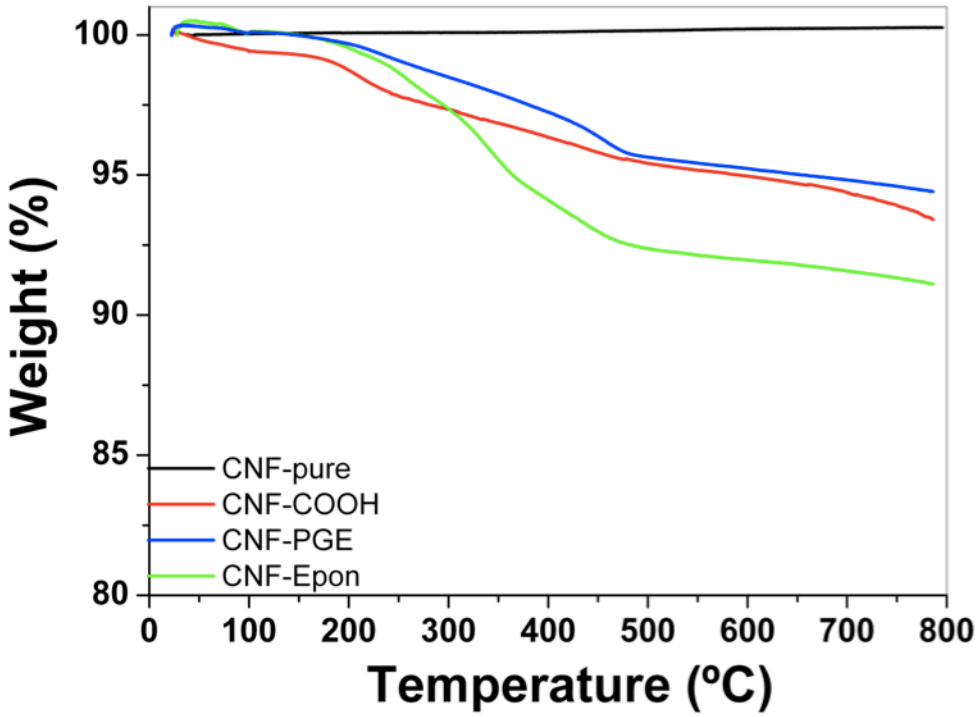

Figure 2.5. Thermal gravimetric analysis (TGA) of pure and functionalized CNFs

The small amounts of mass loss (<1wt %) of the unmodified SWCNT and MWCNT observed in TGA are attributed to the presence of small amounts of amorphous carbon and impurities. On the other hand, unmodified CNF did not show considerable mass loss.

Acidified SWCNTs showed a fast weight loss process ending at about 300ºC, followed by a slowly and continuous weight loss process in the whole temperature range. Most of grafted COOH groups in the SWCNT were lost at about 300ºC and this was followed by a degradation of CNT promoted by the previous acidification treatment. On the other hand, the curves for the acidified MWCNT and CNF show a continuous loss process in the analysed range of temperatures. The organic mass attached to the carbon surface increased after esterification with PGE and EPON, indicating that the reaction proceeded successfully. The amounts of organic groups (COOH, PGE and DGEBA) attached to the structure of the fillers are showed in Table 2.1.

Table 2.1. Amount of the functional groups grafted onto CNTs surface

Functional Groups / Fillers	COOH (%)	COOH-PGE (%)	COOH-EPON (%)	COOH-POSS (%)
SWCNT	8.6	21.1	22.7	14.25
MWCNT	4.9	13.7	15.5	-
CNF	4.7	4.8	8.4	-

2.3.2 Raman Analysis

Raman spectroscopy is a widely used tool for the characterization of various forms of carbon and in particular to observe the vibrational modes of the carbon nanotubes and their composites. There are different peak areas that can be used in Raman analysis. For instance, Radial breathing mode (RBM), which is around 180 cm^{-1}, can be used where all the carbon atoms are moving in-phase in the radial direction. The diameter distribution of the nanotubes in a particular SWCNT bundle can be found by RBM measurements (Graupner, 2007).

G-band is an intrinsic feature of carbon nanotubes that is closely related to vibrations in all sp^2 carbon materials. The most important aspect of this G-band is that it is useful to determine whether the nanotube is semiconducting or metallic. On the other D-band is related to the defects, which breaks the basic symmetry of the graphene sheet. The intensity of the D-band (D for disorder or defects) around 1350 cm^{-1} is known to increase through chemical functionalization. The ratio between the D band and G band (I_d/I_g) is also a good indicator of the quality of bulk samples. If these both bands have similar intensity, this indicates a high quantity of structural defects (Graupner, 2007).

In this study, the changes in D and G bands and the ratio between them were examined. Results are shown in Figure 2.6 and Table 2.2. Results showed that the intensity of the D-band increased after each covalent functionalization. However, the intensity of the D-band decreased after non-covalent functionalization. The reason for the increase in D-band after covalent functionalization was that more defects on the structure were produced after applied strong acids and longer

sonication times. The ratio between the D band and G band (I_d/I_g) also showed that SWCNTs with covalent functionalization had closer D band and G band intensity values. These values also support the theory that quantity of structural defects increased due to covalent functionalization.

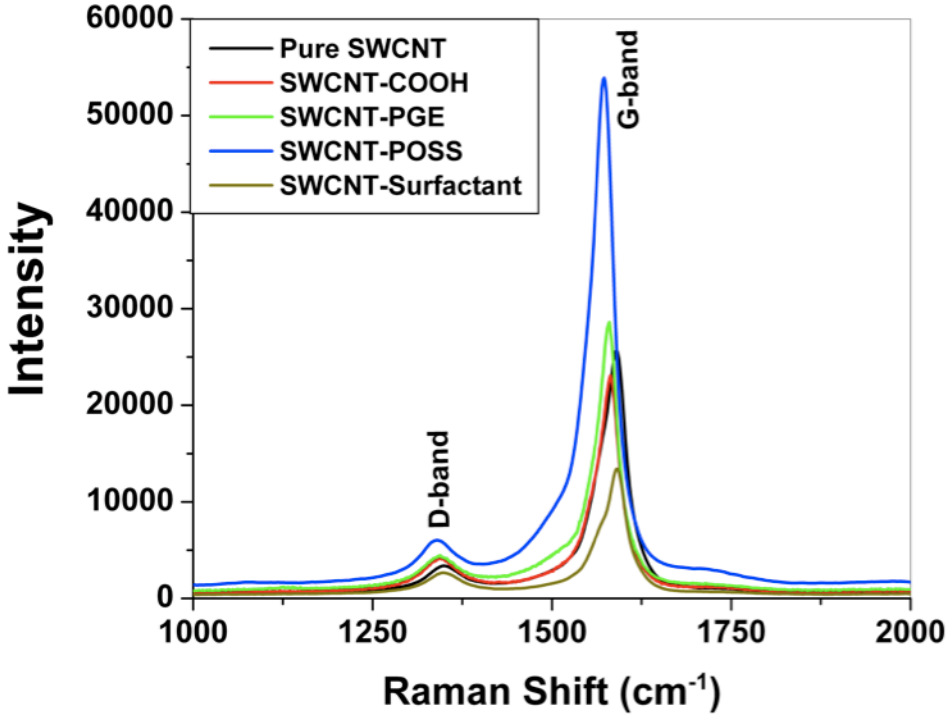

Figure 2.6. Raman (514-nm excitation) of pure and functionalized SWCNTs

Table 2.2. Raman Intensities at D-band and G-band and the ratio of I_D/I_G of pure and functionalized SWCNTs

	Pure SWCNT	SWCNT-COOH	SWCNT-PGE	SWCNT-Surfactant	SWCNT-POSS
G band	27628	23076	28600	13417	53669
D band	3378	4155	4465	2657	5668
I_D/I_G	0.13	0.18	0.15	0.20	0.10

2.3.3 ATR-FTIR Analysis

IR spectroscopy is useful in characterizing functional groups bound to SWCNTs. A variety of organic functional groups on the surface of SWNTs has been identified by IR, such as COOH(R), -CH2, -CH3, -NH2, -OH, etc. In this study, attenuated total reflectance-FTIR (ATR-FTIR) technique was used to corroborate the attachment of PGE to the surface of SWCNT. Figure 2.7 shows the FTIR spectra of pristine and PGE-modified SWCNTs. Peaks located at 2920, 2850, 1460, and 1375 cm^{-1} are characteristic C-H stretching and deformation frequencies. The band at 1734 cm^{-1} is characteristic of the carbonyl group (C=O) while the bands located in the region 1100–1300 cm^{-1} are characteristic of C−O stretching vibrations in esters. The peak at 917 cm^{-1} characteristics of epoxide rings disappeared completely. The absence of this band in the ATR-FTIR spectrum indicates that most of the epoxy groups of DGEBA were consumed during the functionalization reaction.

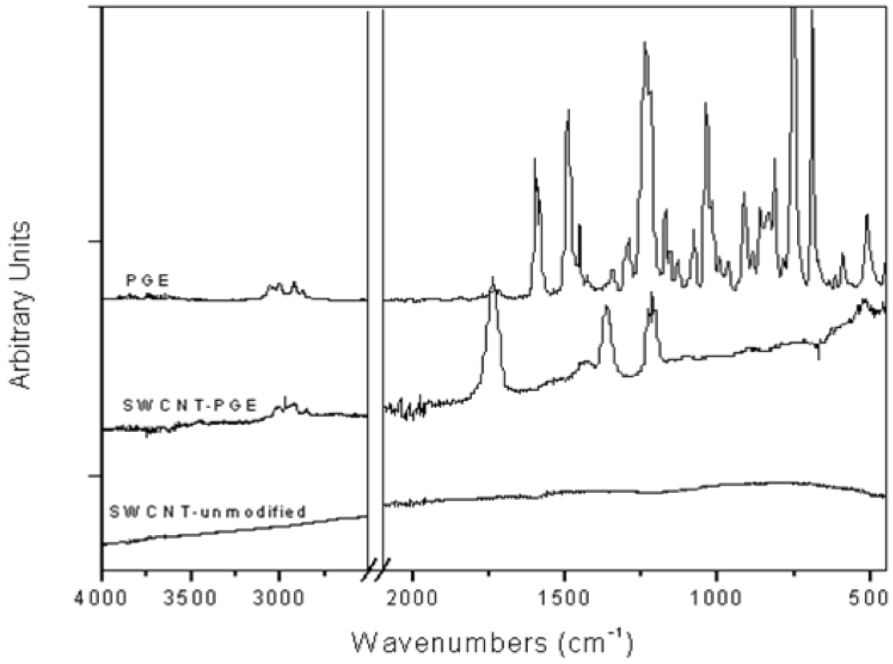

Figure 2.7. ATR-FTIR spectrum of PGE, unmodified SWCNT and SWCNT-PGE

The FTIR analysis of POSS attached single wall carbon nanotubes is shown in Figure 2.8. The FTIR spectrum also includes the untreated SWCNTs and POSS molecules for comparison. The band at 1100 cm^{-1} was assigned to the Si-O-Si stretching vibrations. This peak is a characteristic peak of POSS molecule. The existence of this band in the spectrum of POSS attached single wall carbon nanotubes confirms that POSS molecules were successfully attached onto the carbon nanotube surface.

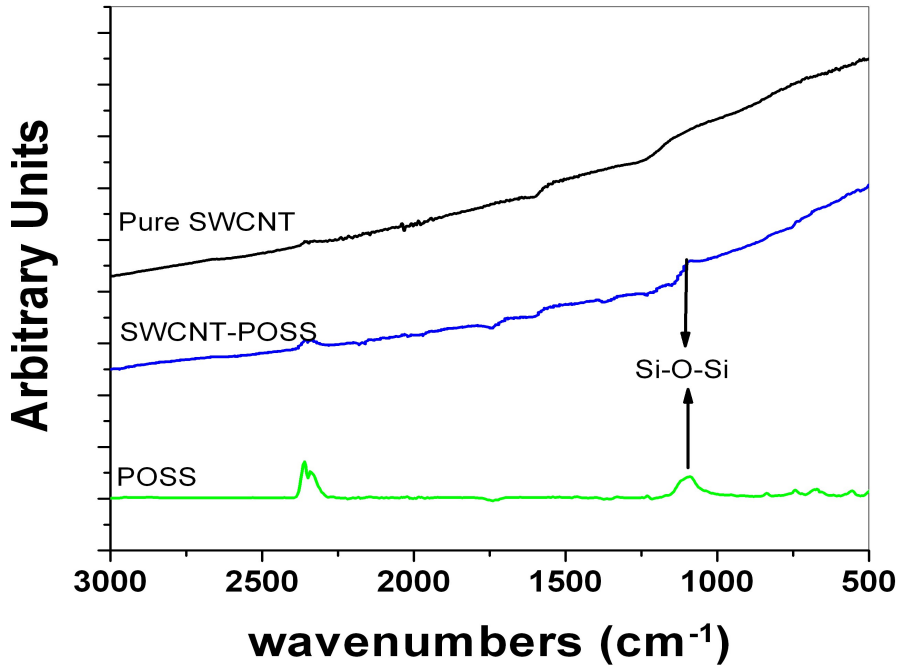

Figure 2.8. FTIR spectrum of POSS functionalized single wall carbon nanotubes

2.4 CONCLUSION

In this chapter defect functionalization of SWCNTs, MWCNTs and CNFs was used in order to attach organic functional groups. Acid groups, ester groups and epoxy groups were attached on CNTs defect sites in order to increase the compatibility with epoxy polymer. In addition, glycidyloxypropyl-heptaisobutyl polyhedral oligomeric silsesquioxane (iBu-Gly-POSS) molecules were attached on CNTs defects sides, which have been studied first time by our group. Furthermore, surfactant adsorption was also used in order to distinguish the effects of covalent and non-covalent functionalization methods. The effectiveness of these functionalization methods was discussed through thermal gravimetric analysis (TGA), Raman spectroscopy and FTIR analysis.

The characterization results showed that functional groups were successfully attached onto the surfaces of nanofillers. The improvement in dispersion of these functionalized nanofillers and the performance of their composites will be discussed in chapter 3.

REFERENCES

1. Alexander I. Zhbanov, Evgeny G. Pogorelov, Yia-Chung Chang, "Van der Waals interaction between two crossed carbon nanotubes", eprint arXiv:0811.0221, 2008

2. Balasubramanian K, Burghard M., "Chemically functionalized carbon nanotubes, Small", 1:180-92, 2005

3. Dyke C.A, James M. Tour, "Covalent functionalization of Single-walled carbon nanotubes for materials applications", J. Phys. Chem. A. Vol, 108 No. 51, 2004

4. Esumi K, Ishigami M, Nakajima A., "Chemical treatment of carbon nanotubes", Carbon 34, 279-81, 1996

5. Georgiakilas V., Kordatos K, Prato M., Guldi D.M., Holzinger M., Hirsch A., "Organic functionalization of carbon nanotubes", J Am. Chem. Soc. 124, 760-761, 2002

6. Hirsch A., "Functionalization of single walled carbon nanotubes", Angew Chem Int Ed 41, 1853-9, 2002

7. J. Chen, M.A. Hamon, H. Hu, Y. Chen, A.M. Rao and P.C. Eklund, "Solution properties of single-walled carbon nanotubes", Science 282, 95, 1998

8. Kelly KF, Chiang IW, Mickelson ET, "Insight into the mechanism of sidewall functionalization of single-wall nanotubes, an STM study", Chem Phys Lett, 313; 445-50, 1999

9. Linda Vaisman, H. Daniel Wagner, Gad Marom, "The role of surfactants in dispersion of carbon nanotubes", Advances in Colloid and Interface Science, 128-130, 37-46, 2006

10. Mickelson ET, Huffman CB, Rinzler AG, "Fluorination of single wall carbon nanotubes", Chem Phys Lett. 296, 188-94, 1998

11. Mohammad Moniruzzaman, Karen I Winey, "Polymer nanocomposites containing carbon nanotubes", Macromolecules, Vol. 39, No. 16, 2006

12. Moore, V. C.; Strano, M. S.; Haroz, E. H.; Hauge, R. H.; Smalley, R. E.; Schmidt, J.; Talmon, Y. "Individually Suspended Single-Walled Carbon Nanotubes in Various Surfactants", Nano. Lett., 3, 1379, 2003

13. R. Graupner, “Raman spectroscopy of covalently functionalized single-wall carbon nanotubes”, J.Raman Spectrosc. 38, 673-683, 2007

14. Rai P.K, Nicholas A, Parra-Vasquez G., Chattopadhyay J., Pinnick R.A., Liang F., Sadana A.K.,Hauge R.H., Billups W.E., Pasquali M., J. Nanosci. Nanotechnol., Vol 7, No.10, 2007

15. Shaffer M. S. P., Fan X., Windle A. H., “Dispersion and packing of carbon nanotube”, Carbon, 36, 1603, 1998

16. Sun Y, Fu K., LIN Y., Huang W., “Functionalized carbon nanotubes: Properties and applications”, Acc. Chem. Res. 35, 1096-1104, 2002

17. Tasis D, Tagmatarchis N, Bianco A, Prato M., “Chemistry of carbon nanotubes”, Chem Rev, 106:1105-36, 2006

18. Tobias Hertel, Robert E. Walkup, Phaedon Avouris, “Deformation of carbon nanotubes by surface van der Waals forces”, Physical Review B, 58, 20, 1998

19. Touhara H, Inahara J, Mizuno T, “Fluorination of cup-stacked carbon nanotubes, structure and properties”, Fluorine Chem, 114,181-8, 2002

CHAPTER 3

EVALUATING THE QUALITY OF NANOTUBE DISPERSION IN EPOXY SUSPENSIONS

3.1 INTRODUCTION

Strong Van der Waals attractions among carbon nanotubes, due to their nanometric size, create agglomerations and decrease the quality of dispersion. This problem must be overcome in order to utilize the unique properties of the nanotubes and develop high performance CNT-based materials. Therefore, there have been many studies in developing approaches for effective and reproducible dispersions of carbon nanotubes (Ajayan et al., 2000, Cui et al., 2003, Cheng et al. 2006). For instance, Advani et al. studied the storage modulus (G'), loss modulus (G''), and complex and steady shear viscosities for MWNT/epoxy suspensions of different dispersion states, aspect ratios, concentrations, network structures, and orientation states. They reported that a good MWNT dispersion, high aspect ratio, and high concentrations aided in the formation of a stronger interacting MWNT network as indicated by higher G' and complex viscosity values (Advani et al., 2007).

There are two main approaches for dispersing carbon nanotubes: mechanical methods and chemical methods. Mechanical dispersion methods, such as ultra-sonication (Qian et al., 2004),

centrifugation (Tan et al., 2005) and high shear mixing (Gojyn et al., 2004) help to separate nanotubes from each other, but can also shorten the nanotubes, decreasing the aspect ratio.

Chemical methods are designed to alter surface character of the nanotubes, either physically (non-covalent functionalization) (Gong et al., 2000, Vaisman et al., 2006) or chemically (covalent functionalization) (Dyke et al., 2004, Chen et al., 2006). Chemical methods include surface functionalization of CNTs to improve their compatibility with polymers or solvents. In general, functionalization provides wetting enhancement and reduce CNTs tendency to agglomerate. However, strong acids and aggressive chemical procedures may create structural defects resulting in poor properties for the nanotubes. On the other hand, non-covalent functionalization methods such as using surfactants or polymers give opportunities of adsorbing various groups on CNT surface without disturbing the π system of graphene sheets (Geng et al., 2008, Liu et al., 2000, Gojyn et al., 2004).

The main goal of this study was to understand and evaluate the problems associated with the dispersion of carbon nanotubes in epoxy systems. Different mechanical and chemical techniques such as sonication, surfactants and covalent functionalization were evaluated. First part of this study, the dispersion of nanotubes in the epoxy suspension was studied through rheological characterization. Second part was built on the observation onto the cured epoxy system with Raman spectrum and SEM images on the fracture surface.

3.2 EXPERIMENTAL

3.2.1 Materials

SWCNTs were obtained from a commercial source (Shenzen Nanotech Port. Co. Ltd., China). The nanotubes were produced by chemical vapor deposition (CVD), and contained ~ 10 wt% impurities, consisting primarily amorphous carbon and transition metals. The diameter range for the SWCNTs was < 2 nm; the length range was 5-15 μm.

During this work, Epon 828 epoxy was used in combination with polyether triamine hardener (Jeffamine T-403, Huntsman) to prepare the composites. Non-ionic polyoxyethylene octyl phenyl ether (Triton X-100) was used as a surfactant agent. Tetrahydrofuran (THF), sulfuric acid (H_2SO_4), nitric acid (HNO_3) and hydrochloric acid (HCl) (Fisher Scientific) were used as received during the oxidation procedure.

3.2.2 Preparation of SWCNT/Epoxy Composites

Epoxy nanocomposites were synthesized employing different concentrations of single wall nanotubes. The nanotubes were dispersed in THF and sonicated for 5 min. The dispersion was mixed one week after adding epoxy. The suspension was mixed for 2 hours and placed overnight in a vacuum oven at 80°C to allow solvent evaporation. Finally, a stoichiometric amount of hardener was added, followed by further mixing (2 min) and degasification (10 min). The solution was cast into a polyetrafluoroethylene (PTFE) mold and cured at 75°C for 3 h., with a post curing process at 125°C for 3 h.

3.2.3 Techniques

Rheological analysis was used to explore the state of nanotube dispersion. The rheological response of epoxy matrix without a curing agent was characterized as a Newtonian liquid; thus, all of the viscoelastic and non-linear behaviors of the suspensions were caused by the addition of SWCNTs (Advani et al., 2007, Chang et al., 1976, K. Gupta et al., 2000). The rheological properties of the epoxy/nanotube suspensions (without hardener) were determined using a commercial strain controlled rheometer (AR-G2, TA Instruments). A cone and plate geometry (diameter 60 mm and 27 μm truncation) was used to register the viscoelastic response of the CNTs/epoxy suspensions. Viscoelastic properties of all samples were measured at 25°C temperature. Dynamic strain sweep at a constant frequency (1Hz) was used to find the linear viscoelastic region in which G' and G'' were independent of strain amplitude. For all samples, 1% strain was chosen in the linear viscoelastic region. A linear viscoelastic response was characterized at the entire range of frequency amplitudes (100 to 0.01 rad/s). During the sample loading procedure, five minutes rest time was used to eliminate the effect of loading history.

Scanning electron microscopy (SEM, Zeiss EVO 50) was used to observe the fractured surfaces of the nanocomposites pre-chilled in liquid nitrogen. Samples were sputter-coated with gold prior to SEM observation.

Raman spectra were obtained at 785 nm using a Renishaw inVia Raman microscope in the backscattering configuration with a 50x objective. The laser beam with a nominal power of 80 mW was focused on a spot of 5 μm diameter.

3.3 RESULTS AND DISCUSSION

3.3.1 Rheological Analysis

Effect of Aspect Ratio

Advani et al. suggested that CNT separation refers to the separation of individual CNTs from the aggregates and CNT interconnection addresses the interconnections between the CNT aggregates and separated CNTs. It is expected to observe a different rheological behavior between these two structures. If a Newtonian plateau of G' develops at low frequencies, it is an indication of the development of an entanglement or network in the suspension (Advani et al., 2007). By comparing the rheological properties of SWCNT-epoxy suspensions with different sonication times (0, 5, 30, 120 min.), the effect of SWCNT network structure on the dispersion of 1wt% SWCNTs with surfactant (SWCNT-$S_{t=0}$, where "t" refers to the total sonication time), were evaluated (Figure 3.1).

In this figure, the highest storage modulus was observed at 5 min. sonication time and the lowest storage modulus was observed for 120 min. The longer sonication time decreased the storage modulus. Aggregated CNTs were separated using longer sonication time producing weaker interconnection between the carbon nanotubes and a considerable decrease at the aspect ratio. It was also expected that the suspension with 5 min sonication time still have aggregated CNTs. In this case, the highest storage modulus is related to a better interconnection between the SWCNT aggregates.

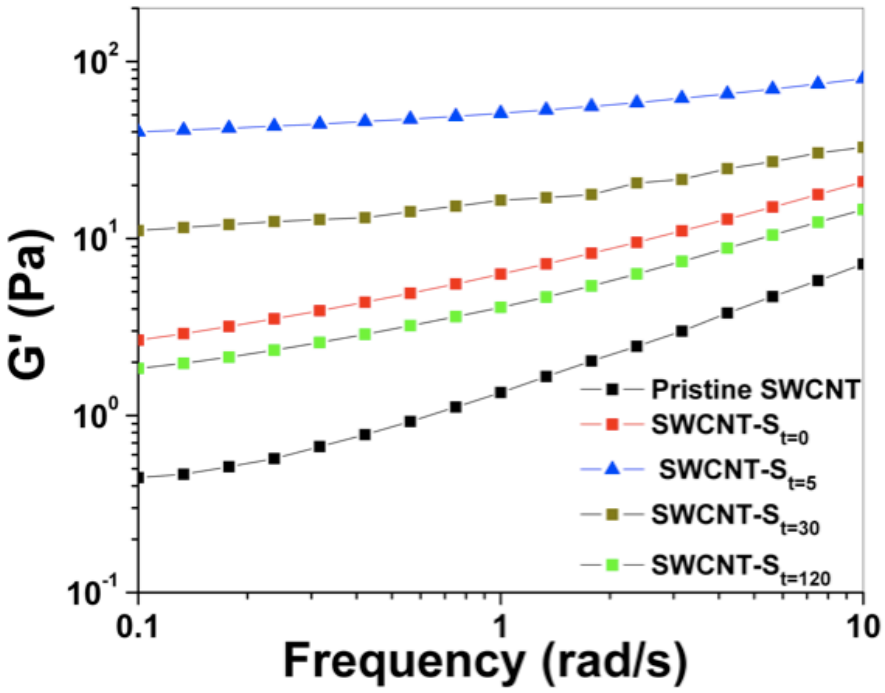

Figure 3.1. Effect of sonication on G' (Pa)

Table 3.1 shows the ultimate sonication time for different concentration of nanofillers. It was observed that the highest storage modulus obtained for 0.25, 0.5 and 1 wt% of SWCNTs with surfactant was with 5 min. sonication. For the 1.5 wt%, the ultimate sonication time was 10 min. The reason for longer sonication time at higher concentration was that the interaction between nanotubes increases at higher concentrations and more energy was required to separate the nanotubes from each other.

Table 3.1. % of increase in storage modulus of different concentration of SWCNTs with surfactants under different sonication time

wt % / time	0.25 wt%	0.5 wt%	1 wt%	1.5 wt%
0	0.16	1.07	2.02	6.03
5	1.59/894%	3.61/237%	40.08/1885%	79.35/1220%
30	1.23/668%	2.60/143%	27.60/1266%	95.32/1480%
120	0.17/6%	2.59/142%	1.79/-11%	70.93/1076%

Effect of Chemical and Mechanical Modification

In this study viscoelastic data of 1wt% SWCNTs with surfactant (SWCNT-$S_{t=0}$), acidified SWCNTs (SWCNT-COOH) and esterified SWCNTs (SWCNT-PGE) were compared with those obtain from 1wt% pristine SWCNTs. Ultra-sonication was also applied in order to improve the dispersion of SWCNTs with surfactant (SWCNT-$S_{t=5}$). Results were shown in Figure 3.2. At low frequency, G' flattened out to a constant value. Both SWCNT-$S_{t=0}$ and SWCNT-$S_{t=5}$ showed higher storage modulus than the pristine SWCNT system. The storage modulus of SWCNT-$S_{t=0}$ system increased 350%. After applying ultra-sonication storage modulus had a value 100 times higher than pristine SWCNT system at low frequencies. In SWCNT-COOH system, the storage modulus at low frequencies increased 250% compared to the pristine SWCNTs.

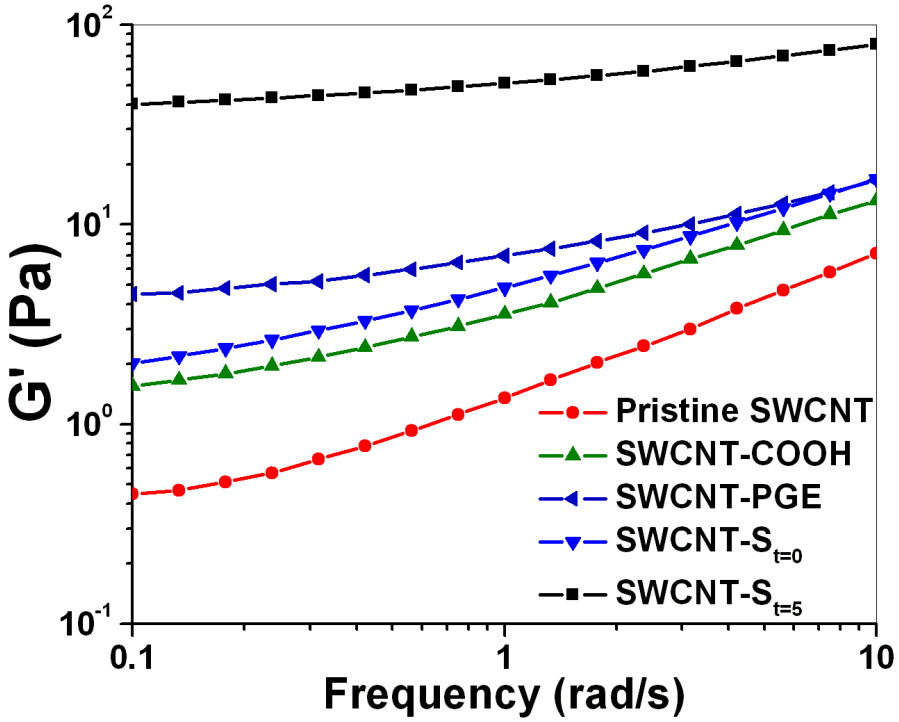

Figure 3.2. Effect of functionalization on G'(Pa)

The aggregated pristine SWCNTs behaved more like a particle suspension and when the frequency was applied, the suspension showed lower flow resistance (lower viscosity and so G') as compared to the SWCNTs with surfactant. On the other hand, surfactants are adsorbed on the nanotube surface by hydrophobic or π-π interactions. In a typical dispersion procedure, further ultra-sonication helps surfactants debundling (or exfoliating) nanotubes by Coulombic or hydrophilic interactions. Therefore, the rubbery plateau for the SWCNTs-$S_{t=5}$ showed higher storage modulus compared to the other suspensions. In the case of chemically modified SWCNTs, the chemical groups provide repulsion forces, which separate the SWCNTs in the suspension. The presence of acid groups provides steric stabilization of SWCNTs, which lowers their tendency to create aggregations and helps to form uniform dispersions. Therefore, the shear resistance (viscosity and G') boosted by adding functionalized SWCNTs into the suspension. For

the SWCNT-PGE system, the reason of higher increase in storage modulus might be because of the strong interaction between the matrix and PGE functionalized SWCNTs.

Effect of Concentration and Critical Percolation Threshold

In a well-dispersed system, after a critical concentration, the nanotubes start forming a 3D network. The suspension shows a solid-like behavior characterized by fixed storage modulus (G') and loss modulus (G'') with the frequency. This critical threshold concentration is called critical percolation threshold. Percolation concentration is simply affected by the quality of the dispersion, the size of the fillers (aspect ratio) and the degree of alignment of the components. These ideas from the percolation theory are commonly applied to the properties of suspensions and composites of impenetrable particles. Power law theory ($P\sim |\phi^* - \phi|^\delta$) has been widely used in the literature to model the behavior of such systems (Du et al. 2004).

$$P\sim |\phi^* - \phi|^\delta$$

where ϕ is the volume fraction of the particles in the suspension, δ is the critical exponent, P is a property (i.e. electrical and thermal conductivity, shear modulus, dielectric constant, transport properties, such as the viscosity of fluid suspensions of rigid particles, etc.) and ϕ^* is the threshold concentration.

Firstly, the systems with acidified SWCNTs were evaluated in order to find the critical percolation threshold. As the concentration increases, the distance between the individual tubes shortens and the interaction between the tubes becomes in a well-dispersed system. It was observed that this stronger interaction increases the storage modulus due to the reducing mobility

and the increased resistance to flow. As the concentration reaches the percolation threshold value that nanotubes start to touch each other and building 3D network, the suspension shows solid-like behavior and creates a plateau in storage modulus vs. frequency graph (Figure 3.3). In Figure 3.4, the critical percolation threshold value for acidified SWCNT system was calculated by using the power law theory. It was found that acidified SWCNT showed percolation threshold value of 0.41 wt%.

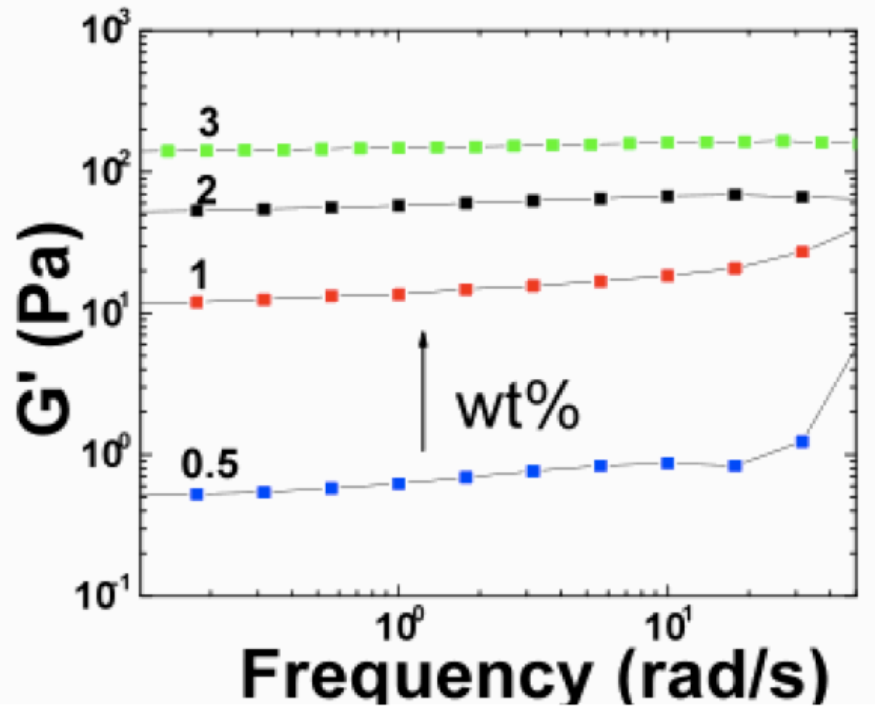

Figure 3.3. Effect of SWCNT-COOH concentration on G' (Pa)

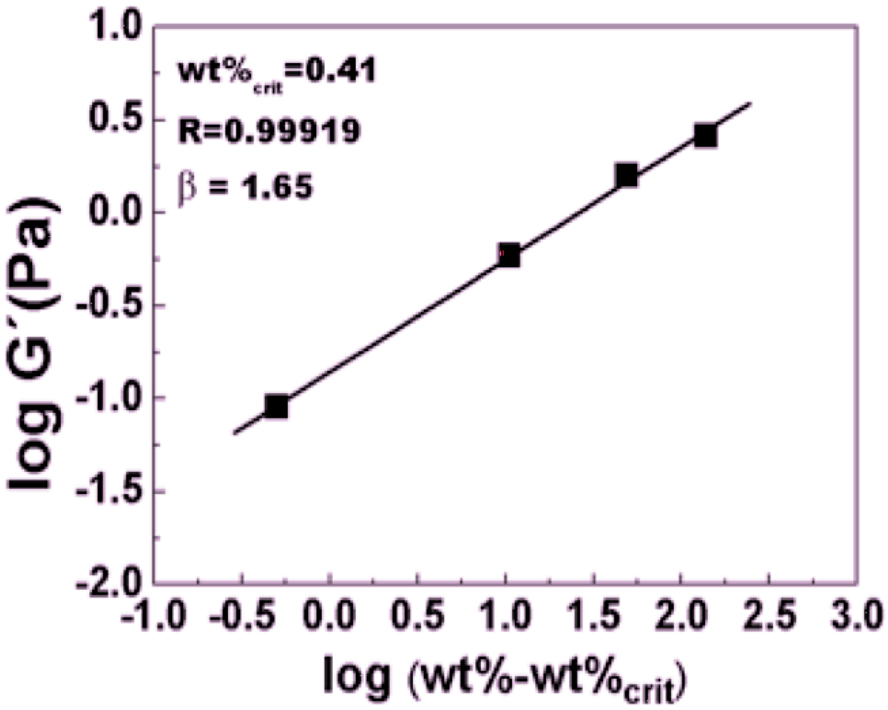

Figure 3.4. Critical percolation threshold of SWCNT-COOH system

Figure 3.5 shows the viscoelastic data of SWCNTs with surfactant at different concentrations. It was observed that as the concentration increased, the storage modulus (G') increased similar to the acidified system. It was also observed that the viscosity increased sharply at low frequencies especially over 0.5wt% CNT loading (Figure 3.6).

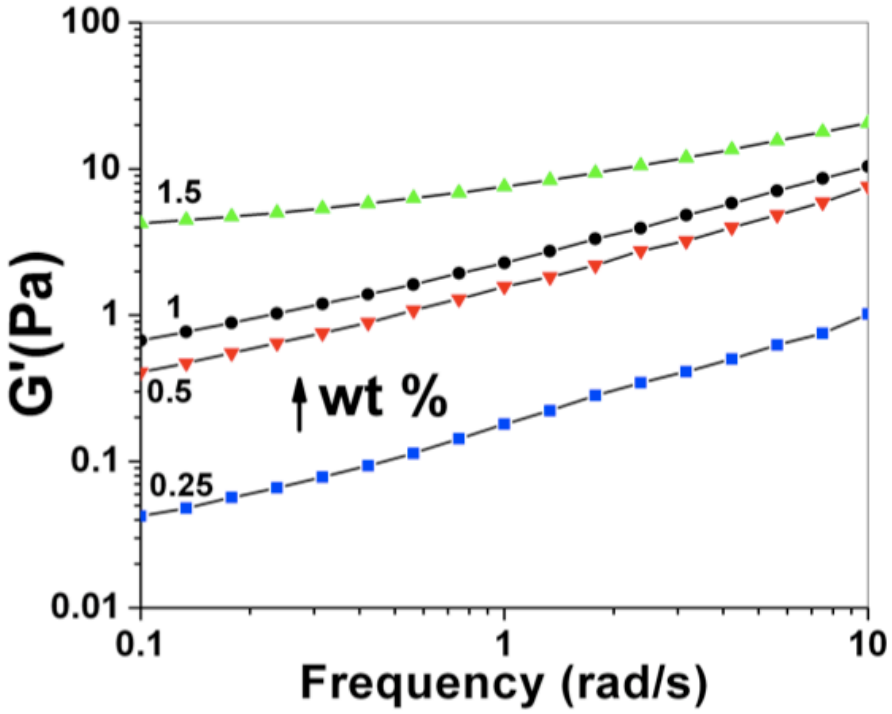

Figure 3.5. Effect of the concentration of SWCNTs with surfactant on G' (Pa)

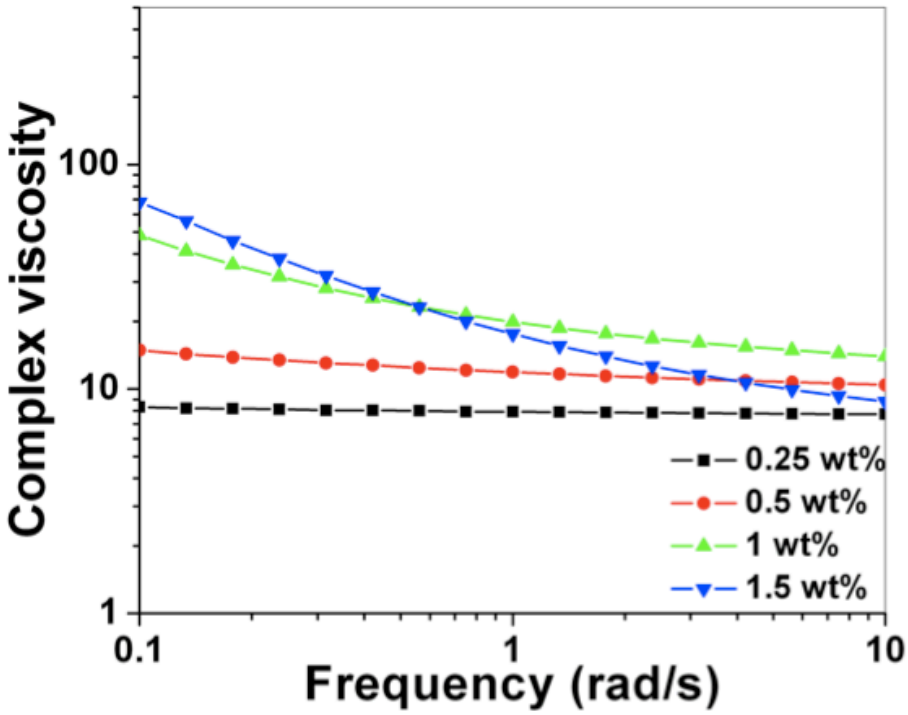

Figure 3.6. Effect of concentration of SWCNTs with surfactant on complex viscosity

In order to obtain better understanding of the transition from the liquid-like to the solid-like behavior, phase angle (δ) vs. complex storage modulus (G*) plot was evaluated (Figure 3.7). This plot can be used to detect the rheological percolation because the phase angle is very sensitive to the fluid–solid transition of a viscoelastic fluid. A typical liquid system shows a delta degree of 90° (in our case the matrix) whereas, a typical solid system shows a delta degree of 0°. Below the percolation threshold, the phase angle tends to 90° at low G*, consistent with a behavior dominated by the viscous flow. At and beyond the percolation threshold, the phase angle significantly decreases with the modulus in agreement with an increasing elastic behavior. In this case, it was observed that the system shows more solid-like behavior after the CNT concentration reaches 0.5 wt%. This value is also close to the percolation threshold value that was observed in acidified systems.

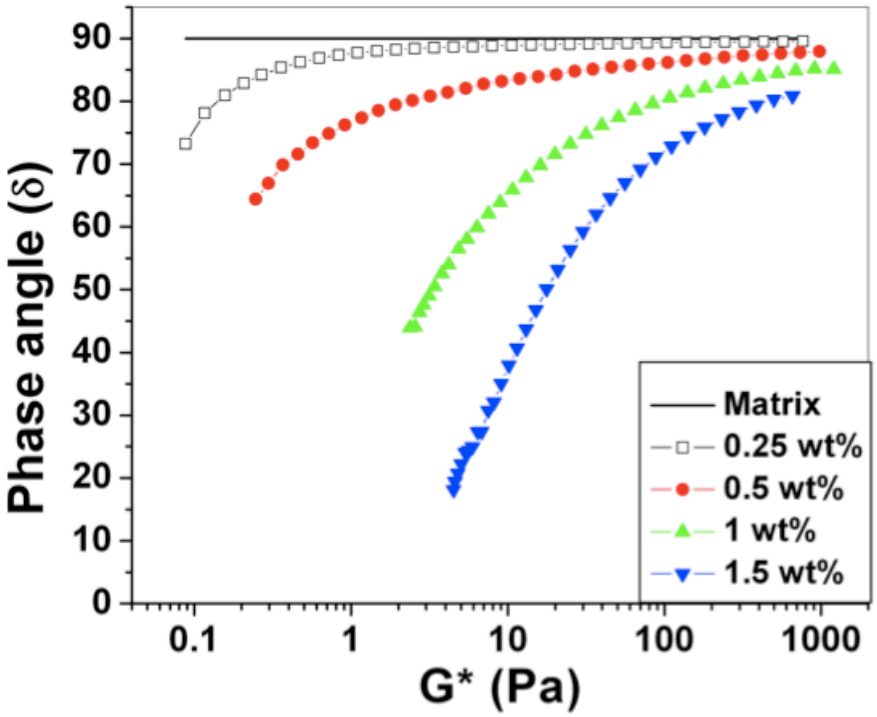

Figure 3.7. Phase angle (δ) vs. complex storage modulus (G*) plot for different concentrations of SWCNTs with surfactant

Several studies have also focused on the percolation threshold of CNT reinforced polymer nanocomposites. Pothschke et al. (2002) found the percolation threshold value to be 2 % by weight for MWCNTs systems. Du et al. (2004) found it to be 0.12 % by weight, while Kinloch et al. (2002) found it to be around 0.5 % by volume. The reason for different percolation threshold values is that research groups might use different aspect ratio CNTs and suspend in different systems. However, all these studies showed that viscosity of the suspension increased by the concentration and viscosity is strongly related to the concentration nanotube forms a network similar to the systems showed above.

Effect of Orientation

Figure 3.8 shows the effect of pre-shear process on the storage modulus of SWCNT-$S_{t=5}$ system. In order to study the effect of the orientation, all samples were tested before and after 20 s^{-1} shear rate for 30 min. It was observed that the storage modulus decreased 80% after the pre-shear period indicating that the pre-shear process aligned the SWCNTs in the shear direction and decreased the flow resistance. It was already mentioned that the 5 min. sonication developed a good CNT network and the pre-shear process, which may break down this network, producing the decrease in the storage modulus.

The use of high shear flow aligns the nanotubes in the shear direction and this aligned suspension shows a lower viscosity and G' than randomly orientated fiber suspension as it experiences lower resistance. At the same time, higher shear flows may break down the 3D network formed by the filler and decrease the viscosity.

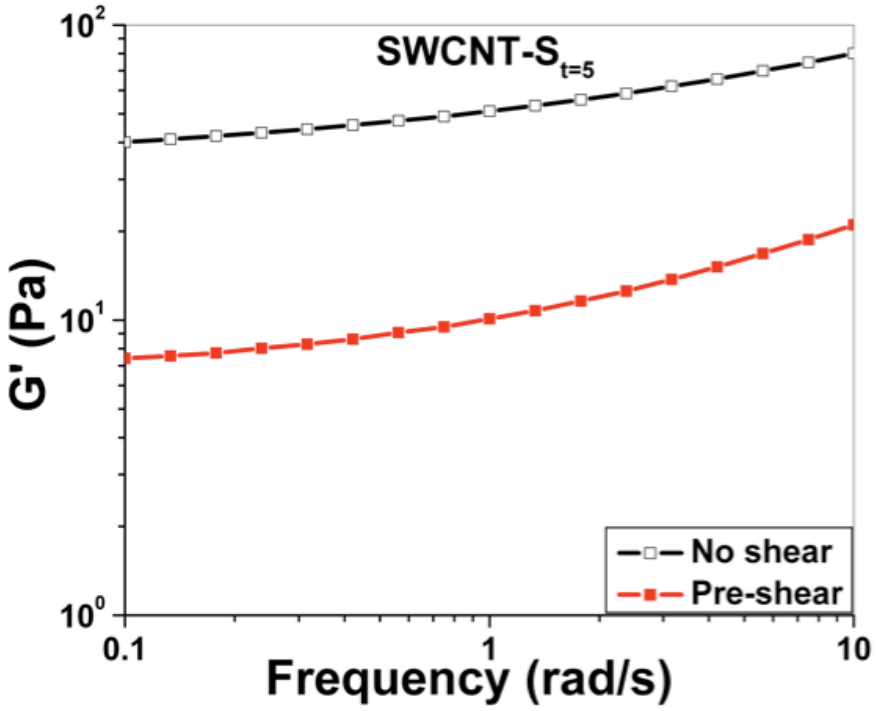

Figure 3.8. Effect of orientation on G' (Pa)

The change in storage modulus with and without pre-shear process for other systems was shown in Table 3.2. It was observed that similar to the SWCNT-$S_{t=5}$ system, acidified system and SWCNT-$S_{t=0}$ systems showed decrease in storage modulus after pre-shear. However, pristine SWCNTs showed an increment. This can be explained with that pre-shear process helped to pristine SWCNTs to break the bundles and create a better network. This better network increased the resistance against the flow and thus the storage modulus of the system.

Table 3.2. Change in G' at 0.1 rad/s with and without pre-shear

Filler Type (1wt%)	G'(Pa) No Shear	G'(Pa) Pre-Shear	% Change
Pristine SWCNT	0.45	0.658	+ 46
SWCNT-COOH	1.55	1.05	- 32
SWCNT-$S_{t=0}$	2.02	0.73	- 64
SWCNT-$S_{t=5}$	40.08	7.93	- 80

3.3.2 Raman Analysis

The dispersion of SWCNT in the epoxy matrix can be also characterized by analyzing the changes in intensity of Raman bands corresponding to radial breathing modes (RBM) associated with isolated and bundled nanotubes. RBM is very sensitive to the diameter of nanotubes. Thus, the single excitation at 785 nm is quite useful to establish differences between isolated and bundled nanotubes. The band at 266 cm^{-1} is a characteristic of bundled nanotubes and that is inversely proportional to the nanotube diameter. For the particular SWCNTs, this frequency is given by :

$$w\ (cm^{-1}) = 223.5/\ d(nm) + 12.5$$

For SWCNT with a diameter close to 1.5 nm as those used in this study, the Raman band characteristic of individual nanotubes may be expected at about 161.5 nm.

Figure 3.9 shows the Raman spectra of nanocomposites containing different types of SWCNT in 100 cm^{-1} – 400 cm^{-1} regions. Two main bands at the expected frequencies are observed for the three samples. Comparing the relative intensities of both bands it may be assessed that the quality of the dispersion, measured by the fraction of individual nanotubes, decreases in the following order: SWCNT-COOH > SWCNT-unmodified > SWCNT-PGE. It is observed that the dispersion of PGE-SWCNT is the worst of the three systems. It was the best dispersion in the initial formulation and the worst dispersion in the cured material. This means that bundling took place in the course of polymerization a process that could be produced by polymerization-induced phase separation.

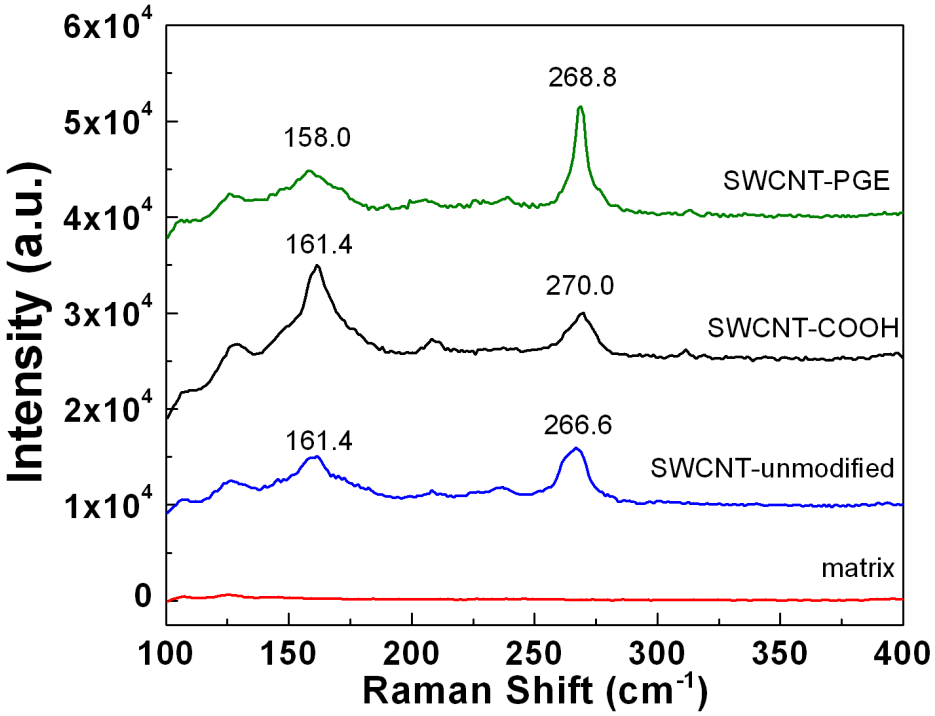

Figure 3.9. Raman spectra of nanocomposites containing different types of SWCNT in the 100 cm^{-1} – 400 cm^{-1} region

A small shift in the frequency characteristic of individual nanotubes has been assigned to an actual variation of the nanotube diameter produced by interactions with the matrix. The shift observed from 161.4 nm for SWCNT-unmodified and SWCNT-COOH to 158.0 nm for SWCNT-PGE, could be explained by a corresponding slight increase in the tube diameter produced by interactions of ester groups with the matrix. In fact, the esterification with PGE was expected to improve the dispersion of SWCNT in DGEBA due to the close similarity of chemical structures. A possible explanation is the occurrence of a polymerization-induced phase separation. Starting from a good dispersion of SWCNT-PGE in epoxy precursors, at a certain conversion in the polymerization reaction the solution becomes metastable mainly due to the

decrease in the entropic contribution to the free energy, and phase separation takes place leading to domains rich in SWCNT-PGE.

3.3.3 Morphological Analysis

Above results were also proven through SEM images of 1 wt% SWCNTs fracture surface broken in liquid nitrogen (Figure 3.10). These images showed that nanotubes were more uniformly distributed in the polymer matrix after covalent and non-covalent functionalization. Considerably smoother surface was observed for SWCNT-COOH and SWCNT-$S_{t=5}$ systems (Figure 3.10-a, 3.10-e, respectively). In figure 3.10-f, the SEM image of SWCNT-$S_{t=120}$, separated nanotubes were observed.

The SEM images confirmed the better dispersion quality at functionalized SWCNT systems compared to the pristine SWCNT system. Large bundles were observed at unmodified and esterified SWCNT systems with the formation of big domains (~20μm and 17μm respectively). Even though the system with esterified SWCNTs (SWCNT-PGE) showed an increase in storage modulus at rheological analysis indicates to a better dispersion, the SEM images and Raman analysis showed that the quality of dispersion is lower in those systems. This indicates that in the rheological analysis, ester groups created a stronger bonding with epoxy matrix and increased the flow resistance of the suspension against shear that increases the storage modulus. However, the SWCNT-COOH/epoxy sample appears to have considerably smaller homogeneously dispersed domains, with sizes in the order of 3-4μm.

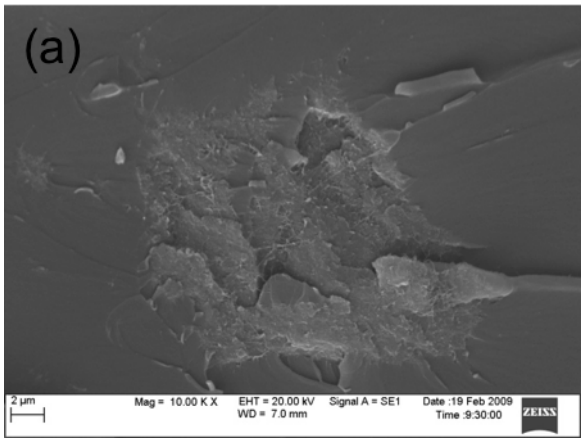
(a)
2 µm
Mag = 10.00 K X
EHT = 20.00 kV
WD = 7.0 mm
Signal A = SE1
Date :19 Feb 2009
Time :9:30:00
ZEISS

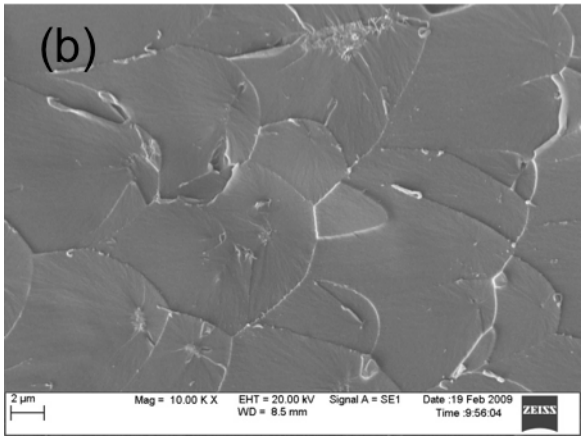
(b)
2 µm
Mag = 10.00 K X
EHT = 20.00 kV
WD = 8.5 mm
Signal A = SE1
Date :19 Feb 2009
Time :9:56:04
ZEISS

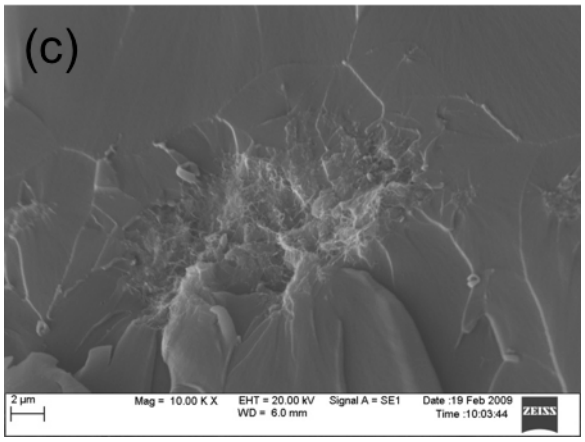
(c)
2 µm
Mag = 10.00 K X
EHT = 20.00 kV
WD = 6.0 mm
Signal A = SE1
Date :19 Feb 2009
Time :10:03:44
ZEISS

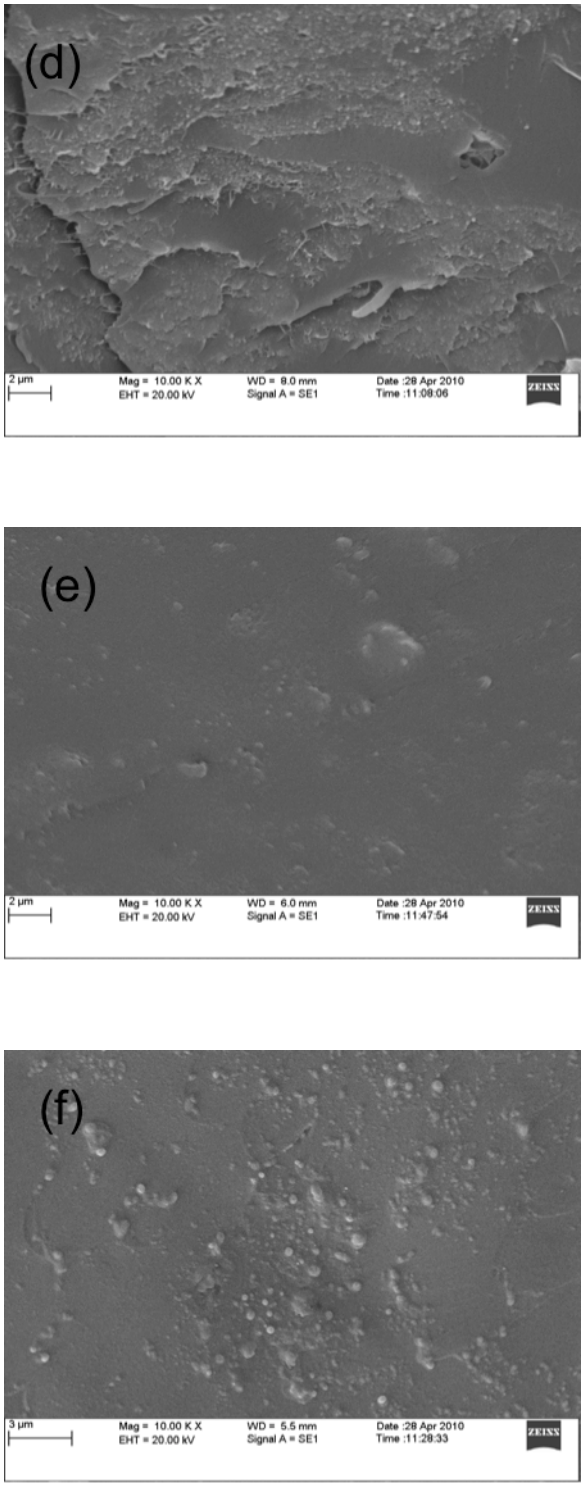

Figure 3.10. SEM images of the epoxy nanocomposites of (a) Pristine SWCNT, (b) SWCNT-COOH, (c) SWCNT-PGE, (d) SWCNT-$S_{t=0}$, (e) SWCNT-$S_{t=5}$, (f) SWCNT-$S_{t=120}$

3.4 CONCLUSION

Using a combination of techniques (rheology, scanning electron microscopy and Raman spectrum), an attempt was made to characterize single wall carbon nanotube/epoxy systems. Several dispersion techniques were chosen such as covalent and non-covalent functionalization, and ultra-sonication. The quality of the dispersion was evaluated through rheological studies. The highest storage modulus (G') value, which indicates better dispersion, was observed for SWCNTs with surfactants after 5 min. sonication.

The effect of carbon nanotubes concentration on the final dispersion was also studied. It was observed that as the carbon nanotube concentration increased, the suspension showed a noticeable transition between a liquid-like to solid-like behavior (percolation concentration). The percolated threshold concentration was found to be approximately 0.41 wt% for acidified SWCNTs, where the storage (G') and loss (G") modulus and the viscosity increased several orders of magnitude compared to the unreinforced system.

It was also observed that the sonication time produced considerable effect on the final dispersion of the fillers. The G' value increased as the sonication time increased indicating a better disentanglement of the SWCNTs bundles. However at longer sonication time storage modulus (G') decreased because of the weaker interconnection between the carbon nanotubes and possible degradation of the final structures. The effect of the orientation on the storage modulus was also discussed. The orientation of SWCNTs in the suspension decreased the resistance to flow and thus decreased the storage modulus of the suspensions.

The dispersion of nanotubes after curing was also discussed through Raman spectrum and SEM images. It was found that the dispersion of carbon nanotubes after acidification improved as it was mentioned through rheological analysis. However, esterified SWCNTs showed a decrease in the quality of dispersion. Due to its similar chemical groups with epoxy matrix, it was expected to observe an improved dispersion with esterified system. Based on the observations from Raman spectrum and SEM images, the reason for bad dispersion quality may be the phase separation during the polymerization.

REFERENCES

1. Ajayan PM, Schadler LS, Giannaris C, Rubio A., Single-Walled Carbon Nanotube-Polymer Composites: Strength and Weakness, Adv. Mater.12, No. 10, 2000

2. Auad L. M, M.A. Mosiewicki, C. Uzunpinar, R.J. J. Williams, "Single-wall carbon nanotubes/epoxy elastomers exhibiting high damping capacity in an extended temperature range", Composite Science and Technology, Volume 69, Issues 7-8, 1088-1092, 2009

3. Chang Dae Han, "Rheology in polymer processing", Academic Press, New York, 1976

4. Christopher A. Dyke, James M. Tour, "Covalent functionalization of Single-walled carbon nanotubes for materials applications", J. Phys. Chem. A. Vol, 108 No. 51, 2004

5. Cui, R. Canet, A. Derra, M. Couzi and P. Delhaes, "Characterization of multiwall carbon nanotubes and influence of surfactant in the nanocomposite processing", Carbon volume 41, Issue 4, 797-809, 2003

6. D. A. Heller, P. W. Barone, J. P. Swanson, R. M. Mayrhofer, and M. S. Strano, J. Phys. Chem. B, 108, 6905, 2004.

7. D. Qian, E. C. Dickey, R. Andrews and T. Rantell, "Load transfer and deformation mechanisms in carbon nanotube-polystyrene composites", Appl. Phys. Lett., Vol. 76, No. 20, 2000

8. Du F, Scogna RC, Zhou W, Brand S, Fischer JE, Winey KI, "Nanotube networks in polymer nanocomposites: rheology and electrical conductivity", Macromolecules 37:9048–9055, 2004

9. E. R. Soulé, J. Borrajo, and R. J. J. Williams, Macromolecules, 40, 8082,2007

10. F.H. Gojny, M.H.G. Wichmann , U. Kopke, B. Fiedler , K. Schulte, "Carbon nanotube-reinforced epoxy-composites: enhanced stiffness and fracture toughness at low nanotube content", Composites Science and Technology 64, 2363–2371, 2004

11. Fuyong Cheng, Dr., Alex Adronov, "Noncovalent functionalization and solubilization of carbon nanotubes by using a conjugated Zn-Porphyrin polymer", Chem. Eur. J. 12, 5053–5059, 2006

12. J Suave, LAF Coelho, SC Amico, SH Pezzin, "Effect of sonication on thermo-mechanical properties of epoxy nanocomposites with carboxylated-SWNT", Materials Science and Engineering: A, 509 (1-2), 57-62, 2009

13. Kinloch, I.A., Roberts, S.A., Windle, A.H., "A rheological study of concentrated aqueous nanotube dispersions", Polymer, 43, 7483-7491, 2002

14. Linda Vaisman, H. Daniel Wagner, Gad Marom, "The role of surfactants in dispersion of carbon nanotubes", Advances in Colloid and Interface Science, 128-130, 37-46, 2006

15. M. J. Bronikowski, P. A. Willis, D. T. Colbert, K. A. Smith, and R. E. Smalley, J. Vac. Sci. Technol. A, 19, 1800, 2001

16. M. J. O'Connell, S. Sivaram, and S. K. Doorn, Phys. Rev. B, 69, 235415, 2004

17. Pötschke P, Fornes TD, Paul DR, "Rheological behavior of multiwalled carbon nanotube/polycarbonate composites", Polymer 43:3247–3255, 2002

18. Rakesh K. Gupta, "Polymer and composite rheology", 2nd edition, Marcel Dekker INC., New York, 2000

19. Xiaoyi Gong, Jun Liu, Suresh Baskaran, Roger D. Voise, James. S Young, "Surfactant-Assisted Processing of Carbon Nanotube/ Polymer Composites", Chem. Mater.,12 (4), 1049-1052, 2000

20. Yan Geng, Ming Yang Liu, Jing Li, Xiao Mei Shi, Jang Kyo Kim, "Effects of surfactant treatment on mechanical and electrical properties of CNT/epoxy nanocomposites", Composites: Part A 39, 1876-83, 2008

21. Yongqiang Tan and Daniel E. Resasco, "Dispersion of Single-Walled Carbon Nanotubes of Narrow Diameter Distribution", J. Phys. Chem. B, 109, 14454-14460, 2005

22. Zhihang Fan, Suresh G. Advani, "Rheology of multiwall carbon nanotube suspensions", J.Rheol. Volume 51, Issue 4, pp. 585-604, 2007

CHAPTER 4

DISPERSION INDUCED BY PHASE SEPARATION

4.1 INTRODUCTION

In this chapter, the reaction induced phase separation process was studied with epoxy/diamine system incorporated with modifiers such as polyhedral oligomeric silsesquioxanes (POSS), unmodified and modified SWCNTs. Whether phase separation occurs in the presence of these modifiers was discussed. Furthermore, the effect of phase separation process during the curing reaction on the dispersion of SWCNTs was discussed.

Various epoxy systems containing various modifiers (e.g. rubber, liquid crystal) have been used frequently in industry and research. These modifiers can be used for toughening of the polymer network, improving the quality of molding surfaces, producing interconnected structures as coating layer or improving the thermal and mechanical properties. Based on their structure, modifiers may initially be immiscible or may phase-separate during the curing process (Williams et al., 1997).

Phase separation process takes place when a polymerization is carried out employing a solution of a suitable modifier (e.g., rubber, thermoplastic polymer or liquid crystal) in the starting monomers, which is called reaction or polymerization induced phase separation. This produces a

decrease in the contribution of the entropy and the increase in cross-link density during the post-gel state that generates an elastic contribution, which limits the amount of modifier in the swollen network (Elicabe et al., 1997).

Reaction-induced phase separation process has some advantages and disadvantages depending on the application. The stability and low viscosity of the starting homogeneous solution are advantages of these systems. However, the production of undesired morphologies during the curing process or remaining modifiers in solution even at complete conversion are the disadvantages. If the remaining modifiers have lower glass transition temperature, they act like plasticizers that decrease the glass transition temperature of the cured system. On the other hand, if the modifiers are high T_g thermoplastics, the remaining parts do not create a problem.

In order to evaluate the phase separation during the reaction, thermodynamic and kinetic factors need to be understood well. These analysis help to observe whether the systems remain stable (no phase separation), metastable (phase separation may take place), or unstable (phase separation does take place). In the following section, basic information in Flory-Huggins model will be explained in order to provide a better understanding in the thermodynamic of the phase separation process (Sperling, 2006; Williams et al, 1997).

Flory-Huggins Model

Flory and Huggins developed a model in 1941 to explain the mixing behavior of polymer systems that creates a basic understanding on different types of phase diagrams, under the effect of temperature and molar masses. This model was based on the changes in Gibbs free energy (ΔG_{mix}) during mixing that can be shown as

$$\Delta G_{mix} = G_{AB} - (G_A + G_B)$$

where G_A, G_B, and G_{AB} denote the Gibbs free energies of the compounds A and B in separate states and the mixed state, respectively.

When a polymer dissolves in a solvent, the Gibbs free energy can be decreased by the addition of polymer into the solution at constant temperature and pressure. The Flory-Huggins model represents ΔG_{mix} as a sum of two contributions, which describe two main aspects of the mixing process. Firstly, mixing leads to an increase of the entropy associated with the motion of the centers of mass of all polymer molecules, and secondly it may change the enthalpic contribution. The latter part is called ΔH_{mix} and the increase in the translational entropy ΔS_{mix}.

$$\Delta G_{mix} = \Delta H_{mix} - T\Delta S_{mix}$$

In order to favor the mixing, ΔS_{mix} needs to be decreased. On the other hand, enthalpic contribution may act favorably or unfavorably depending on the monomer-monomer interactions. In most cases, for van der Waals interactions generally, attractive energies between equal monomers are stronger than those between unlike pairs. This behavior implies $\Delta H_{mix} > 0$ and therefore opposes a mixing. As enthalpic contribution, ΔH_{mix} also accounts for changes in the

entropy due to local effects. For example, a shrinkage or an expansion of total volume on mixing results in a change in the number of configurations available for local motions of the monomeric units. The Flory-Huggins treatment is based on approximate equations for both ΔH_{mix} and ΔS_{mix}. Based on Flory-Huggins model

$$\frac{\Delta S_{mix}}{R} = n_P ln \frac{V}{V_P} + n_M ln \frac{V}{V_M}$$

where R is the gas constant, n_P is the moles of a polymer, n_M is the moles of a modifier. Introducing the volume fractions $\emptyset_P = {}^{V_P}/_{V}$ and $\emptyset_M = {}^{V_M}/_{V}$ of the two components in the mixture, ΔS_{mix} can be written as

$$\frac{\Delta S_{mix}}{R} = -n_P ln\emptyset_P - n_M ln\emptyset_M$$

By calling V_P and V_m the molar volumes of polymer and modifier, and $V_T = N_P V_P + N_M V_M$ the total volume of the system, the entropy of mixing per unit volume may be written as;

$$\frac{\Delta S_{mix}}{R} = -\frac{\emptyset_P}{V_P} ln\emptyset_P - \frac{\emptyset_M}{V_M} ln\emptyset_M$$

"In the case of polycondensation reaction of polymer (P), V_M remains constant and V_P increases with conversion depending on the functionality of reactants. As V_P increases with conversion, the absolute value of the entropy of mixing decreases, i.e. there is less contribution of the entropy of mixing to the free energy" (Williams et al., 1997)

The enthalpy of mixing is expressed by the equation

$$\Delta H_{mix} = RT\frac{V}{V_R}\chi \emptyset_P \emptyset_M$$

where V_R is a molar volume of a unit cell common to both polymers, χ is the Flory-Huggins interaction parameter which is dimensionless and determines the empirical manner the change in the local free energy per reference unit. Based on the equation $\Delta G_{mix} = \Delta H_{mix} - T\Delta S_{mix,}$ Gibbs free energy per unit volume system can be given by;

$$\Delta G_{mix} = \Delta H_{mix} - T\Delta S_{mix} = RT\{\frac{\emptyset_p}{V_P}\ln \emptyset_p + \frac{\emptyset_M + \chi}{V_M \ln \emptyset_M} + \frac{\chi}{V_r}\emptyset_p \emptyset_M\}$$

If $V_M > V_P$, the contribution of the monomer to the entropy mixing is much more important in absolute value than the modifier contribution. Therefore, the increase of V_P with conversion process is feasible. For this reason it is usually stated that phase separation is the result of the decrease in the entropic contribution to the free energy of mixing during polymerization (William et al., 1984).

Following this phenomenon, monofunctional POSS structures, which contain only one reactive groups in the structure, may induce phase separation during polymerization due to lack of compatibility with organic network similar to different types of rubbers, thermoplastics and liquid crystals. By controlling the monofunctional group and the nature of the inert organic groups on the phase separation, either amorphous or crystalline POSS aggregates can be generated (Zucchi et al., 2008).

In this chapter, POSS attached CNTs (produced through covalent reaction between the existing functional groups on the CNTs surface and functional group that POSS molecule holds-See Chapter 2) were developed in order to observe whether phase separation of monofunctional POSS molecules creates some kind of ordered arrays during polymerization that helps the dispersion of CNTs in the epoxy/diamine system. This technique leads to combine the two types of nano-reinforcement agents. To best of our knowledge, this functionalization method has not been reported before. The kinetics and dynamics of phase separation process during the polymerization process were studied and explained with details through differential scanning calorimetry (DSC), rheology, dynamic mechanical analysis (DMA), scanning electron microscopy (SEM) and optical methods.

4.2 EXPERIMENTAL

4.2.1 Materials

Monofunctional glycidyloxpropyl-heptaisobutyl POSS (iBu-Gly-POSS, EPO 418 Hybrid Plastics) was a crystalline powder with a molar mass of 931.6 g/mol. Single-wall carbon nanotubes were purchased from NTP (Nanotech Port, Shenzhen, China). Technical specifications of SWCNT were a diameter <2 nm, length <20 μm, purity of CNTs >90%, amorphous carbon < 5%.

The elastomeric epoxy/diamine matrix was formulated using different stoichiometric amounts of an epoxy monomer based on diglycidylether of bisphenol A (DGEBA, Epon 828, Miller-Stephenson) with a molar mass of 180 g/mol per epoxy group and a selected hardener 4,4' – methylenebis (2,6-diethylaniline) (MDEA) ($C_{21}H_{30}N_2$) with a molar mass of 310.45 g/mol.

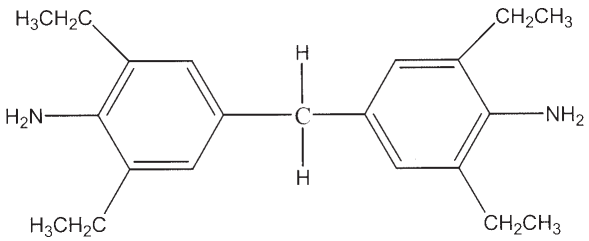

Figure 4.1. Structure of 4,4′-methylenebis (2,6-diethylaniline) (MDEA)

4.2.2 Synthesis of POSS-Modified DGEBA-MDEA Networks

Networks were synthesized using different stoichiometric proportions (R) of epoxy and hardener. The stoichiometric ratio was calculated as the ratio of the equivalent molar amount of the MDEA to the equivalent molar amount of the DGEBA. POSS (1 mol), MDEA (10 mol), DGEBA (19.5

mol) were used to provide an overall stoichiometric ratio of 1 (R=1) of epoxy and NH functionalities. The mass fraction of iBu-Gly POSS in the final network was 8.1 wt%. 1 wt% of SWCNTs were also added into the system. All systems were mixed with THF in order to increase dispersion quality. The systems with SWCNTs were sonicated with a tip-sonicator in THF for 5 minutes. Furthermore, THF was evaporated at 80°C for 24 hr. and in order to be sure that all solvent was removed, the weight of the suspensions was measured before and after THF evaporation. Because of the high melting temperature of POSS molecules and MDEA crystals, suspensions were immediately poured onto the mold without extra bath sonication. In every case, the polymerization carried out at 135°C for 3 hr, followed by a 3 hr post-cure at 190°C.

4.2.3 Characterization

All samples were run with parallel plate geometry in rheometer during curing process and reaction was checked under 135°C at 1 Hz frequency during a time sweep experiment. The gel point where the polymers are cross-linked during the curing process was determined. The same procedure was followed in order to observe gelation time and phase separation.

Differential Scanning Calorimetry (DSC) was used to observe the polymerization kinetics and also the glass transition temperature of the samples before post curing. The polymerization was performed at 135°C. The total reaction heat obtained from an isothermal scan at 135°C was divided by the maximum reaction heat determined from a dynamic scan at 10°C/min in order to find the maximum conversion at 135°C.

In order to have additional information on where gel point is reached, a visual experiment were run. The solutions were prepared in a glass tube and put into the pre-heated 135°C oil bath. The polymerization was checked periodically and the time, when the gelation was observed, was recorded.

The post-cured samples were tested using dynamic mechanical analysis with 3-point bending tool. The dynamic temperature ramp test was performed at 0.1% strain at a frequency of 1Hz from 25°C to 200°C with a heating rate of 5°C/min.

4.3 RESULTS AND DISCUSSION

4.3.1 Curing Process

The curing occurs through the transformation of low molecular weight monomers from liquid to solid state by the formation of a polymer network, through the chemical reaction of the reactive groups. In this network formation, one of the most important parameters is the development of gel point where the transition from liquid to solid occurs.

In this study, the curing process of DGEBA/MDEA system with and without modifiers was evaluated through visual observation, calorimetric (DSC) and rheological analysis. In the rheological characterization two stages can be distinguished during the curing process, limited by the gel point. The initial part of the process is dominated by the viscous behavior of the oligomeric growing species. Thus, the loss modulus of the material is larger than the storage modulus, which represents the elastic part of the response and is negligible at this stage. Close to the gel point, the G' will increase rapidly. As it reaches the gel point, the G" and G' will cross and level off (Auad et al., 2005). Viscosity of the system starts to increase during the polymerization and after gel point viscosity reaches an infinite value. When phase separation occurs, a sudden drop in G' should be observed. After phase separation completes, the G' will continue to increase as the time increases.

Rheological Study of the Reaction Process

Time sweep experiments were performed for DGEBA/MDEA and DGEBA/MDEA/POSS. Results are shown in Figure 4.2 and 4.3. In both graphs, left x-axis shows G' and G'' and right x-axis shows the complex viscosity. In these graphs, G' and G'' crossed at gel point (or close to gel

point) (Auad et al., 2005) and viscosity increased dramatically. However, the system where POSS molecules were incorporated into the mixture, showed a plateau in G' before reaching the gel point. This can be explained with the phase separation process that occurred before system reached the gel point. At the beginning of the reaction, the homogenous blend behaved more like a polymer solution. When phase separation occurred, the system showed a plateau in G' and a slower increase in viscosity (Figure 4.3). This gradual increase in viscosity occurred due to formation of bi-continious structures. However, when the system reaches a continuous modifier-rich phase up to the end of the phase separation process, a faster increase was observed at viscosity and also G'.

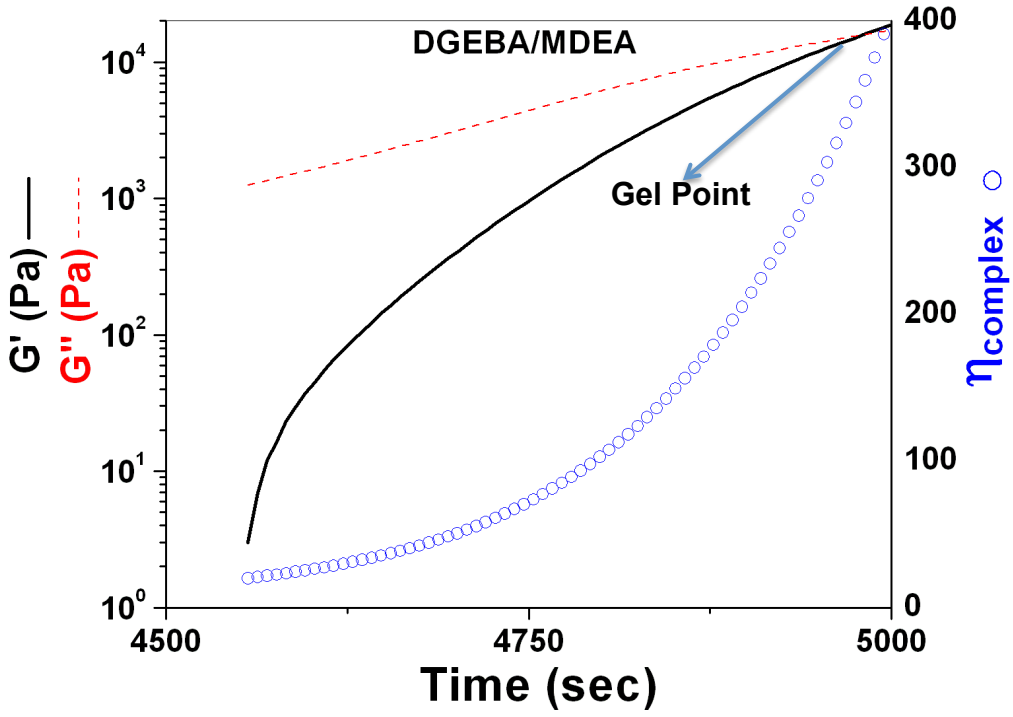

Figure 4.2. Time sweep experiment for DGEBA/MDEA matrix

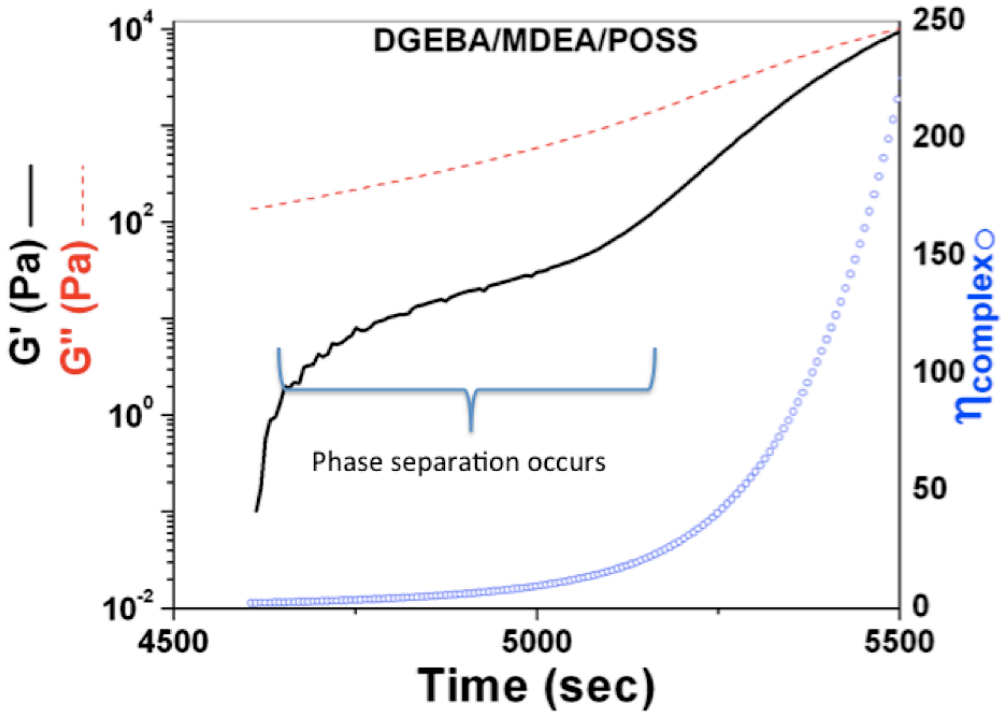

Figure 4.3. Time sweep experiment for DGEBA/MDEA/POSS

Calorimetric Calculation of the Conversion

In order to observe the conversion during polymerization, a conversion vs. time curve at 135°C for a stoichiometric DGEBA/MDEA with and without modifiers was obtained by differential scanning calorimetry (DSC). Since the epoxy/amine reaction is exothermic, the heat generated during isothermal heating is proportional to the number of bonds reacted in the system (Wasikiewicz et al., 2010). Thus, the measurements of heat developed at any time should be a direct indication of the degree of reaction (i.e. conversion) based on the equation:

$$\alpha = \frac{\Delta H_t}{\Delta H_{max}}$$

where α is the conversion, ΔH_t is the heat evolved at the time and ΔH_{max} is the total heat of reaction including residual heat.

Applying the gelation theory of Flory (1953), the degree of the reaction at the gel point can be described theoretically by the following equations.

$$\alpha_E = \left\{\frac{m_a f_a}{m_e f_e (f_a - 1)(f_e - 1)}\right\}^{1/2} \quad \alpha_A = \left\{\frac{m_e f_e}{m_a f_a (f_a - 1)(f_e - 1)}\right\}^{1/2}$$

where α is the fraction of the epoxy group that reacted at the gel point, m_e , m_a are the number of moles of epoxy (DGEBA) and hardener (MDEA), respectively and f_e , f_a are the functionality of the epoxy and amine component present, respectively.

If a stoichiometric ratio of components is used, then above equations can be written in function of the functionality only.

$$\alpha_E = \alpha_A = \alpha_{gel} = \left\{\frac{1}{(f_a - 1)(f_e - 1)}\right\}^{1/2}$$

where $\alpha_{gel}$is the extension of reaction at gel point. In the case of DGEBA and MDEA system, $f_E = 2$ and $f_a = 4$. Based on these values the theoretical conversion value was found $\alpha_{gel} = 0.57$. In the experimental work, this value was reported greater than theoretical value due to unequal reactivities of the same functional groups and intra-molecular ring formation.

Figure 4.4 shows how incorporation of POSS molecules affects the curing process in DGEBA/MDEA system. The results obtained from time sweep experiment and DSC were compared and the conversion at the time of G' and G'' cross over (close to gel point) was obtained. DGEBA/MDEA system reached the gel point around 83 min. and the conversion at

this time was measured as 0.76. The system with POSS, the conversion value was 0.79 at the time of 93 min. when the system reached its gel point. The difference between the theoretical conversion value and experimental conversion value was due to unavoidable changes of exact stoichiometry and formation of cyclic oligomers. The main finding of this graph is that POSS molecules showed a clear plateau at the low conversion indication the phase separation during the polymerization. POSS-rich domains formed during this phase separation and these domains strongly disturbed the polymerization kinetics (slower reaction) and caused reduction in the mobility of chains. The phase separation process in DGEBA/MDEA/POSS system took place in approximately 9 min. between the conversion value of 0.67 and 0.74.

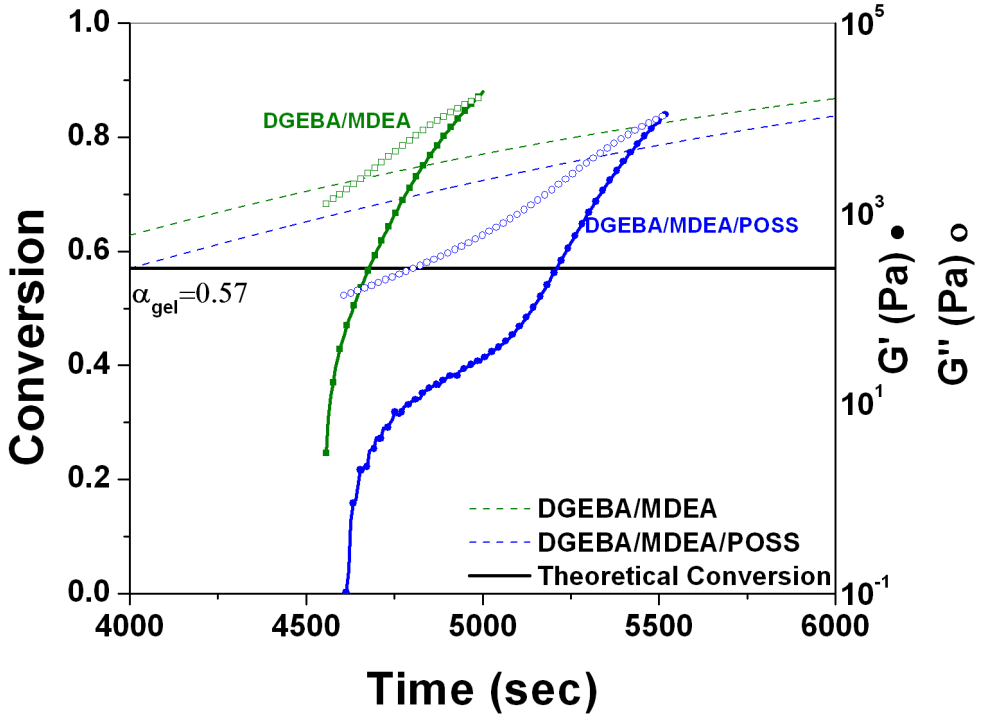

Figure 4.4. Curing analysis of DGEBA/MDEA system with and without POSS molecules

Figure 4.5 shows how single wall carbon nanotubes (SWCNT) affects the curing process of DGEBA/MDEA system. Similar to the POSS system, SWCNT system also showed a plateau at

G' which refers to phase separation. Phase separation process took place between 0.46 and 0.56 conversion during 8 min. When the system reached its gel point, the conversion was 0.64, which is lower than matrix and the system with POSS. It is possibly because that the existence of the CNTs physically obstructed the mobility of the epoxy monomers and also affected the optimized curing ratio between DGEBA and MDEA. On the other hand, SWCNTs accelerated the polymerization where the gel point was reached in 58 min. It is clear from the rheological results that CNTs caused an acceleration effect on the epoxy reaction at the initial stage of curing. Similar results on the different effects of SWCNTs on the curing kinetics were discussed by Puglia et al. (2003), as well. They showed that SWCNTs accelerated the curing at DGEBA/DETA system. They explained the increase in terms of the extremely high thermal conductivity of nanotubes and their high surface area for heat propagation.

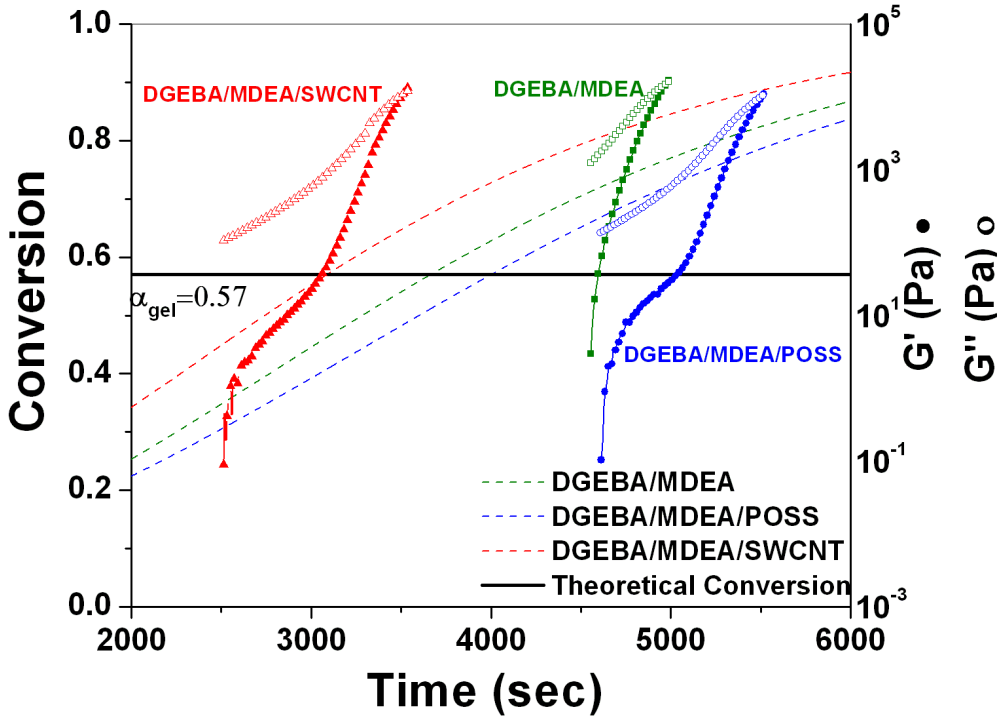

Figure 4.5. Curing analysis of DGEBA/MDEA with POSS and SWCNT

Figure 4.6 shows the curing analysis of DGEBA/MDEA/SWCNT system with and without POSS molecules. In both systems, phase separation occurred with the addition of modifiers. They system with POSS molecules showed phase separation during 8min., between the conversion value of 0.45 and 0.53. This result shows that the incorporation of POSS molecules did not extend the phase separation time and did not show a considerable change in conversion. However, the addition of POSS molecules increased the time to reach the gel point. While the system with POSS molecules reached the gel time at 62 min., the gel time for the system without POSS molecules was 58 min. Both systems showed a conversion around 0.64 at the gel point. As it is mentioned above, the incorporation of POSS molecules slowed down the reaction. However, the polymerization occurred earlier than DGEBA/MDEA system by the incorporation of SWCNTs, because of the high thermal conductivity of nanotubes.

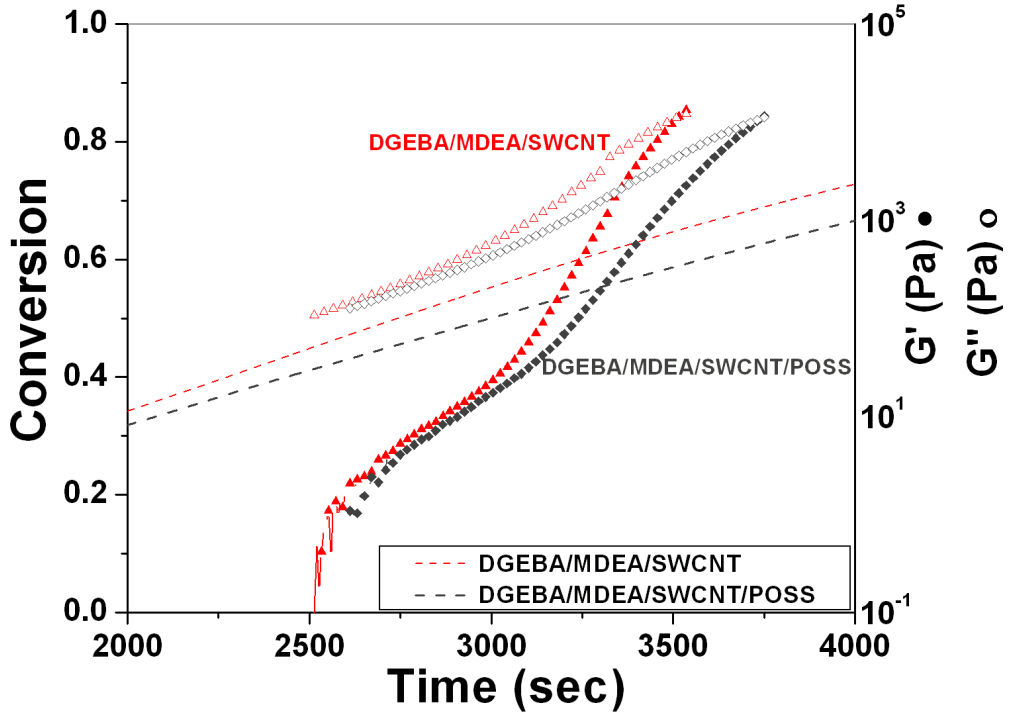

Figure 4.6. The curing analysis of DGEBA/MDEA/SWCNT with and without POSS

Incorporation of functionalized carbon nanotubes into the system affects the curing kinetics and rheological behavior. Attached functional group may participate in curing reaction and change the conversion of curing reaction. For instance, Qiua et al. (2010) showed that functionalization of carbon nanotubes has two-edge effects on the reaction kinetics; first, the change in the size of interface due to functionalization and second the reaction between the functional group and polymer. They reported that amino functionalized SWCNTs increased the activation energy of the system, while epoxide functionalized SWCNTs decreased the activation energy of the system.

In Figure 4.7, the effect of acid functionalization on the kinetics and rheology of the DGEBA/system was studied. Adding acidified SWCTNs into the system accelerated the polymerization. Similar to the pure SWCNT epoxy system, the mixture with acidified SWCNTs also showed phase separation in DGEBA/MDEA system. However, acidified SWCNTs showed a longer plateau, so that, longer phase separation of domains. The phase separation process took place for approximately 23 min., at a starting conversion value of 0.47 and finished at 0.72. This longer phase separation process can be explained by the good dispersion of carbon nanotubes in the system. On the other hand, acidified SWCNTs showed a conversion value of 0.77 at gel point, which is higher than unmodified SWCNT system due to the possible reaction between the acid groups and the matrix. This reaction can increase the cross-linking density and thus, decrease the mobility of chains.

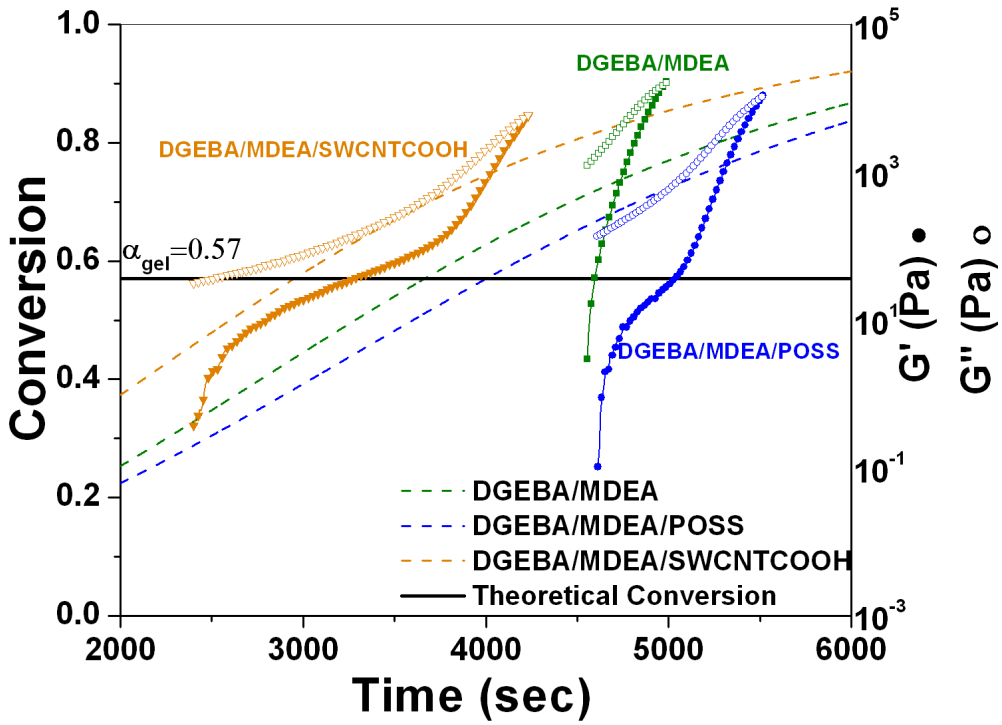

Figure 4.7. Curing analysis of DGEBA/MDEA with POSS and SWCNT-COOH

Figure 4.8 shows how POSS molecules affect the curing of DGEBA/MDEA/SWCNTCOOH system. As it was observed on the previous systems, adding POSS molecules into the system slowed down the polymerization reaction. It needs to be noted that a plateau (solid-like behavior) was observed in G' from the beginning of the experiment. This solid-like behavior occurred because of the increased viscosity of the system after adding POSS molecules that showed higher resistance against flow and thus an increase in the storage modulus. However, it is not clear on the rheological results whether phase separation occurred after incorporation of POSS molecules.

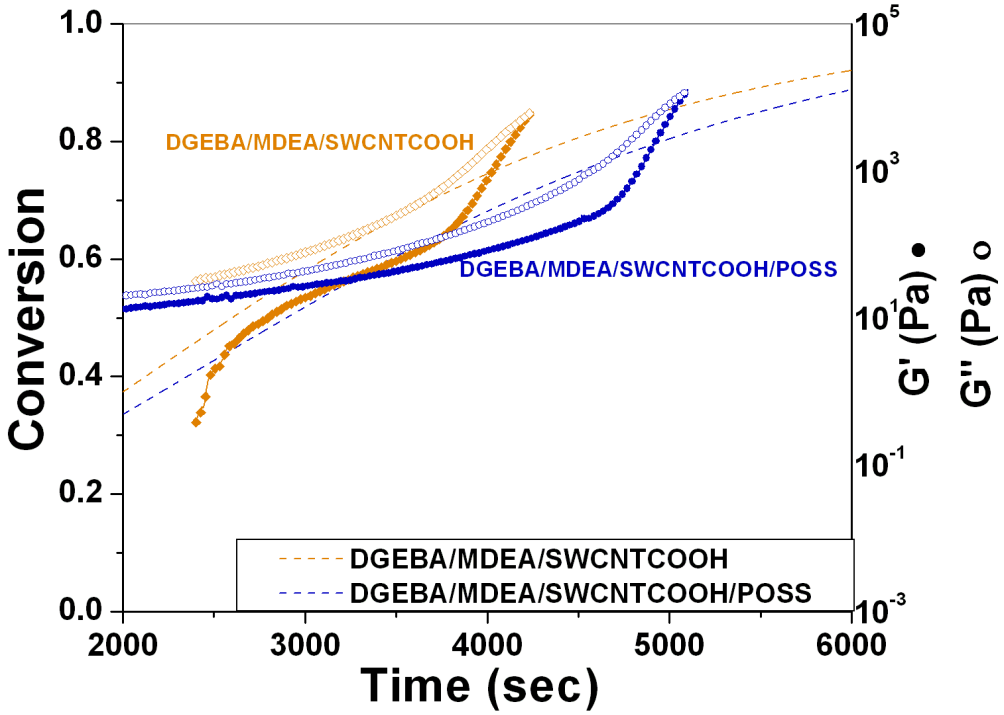

Figure 4.8. The curing analysis of DGEBA/MDEA/SWCNT-COOH with and without POSS

The difference in curing of the unmodified and the acidified system was shown in Figure 4.9. Compared to the unmodified SWCNT system, acidified system showed higher conversion (0.64, 0.77. respectively). The DSC analysis showed that incorporation of acidified system accelerated the system. However, the rheological analysis showed that the solution reached its gel point later than pristine system. This difference might be due to longer phase separation process took place in the acidified system. Moreover, unmodified SWCNT system had lower conversion than acidified SWCNT system. Since CNTs are in the same size scale of epoxy molecules and disturb the curing reactions by influence the molecular diffusivity, unmodified SWCNTs reduced the conversion of curing reaction. However, acidified SWCNTs counteract this effect and increase the conversion.

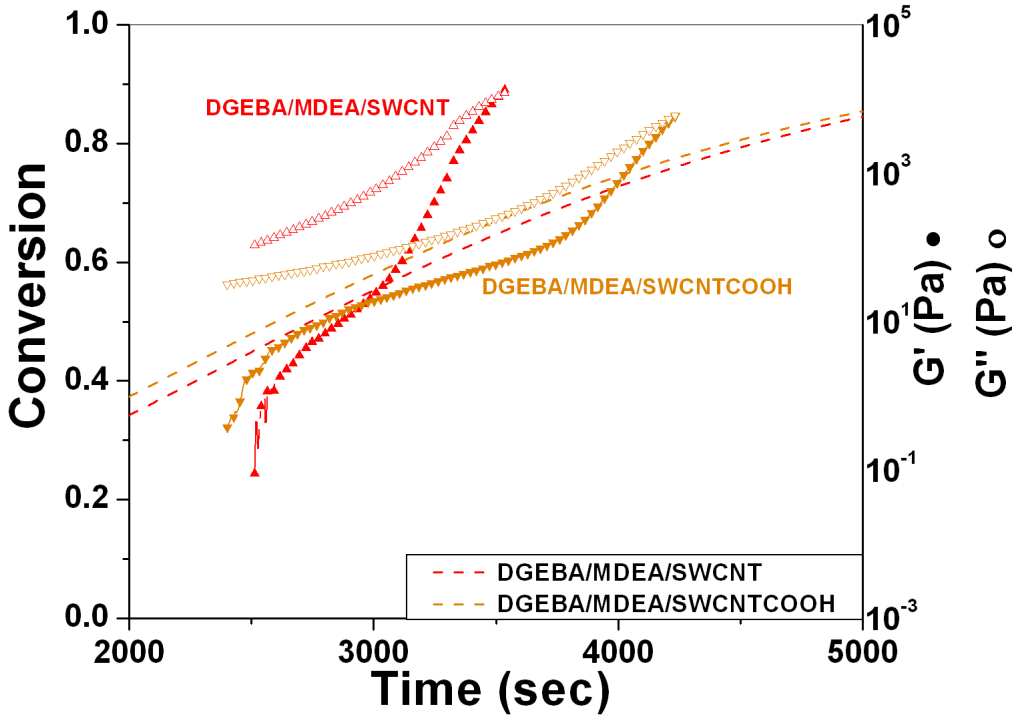

Figure 4.9. The curing analysis of DGEBA/MDEA/SWCNT and DGEBA/MDEA/SWCNT-COOH

Figure 4.10 shows the conversion of DGEBA/MDEA system during curing process with esterified SWCNTs (SWCNT-PGE). Similar to the first two systems, esterified SWCNT systems also showed a phase separation plateau and acceleration in the polymerization. The system started to show phase separation at conversion of 0.50 and it reached the end at the conversion of 0.69. Phase separation process took place during 19 min. However, incorporation of SWCNT-PGE did not affect the conversion at the gel point compared to the matrix. The reason might be the existence of similar functional groups between SWCNT-PGE and epoxy matrix. Tao et al. also studied the effect of SWCNT in DGEBF/DETD epoxy system and they just observed a small difference in conversion by adding the SWCNTs during their isothermal DSC run.

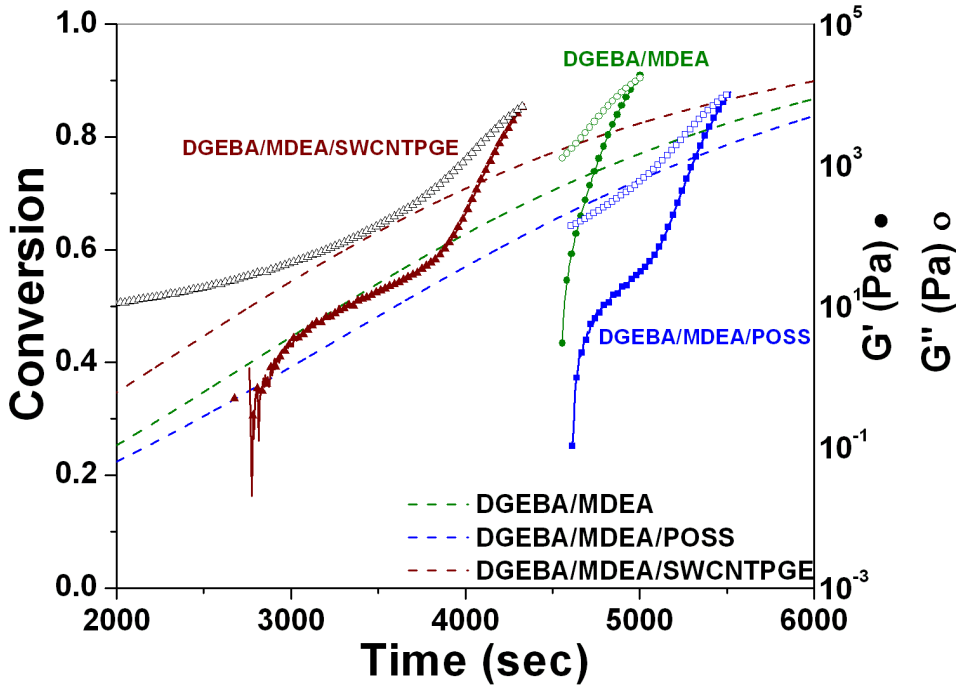

Figure 4.10. Curing analysis of DGEBA/MDEA with POSS and SWCNT-PGE

Figure 4.11 shows how POSS molecules affect the curing of DGEBA/MDEA/SWCNTPGE system. Similar to the first two systems, incorporation of POSS molecules retarded the polymerization. Both systems showed same duration of phase separation process and the phase separation took place between similar conversion values. Similar to the acidified system, adding POSS molecules increased the conversion of the system at the gel point. As it was mentioned in the experimental section, POSS molecules used in this study are monofunctional molecules with an epoxy group attached to the chemical structure. The reason for the higher conversion might be the interaction between these groups and esterified SWCNTs that created more reacted domains in the system.

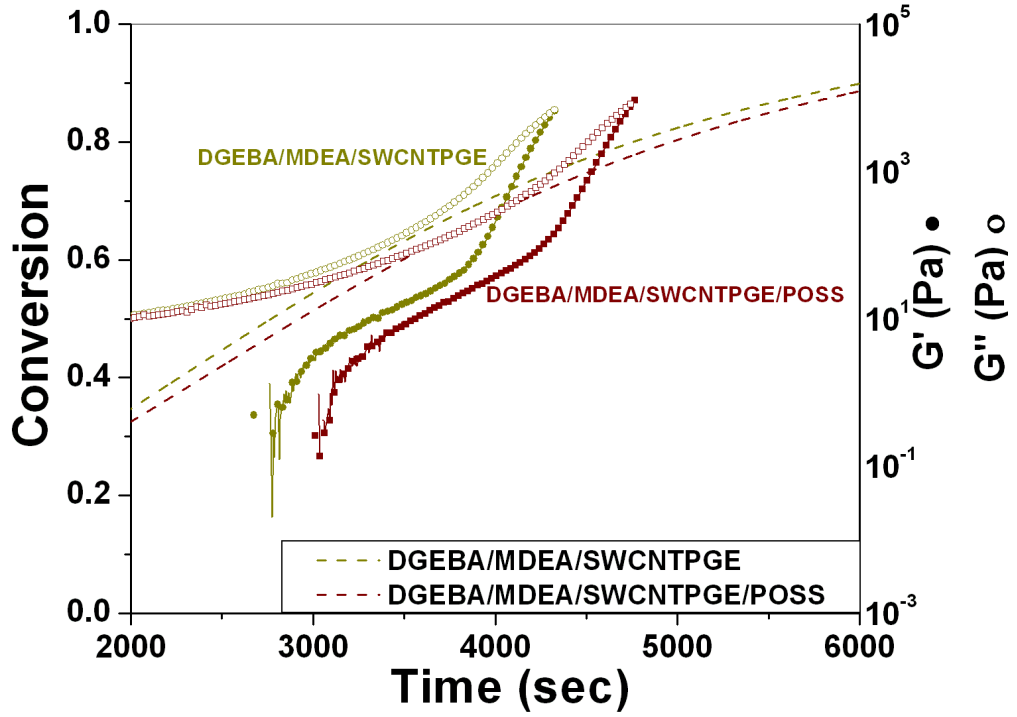

Figure 4.11. The curing analysis of DGEBA/MDEA/SWCNT-PGE with and without POSS

In previous sections, the curing analysis of DGEBA/MDEA with unmodified, acidified and esterified SWCNT was discussed. Results were summarized in Table 4.1. The main idea of this research was to analyze whether this phase separation process can be used as a tool to obtain well-dispersed carbon nanotubes in epoxy system. To do that, SWCNTs were functionalized with monofunctional POSS molecules. It was already mentioned that monofunctional POSS molecules are not different than other fillers such as rubber, thermoplastics or liquid crystals that induce the phase separation. In this section, the curing analysis of POSS functionalized SWCNTs was studied.

Table 4.1. Curing analysis of DGEBA/MDEA system with and without modifiers (PS refers to Phase separation, α_1 and α_2 are the conversion at the beginning and end of the phase separation, respectively, α_g is the conversion at the gel point)

	Time at Gel Point (min)	Time at Visual (min)	α_g	Duration of PS (min)	α_1	α_2
Epoxy MDEA	83	85	0.76	-	-	-
Epoxy MDEA POSS	93	95	0.79	9	0.67	0.74
Pure SWCNT	58	62	0.64	8	0.46	0.56
Pure SWCNT-POSS	62	65	0.62	8	0.45	0.53
SWCNT-COOH	71	72	0.77	23	0.47	0.72
SWCNT-COOH-POSS	85	86	0.81	-	-	-
SWCNT-POSS	76	76	0.79	32	0.38	0.73
SWCNT-PGE	72	72	0.75	19	0.50	0.69
SWCNT-PGE-POSS	80	81	0.78	19	0.51	0.70

Figure 4.12 shows how POSS functionalized SWCNTs affect the curing of DGEBA/MDEA system. Incorporation of POSS functionalized SWCNTs created domains that caused phase separation. This system showed the longest phase separation process which is around 32 min. and phase separation occurred at the conversion value of 0.38 to 0.73. It needs to be noted that as the only adding POSS molecules slowed down the polymerization, whereas POSS functionalized SWCNTs accelerated the polymerization and compared to the matrix, system showed a higher conversion value at the gel point.

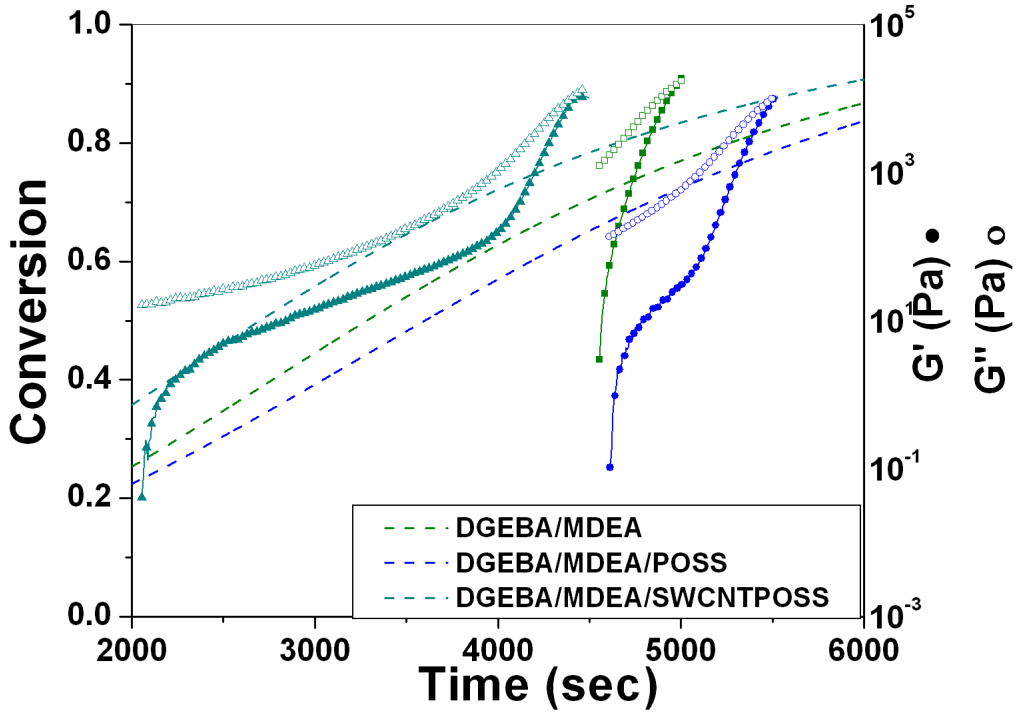

Figure 4.12. Curing analysis of DGEBA/MDEA with POSS functionalized SWCNTs (SWCNT-POSS)

Based on the results obtained from curing analysis with DSC and rheometer, it is known that incorporation of POSS functionalized SWCNTs showed a clear and the longest phase separation process. Since these two methods (DSC, rheology) are not similar experimental methods, a visual analysis was also performed to compare the conversion values. Whether this phase separation process improved the dispersion of SWCNTs and potentially provided effective percolation compared to the other functionalization methods will be discussed with SEM images and DMA experiments.

4.3.2 SEM Analysis

SEM micrographs of cured DGEBA/MDEA and DGEBA/MDEA/POSS system were shown in Figure 4.13 and 4.14, respectively. After adding POSS molecules into the DGEBA/MDEA, rich POSS domains were observed. Those dispersed individual domains were spherical with sizes in the range of several micrometers. These are typical results for polymerization induced phase separation through a nucleation growth coarsening mechanism.

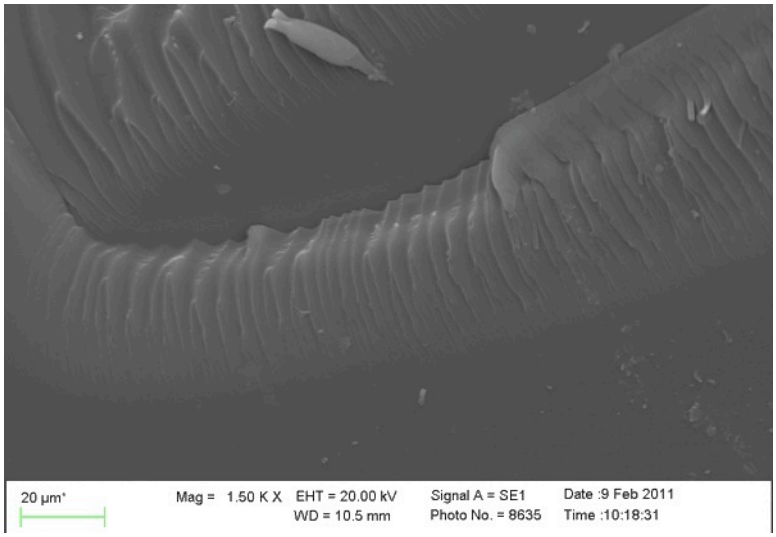

Figure 4.13. SEM image of DGEBA/MDEA system

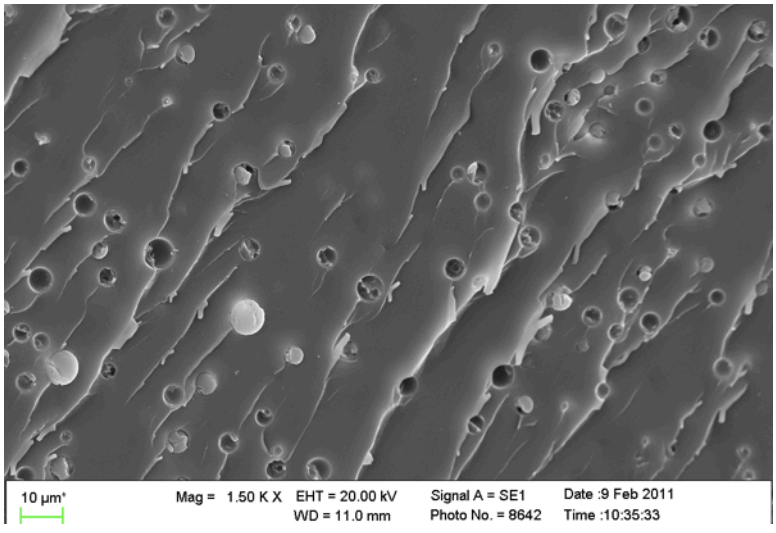

Figure 4.14. SEM image of DGEBA/MDEA/POSS system

In the SEM images of DGEBA/MDEA/POSS system (Figure 4.14), a rougher surface, that contains many small smooth regions, was observed compared to the matrix. Smooth regions formed partly oval areas in the materials that localized during the deformation. These oval areas can be considered as second-phased POSS domains. Higher magnification of SEM images of DGEBA/MDEA/POSS system (Figure 4.15) also showed that during the failure process, the crack propagation stopped or changed the direction as it crossed the POSS-rich domains. It also needs to be noted that POSS rich domains did not create a good adhesion with epoxy matrix.

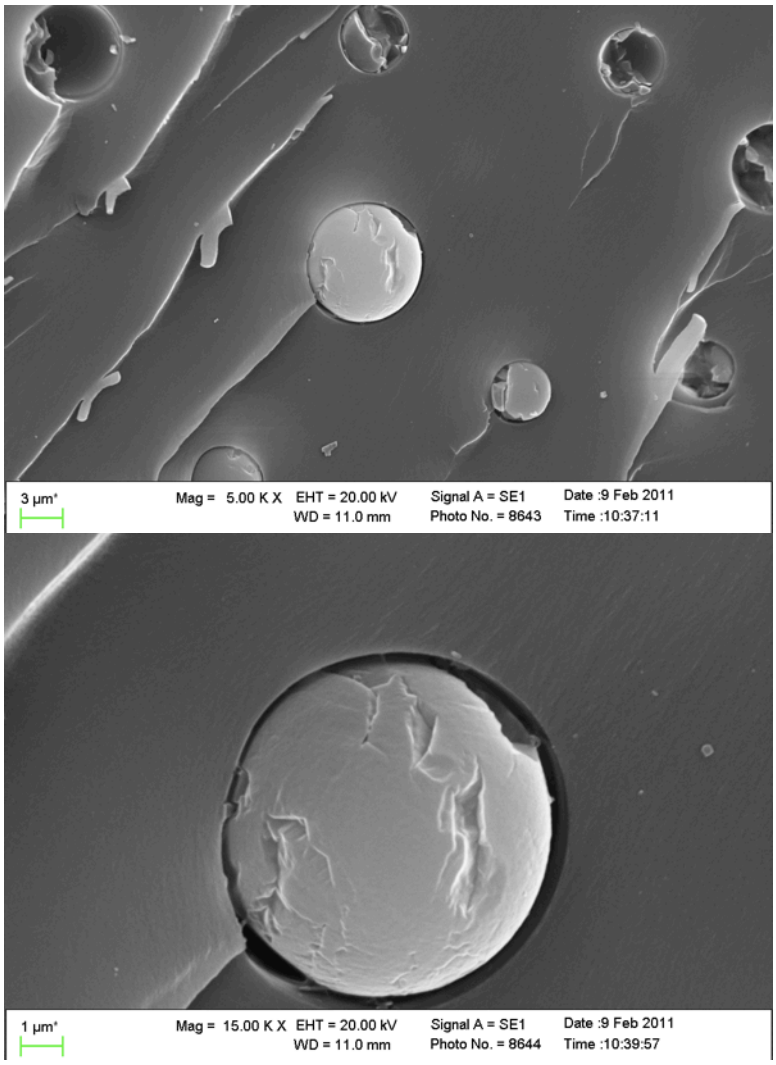

Figure 4.15. SEM images of DGEBA/MDEA/POSS composites (a) 5 KX, (b) 15 KX

In Figure 4.16, SEM images of DGEBA/MDEA/SWCNT system with POSS molecules were shown. Similar to the DGEBA/MDEA/POSS system, domains of POSS aggregates were observed. SWCNTs could not be observed due to their smaller size. However, in Figure 4.16 (c), it can be clearly observed that POSS molecules with SWCNTs had better adhesion to the polymer matrix compared to the system without SWCNTs. This result also confirms that adding SWCNTs into the system accelerated the polymerization and increased crosslinking. Thus, monofunctional POSS molecules with SWCNTs created better adhesion with matrix through chemical bonding.

On the other hand, the system with only pure SWCNTs showed aggregation of SWCNT bundles. This agglomeration can be explained as the high interaction between the nanotubes due to their nanoscale size. Same behavior was also shown in Chapter 3 with a different hardener system (DGEBA/T-403). Higher magnification SEM image of this system also shows SWCNT bundles around 70-80 nm (Figure 4.17c). However, DGEBA/MDEA/SWCNT system showed phase separation during the polymerization that confirms the results from rheological analysis (Figure 4.17).

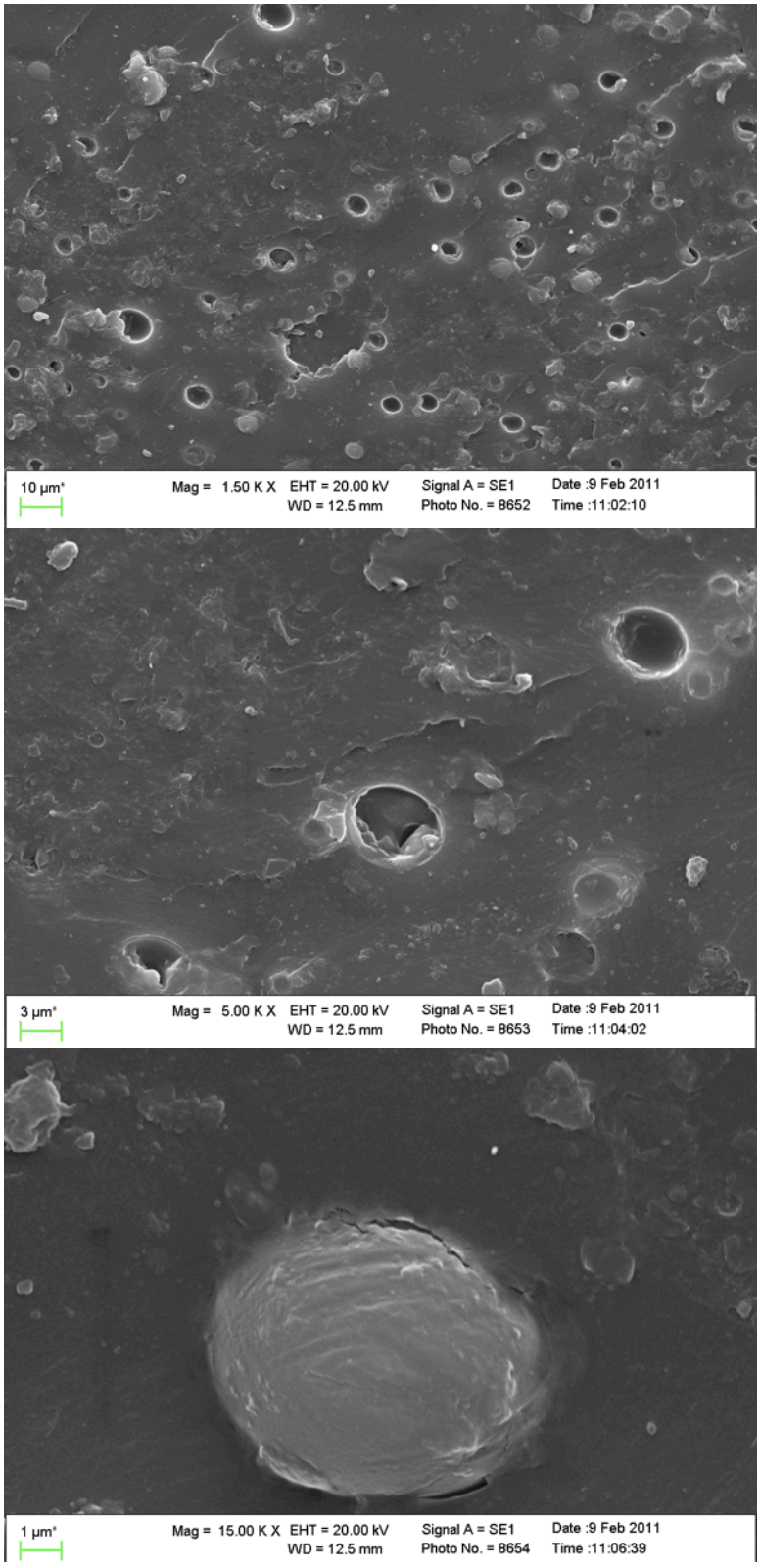

Figure 4.16. SEM images of DGEBA/MDEA/SWCNT/POSS (a) 1.5 KX, (b) 5 KX, (c) 15 KX

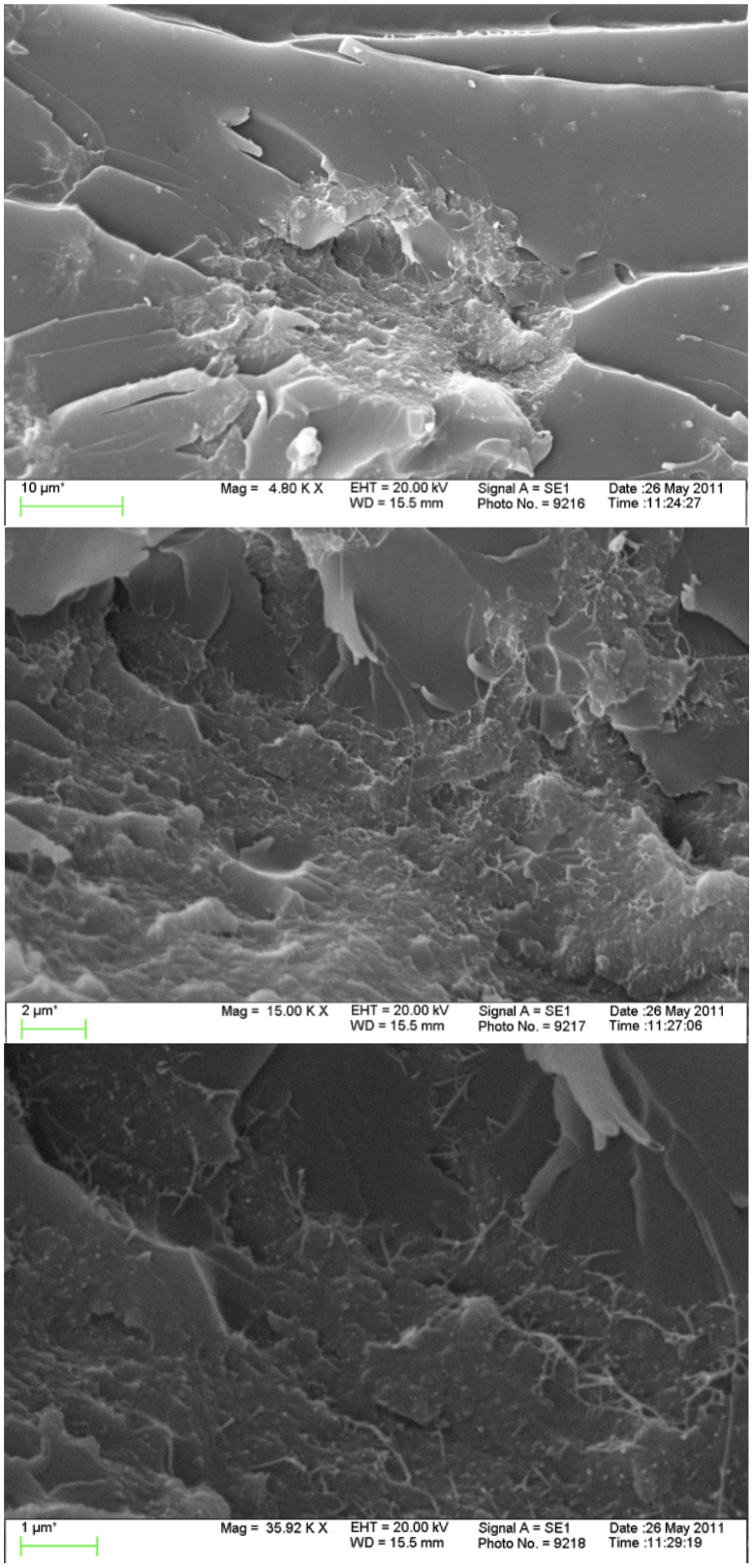

Figure 4.17. SEM images of DGEBA/MDEA/SWCNT (a) 4.8 KX, (b) 15 KX, (c) 35 KX

Figure 4.18 shows the SEM image of DGEBA/MDEA system with acidified SWCNTs. It was observed that a clear phase separation process took place during the polymerization of this system. This result also proves the results obtained from rheological analysis. Moreover, some domains of aggregated SWCNTs were observed. This result was unexpected based on the information that we obtained from Chapter 3. However, phase separation process in this system might cause a bad dispersion of SWCNTs in the epoxy matrix.

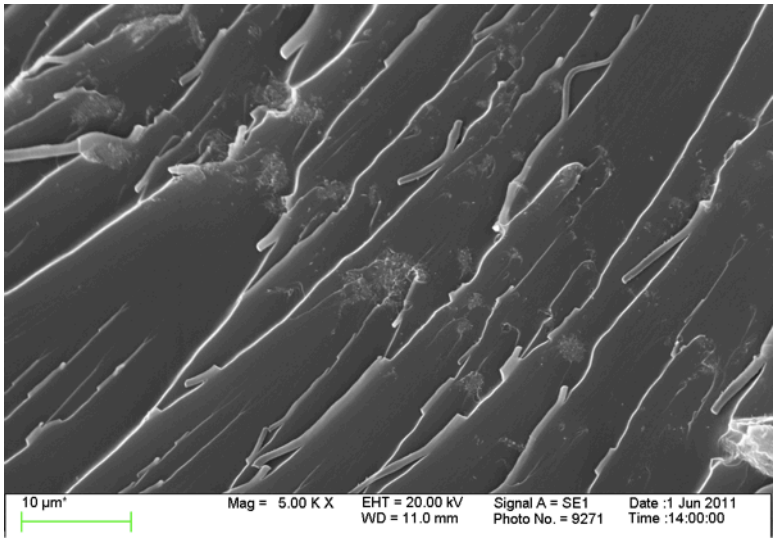

Figure 4.18. SEM image of DGEBA/MDEA/SWCNTCOOH system

Figure 4.19 shows the SEM images of DGEBA/MDEA system with POSS functionalized SWCNTs. Compared to the systems with only POSS molecules, spherical could be observed. It is due to the fact that the small fraction of POSS molecules was attached onto the 1 wt% SWCNTs. Similar to the systems with only POSS and only SWCNTs, this system also showed a rougher surface compared to matrix. Small domains of SWCNT bundles were also observed. In the rheological analysis, phase separation was observed for POSS functionalized SWCNT system. This result was confirmed after the SEM images that showed phase separation in the system after the curing process.

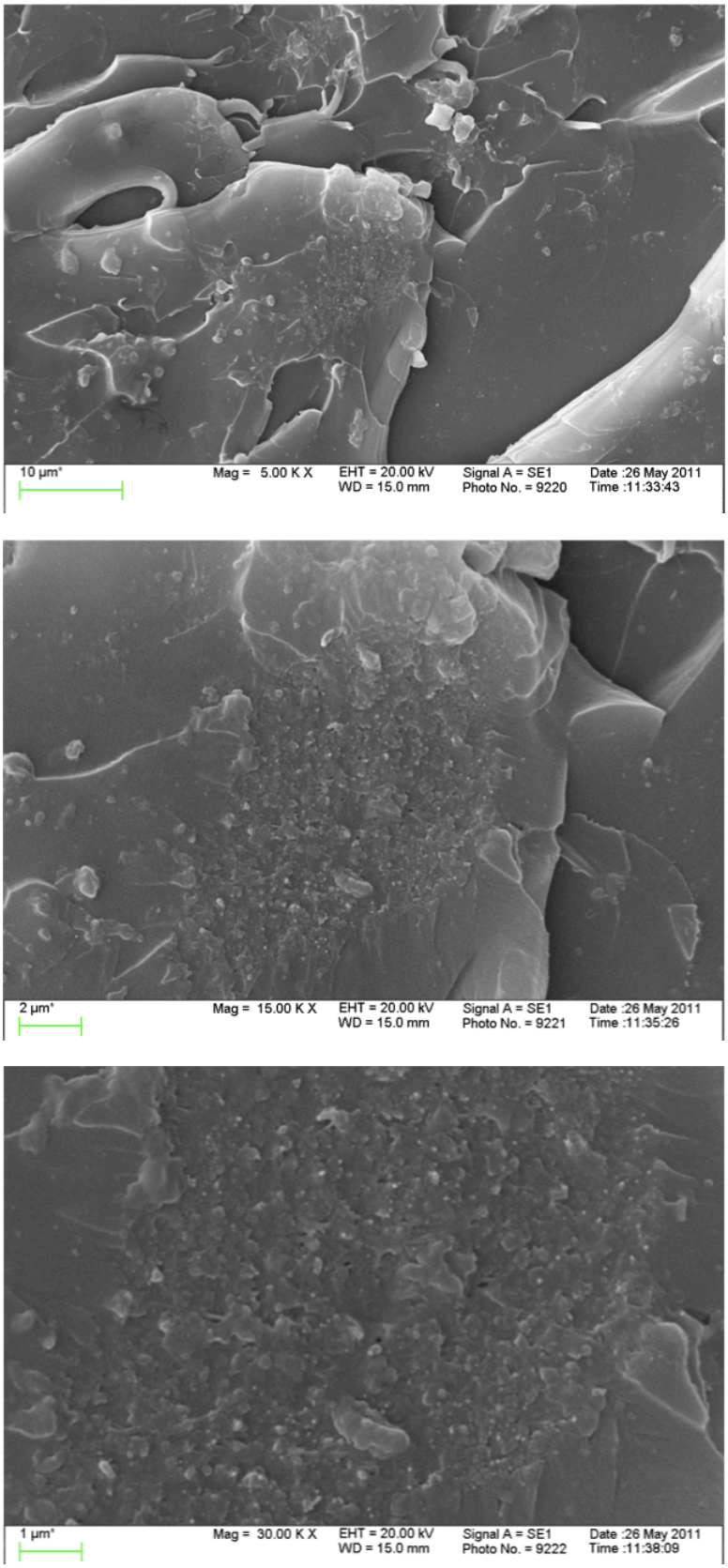

Figure 4.19. SEM images of DGEBA/MDEA/SWCNT-POSS (a) 5 KX, (b) 15 KX, (c) 30 KX

4.3.3 Dynamic Mechanical Analysis

DMA plots in Figure 4.20 show the storage modulus (E') versus temperature for DGEBA/MDEA matrix and modified systems with SWCNT and POSS molecules. It was observed that incorporation of POSS molecules decreased the storage modulus, as well as adding acidified and POSS functionalized SWCNTs. However, at room temperature, the highest modulus was observed for matrix and DGEBA/MDEA/SWCNT systems. The lowest modulus was observed after POSS molecules added into the SWCNT system. In the literature, while some groups reported increase in storage modulus, some groups reported decrease (Qiua et al., 2010, Puglia et al., 2003). This difference can be due to different hardener and matrix, dissimilar dispersion techniques and also unlike filler structures. Based on our findings, the decrease in storage modulus compared to the matrix can be related to the bad dispersion of fillers in the polymer matrix.

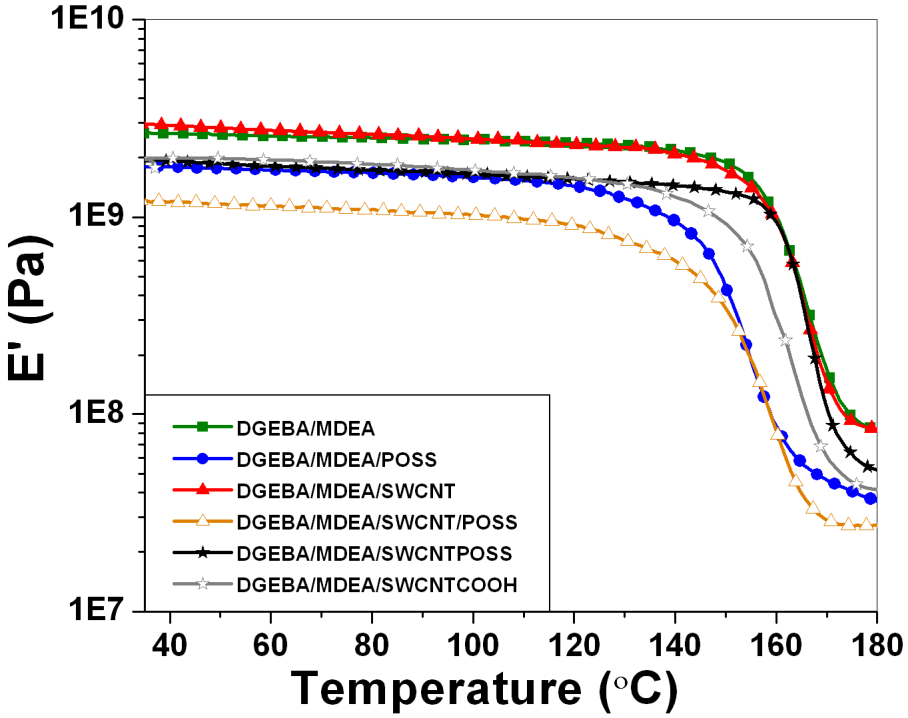

Figure 4.20. Storage modulus (E') vs. Temperature for DGEBA/MDEA systems

Figure 4.21 shows the DMA plots of tan delta versus temperature for the DGEBA/MDEA system with and without POSS molecules and SWCNTs. The glass transition temperature, T_g, was taken as the peak temperature in tan delta curves as presented in Table 4.2.

Table 4.2. DMA results for DGEBA/MDEA with and without modifiers

	E'	% increase in E'	T_g (C)
DGEBA/MDEA	2.64887E9	-	168
DGEBA/MDEA/POSS	1.79431E9	-32	158
DGEBA/MDEA/SWCNT	2.90774E9	9.7	168
DGEBA/MDEA/SWCNT/POSS	1.19721E9	-54.8	162
DGEBA/MDEA/SWCNT-POSS	1.9239E9	-27.4	169
DGEBA/MDEA/SWCNT-COOH	1.99E9	-24.9	165

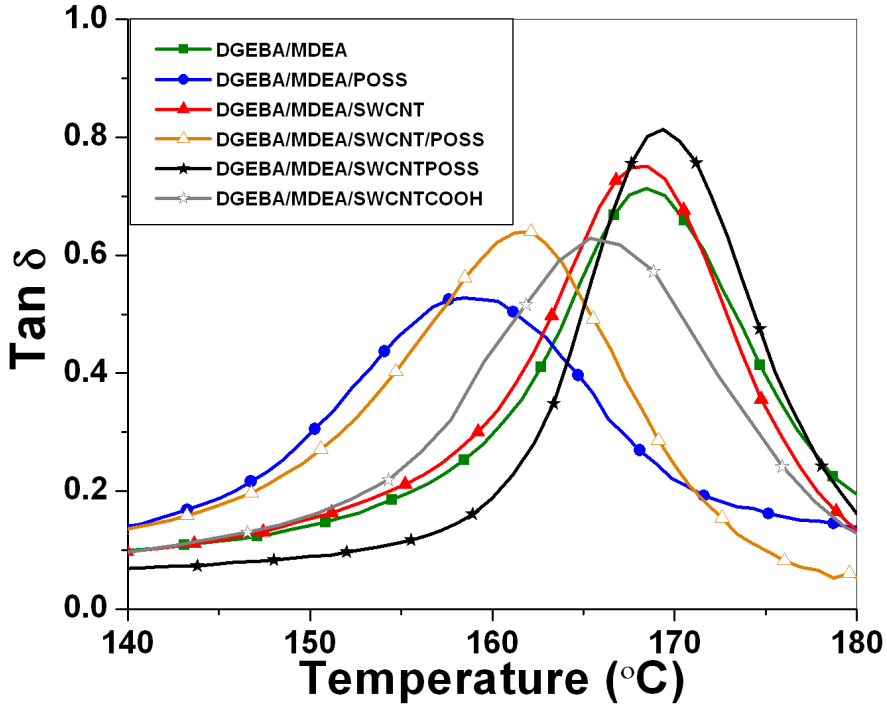

Figure 4.21. Tan δ vs. Temperature for DGEBA/MDEA systems

The glass transition temperature of DGEBA/MDEA system decreased after incorporation of POSS molecules. This can be explained by the fact of POSS molecules reduced the polymer chain interactions and interrupt the crosslinking formation during curing reaction. This result can be also confirmed with the rheological data obtained through curing process showing that POSS molecules slowed down the polymerization.

On the other hand, the glass transition temperature of the systems with unmodified, acidified and POSS functionalized SWCNTs kept the similar glass transition temperature with matrix. These results also confirm the rheological data that adding SWCNTs into the system created faster polymerization kinetics and higher crosslinking densities. Even though adding SWCNTs into the system might creates non-stoichiometric regions where a decrease in T_g is expected, because of their assistance to crosslinking process, the glass transition temperature kept the same value with matrix. It is also interesting that adding POSS molecules into the DGEBA/MDEA/SWCNT system also decreased the glass transition temperature. However, this system showed higher T_g compared to the DGEBA/MDEA/POSS system.

4.4 CONCLUSION

In this chapter, the epoxy network DGEBA/MDEA was modified by monofunctional POSS units as well as unmodified, acidified, esterified and POSS functionalized SWCNTs. The curing analysis of these systems was studied through rheology, DSC and visual observations. The time where the gel point was reached and the conversion at that time were calculated. It was observed that adding POSS molecules slowed down the polymerization process, however they did not have any effect on the conversion value. On the other hand, incorporation of SWCNTs accelerated the polymerization because of the high thermal conductivity of nanotubes. Unmodified SWCNTs showed lower conversion value due to the hindrance effect on the crosslinking process. However, acidified and esterified system did not create a significant change on the conversion because of the side reaction with the epoxy/amine system. The main finding of this research is that all these systems with fillers showed a plateau at G' before the gel point that refers to the phase separation.

By using these results and confirming that phase separation may take place in DGEBA/MDEA system with the incorporation of POSS and SWCNTs, POSS functionalized SWCNTs were prepared and characterized. After rheological experiences, it was observed that this system also showed phase separation and accelerated the polymerization. Compared to the matrix, higher conversion value was observed. After confirming the existence of phase separation, whether this phase separation process could help the dispersion of SWCNTs and created an effective percolation was discussed with SEM images and DMA analysis.

SEM images of these system showed that adding POSS molecules into the system created spherical domains that were result of phase separation process. Moreover, these systems showed rougher surface compared to the epoxy matrix. It is notable that pure SWCNT system and POSS functionalized SWCNTs showed phase separation process. However, pure SWCNT system showed clear nanotube bundles around the size of 70 nm. On the other hand, small domain of bundles were observed at the POSS functionalized SWCNT system.

During DMA experiments, it was expected to observe a higher storage modulus value compared to the matrix for the systems with acidified SWCNTs and POSS functionalized SWCNTs. However, both systems showed decrease in storage modulus at both glassy and rubbery regions. The system with pure SWCNT showed similar storage modulus with the epoxy matrix. It is notable that incorporation of only POSS molecules decreased the glass transition temperature while the incorporation of nanotubes did not have any harmful effect on the glass transition temperature. This shows that POSS molecules acted like a plasticizer in the system and it also confirms the results obtained from rheological analysis and DSC.

REFERENCES

1. Williams R.J.J., Rozenberg B.A., Pascault J.P., " Reaction-induced phase separation in modified thermosetting polymers", Advances in Polymer Science, Vol.128, 1997

2. Elicabe G.E., Larrondo H.A., Williams R.J.J, "Polymerization-induced phase separation: A maximum in the intensity of scattered light associated with a nucleation-growth mechanism", Macromolecules, 30, 6550-6555, 1997

3. Sperling L. H., "Introduction to physical polymer science", Wiley Interscience, 4th edition, 2006

4. William R.J.J., Borrajo J., Adabbo H.E., Rojas A.J., "Rubber modified thermoset resins", Am Chem Soc, 195, 1984

5. Zucchi I. A., Hoppe C.E., Galante M.J., Williams R.J.J., Quintela L.M.A., Matejka L., Slouf M., Plestil J., "Self-assembly of gold nanoparticles as colloidal crystals induced by polymerization of amphiphilic monomers", Macromolecules, 41, 4895-4903, 2008

6. Auad L.M., Nutt S.R., Stefani P.M., Aranguren M.I., "Rheological study of the curing kinetics of epoxy-phenol novolac resin", J. Applied Science, Vol. 102, 4430-4439, 2006

7. Wasikiewicz J.M., Yeates S.G., "Determination of gel point of epoxy thermosets via electric resistance measurements", Macromol. Eng., 295, 511-514, 2010

8. Flory P.J., "Principles of Polymer Chemistry", Cornell University, Ithaca, N.Y. 1953

9. Puglia D., Valentini L., Armentano I., Kenny J.M., "Effects of single-walled carbon nanotube incorporation on the cure reaction of epoxy resin and its detection by Raman spectroscopy", Diamond and Related Materials 12, 827–832, 2003

10. Qiua J., Wang S., "Reaction kinetics of functionalized carbon nanotubes reinforced polymer composites", Materials Chemistry and Physics 121, 295–301, 2010

CHAPTER 5

EFFECT OF INTERPHASE IN EPOXY NANOCOMPOSITES

5.1 INTRODUCTION

Nanocomposite technology is taking advantage of the high strength and high stiffness of nanofillers, which are combined with matrix materials of similar/ dissimilar natures in various ways, creating unavoidable interfaces. In polymer nanocomposites, both the nanofiller and the matrix retain their original physical and chemical identities. Final properties of these materials depend primarily on the characteristics of the filler, polymer and the interphase between the filler and the polymer (Andrews et al., 2004). Among these factors, the effectiveness of the interphase plays a predominant role in the nanocomposite properties. In particular, there is a lack of understanding of processes occurring at the atomic level of the interphase region and how these processes influence the final material behavior.

As a definition, the interphase is the geometrical area of the classic fiber-matrix contact as well as the region of finite volume extending therefrom. In this region, the chemical, physical and mechanical properties vary either continuously or in a stepwise manner between the bulk fiber and matrix material (Drzal et al., 1993 and 2004,). Even though, the size of the interphase has not been studied in detail, the interphase size has been reported to be as small as 2 nm and as large as about 50 nm (Schadler et al., 1998). Even if the interphase is only a few nanometers, very

quickly the entire polymer matrix may have a different behavior than the bulk. If the interfacial region is more extended, then the polymer matrix behavior can be altered even at low loadings (i.e., at the percolation condition of the system). This interfacial area provides an opportunity for altering the mobility and properties in this zone (i.e., the interphase region). Therefore, by controlling the degree of interaction between the polymer and the nanofiller, the properties of the entire matrix can be controlled. With improved dispersion of the nanotubes in the polymer matrix, the influence of this region can be increased (Putz et al., 2008, Schadler et al., 1998).

As it is mentioned in previous chapters, the intrinsic Van der Waals attraction between nanotubes holds them together as bundles and ropes in most solvents and polymers. It is also discussed that the functionalization of carbon nanotubes can provide adequate dispersions of carbon nanotubes in polymers in particular epoxy precursors. When nanotubes are bundled, they stand as macro-fillers with less the available surface area. With improved dispersion through functionalization, the nanotubes can be separated from each other and available surface area can be increased. However, the generation of a high surface area per unit volume introduces a new problem into consideration related to the partitioning of the epoxy monomer and hardener at the carbon interface. Although it is already known that in conventional epoxy composites a non-stoichiometric region may be formed at the fiber interface, the use of nanotubes extends the area of the interphase region that influences the properties of epoxy nanocomposites. Variations in stoichiometry may be produced by the preferential physical adsorption of one of the monomers at the interface or by chemical reaction with a functional group previously attached to the carbon surface.

In particular, the glass-transition temperature (T_g), one of the most important design parameter for the engineering application of polymers, can be largely influenced by the interphase. In the literature, substantial changes in the glass transition temperature have been reported depending on the nature of the matrix-filler interaction because of alteration of the mobility and the composition of the polymer chains in the interphase region. Miyagawa and Drzal (2004) reported a decrease of about 70 ºC in the glass transition temperature of an epoxy/anhydride formulation produced by the dispersion of 0.5 wt % fluorinated-SWCNT. A broadening of the tan δ peak was also observed. This was assigned to adsorption of the epoxy monomer at the SWCNT interface that produced a decrease of the crosslink density of the anhydride-rich matrix and was corroborated by the decrease of the rubbery modulus with the amount of SWCNT in the composite.

A significant decrease in the glass transition temperature by the addition of amine-functionalized MWCNT to an epoxy-amine matrix was also reported by Shen et al. (2007). Abdalla et al. (2007) reported the presence of a shoulder in the tan δ peak of an epoxy/amine matrix containing MWCNT functionalized with COOH groups. The relaxation behavior was attributed to a physical partitioning effect in which the presence of MWCNT interrupts the local stoichiometry. A slight drop in the T_g of an epoxy/amine matrix by the addition of unmodified SWCNT was recently reported by Sun et al. (2008). The proposed explanation was the alteration of the stoichiometric ratio by preferential adsorption of one of the monomers at the fiber interface.

The main goal of this chapter is to analyze the interphase of epoxy/nanotube nanocomposites measuring the changes in the thermo-mechanical properties. Whether partitioning of monomers at the nanofiller interface or phase separation occurs for a typical epoxy/amine formulation will be discussed. The analysis will be performed for three types of nanofillers: SWCNT, MWCNT and carbon nanofibers (CNF) with three types of functionalization: unmodified, oxidized (functionalized with COOH groups), and esterified (by reaction of COOH groups with phenyl glycidyl ether). Furthermore, the effects of these fillers on the flexural properties of epoxy nanocomposites were evaluated.

5.2 EXPERIMENTAL

5.2.1 Materials

Single-wall and multi-wall carbon nanotubes were purchased from NTP (Nanotech Port, Shenzhen, China). Technical specifications of SWCNT were a diameter < 2 nm, length < 20 μm, purity of CNTs >90%, amorphous carbon < 5%. For MWCNT, the diameter range was 40– 60 nm, the length range was 5–15 μm, and the purity was 95%. The CNFs were provided by Pyrograf Products (Pyrograf III PR-19, PS Grade). The diameter was comprised between 100 and 200 nm, and the length was in the range of 30–100 μm. The PS grade of CNF is characterized by the presence of a chemically vapor deposited layer of carbon over a graphite tubular core. The selection of PS grade of CNF intended to investigate the effect of a non-graphitic surface on the partitioning of epoxy precursors.

5.2.2 Sample Preparation

The epoxy/amine matrix was formulated using an epoxy monomer based on diglycidyl ether of bisphenol A (DGEBA, Epon 828, Miller-Stephenson) and a polyether triamine (Jeffamine T-403, Huntsman) as hardener (Figure 5.1). Esterification of oxidized nanotubes and nanofibers was performed using PGE (Aldrich) and triphenyl phosphine (TPP, Aldrich) as catalyst.

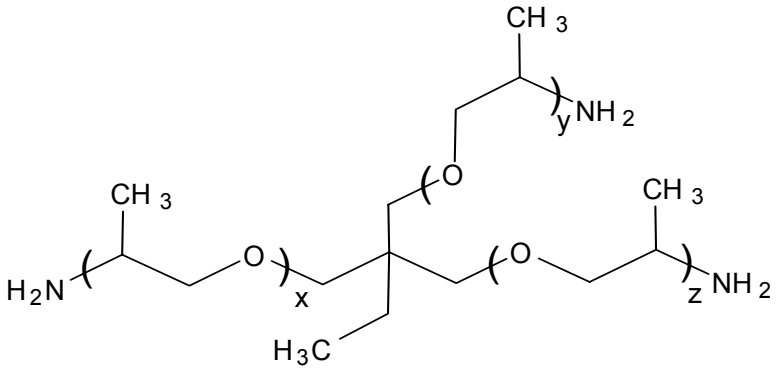

Figure 5.1. The structure of polyether triamine (Jeffamine T-403, Huntsman)

Epoxy nanocomposites were synthesized employing 1 wt% of the different nanotubes and nanofibers (for surface-modified nanotubes or nanofibers, the weight refers to the amount of neat nanotube or nanofiber calculated from thermal gravimetric analysis). The nanotube or nanofiber were dispersed in THF and sonicated for 5 min. Following DGEBA addition, the dispersion was sonicated for 20 min. and placed overnight in a vacuum oven at 50° C to allow solvent evaporation. Finally, a stoichiometric amount of hardener was added, followed by further mixing (2 min.) and degasification (10 min.). The solution was cast into a polyetrafluoroethylene (PTFE) mold and cured at 75°C for 3 h, with a subsequent post-curing step at 125°C for 3 h.

Epoxy/T-403 flexural tests were performed with a 3-point bending tool. The dynamic temperature ramp test was performed at 0.1% strain at a frequency of 1Hz. from 25°C to 160°C with a heating rate of 5ºC/min. The flexural modulus was calculated by using the equation of $E = ((L^3 \times m) / (4 \times b \times d^3))$ (ASTM D790M) where E is the modulus of elasticity in bending (MPa), L is the support span length which is 10 mm in this study, b is the width of the beam tested (mm) and m is the slope of the tangent to the initial straight-line portion of the load deflection curve (N/mm of deflection).

5.3 RESULTS AND DISCUSSION

In this study, the dynamic mechanical analysis of the pristine, acidified and esterified SWCNT, MWCNT and CNF was studied. Firstly, frequency and strain sweep experiments were run in order to find the ultimate strain and frequency values in the linear viscoelastic regions. The results are shown in Figure 5.2 and Figure 5.3. Based on these two figures 0.1 % strain and 1 Hz frequency were chosen in the linear viscoelastic region. These values were used for the further dynamic temperature ramp experiments.

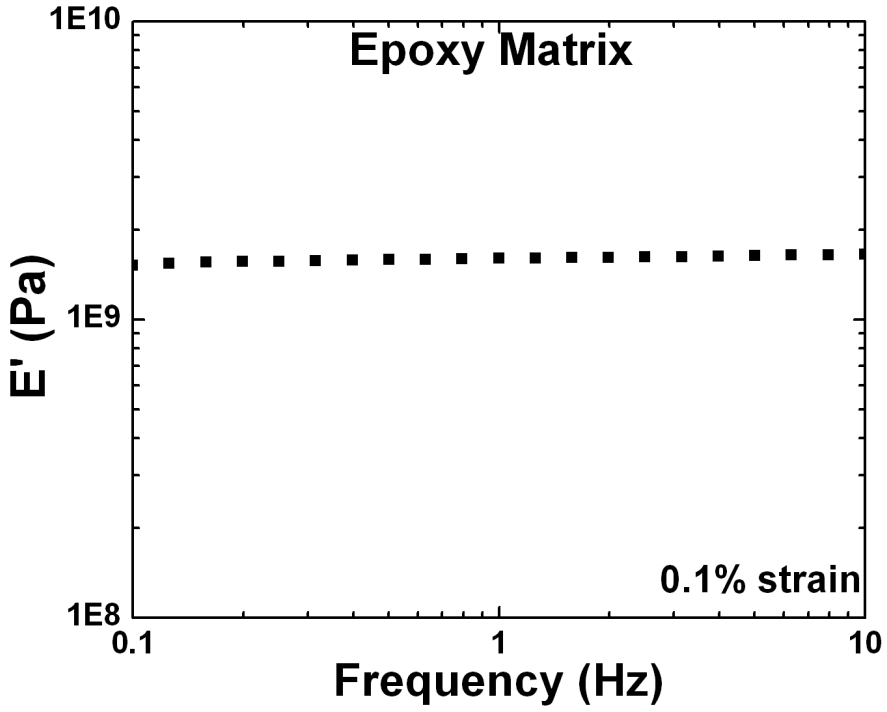

Figure 5.2. Frequency sweep test for rigid epoxy matrix

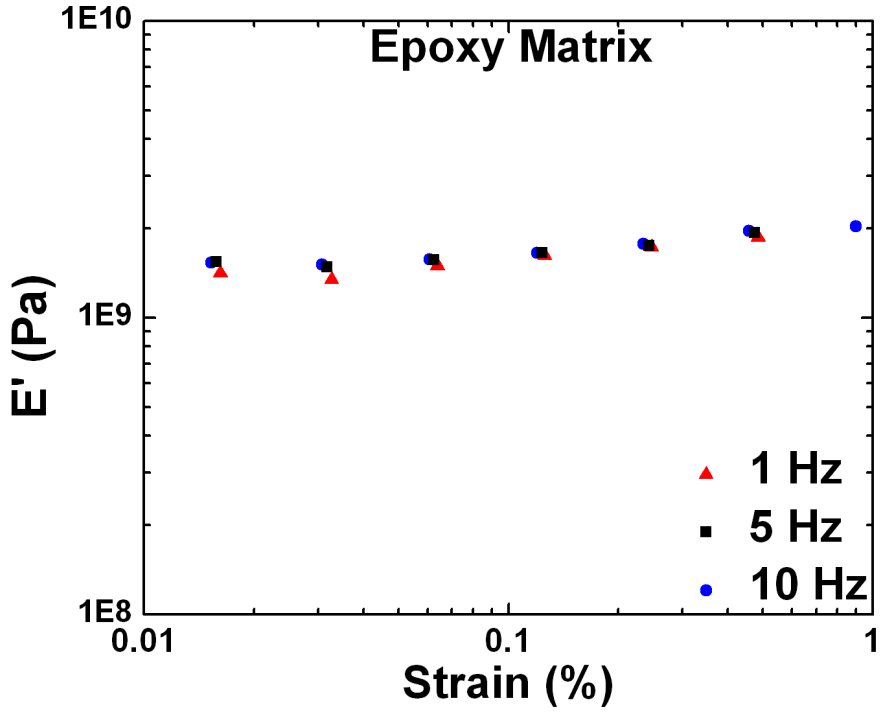

Figure 5.3. Strain sweep test for rigid epoxy matrix

5.3.1 Effect of Interphase on the Glass Transition Temperature (T_g)

The glass transition temperature of the nanocomposites was determined through the dynamic mechanical analysis. The temperature, where loss peak (tan δ) reached its maximum, was chosen as glass transition temperature. Whether the nanocomposites showed one or two relaxation peaks gave ideas about the features at the carbon interface such as monomer partitioning and phase separation. Figure 5.4, 5.5 and 5.6 show the results for the three nanofillers (SWCNT, MWCNT and CNF, respectively) used pristine, oxidized and esterified.

It is already known that the T_g will have maximum value at the stoichiometric ratio of 1 for the epoxy/amine system. If the stoichiometric is lower or higher than 1, the glass transition value

will drop down. Based on this information, the lower peak at the dynamic mechanical analysis can be related to the non-stoichiometric region (i.e. interface) of the nanocomposites.

The use of unmodified and oxidized nanofillers produced a heterogeneous matrix exhibiting two relaxation peaks. The larger peak located at low temperatures assigned to a non-stoichiometric interphase surrounding carbon nanofillers and the smaller peak corresponds to nearly stoichiometric region. This peak is also close to the peak of the neat matrix that can be related to the stoichiometric region in the unmodified and oxidized nanofillers. Since this effect was observed for unmodified and oxidized SWCNT, MWCNT and CNF, it cannot be associated with the surface treatment but possibly reflects to a preferential adsorption of the aromatic monomer (DGEBA) at the carbon interface.

On the other hand, the esterification of COOH groups with PGE avoided the partitioning of monomers and led to a single relaxation peak of the epoxy matrix for the three types of nanofillers. The explanation is related to the fact that PGE-modified nanofillers created a stronger physical interaction (improved adhesion) with the epoxy matrix and were phase-separated from the matrix in the course of polymerization. Matrix exclusion from these domains reduced the partitioning of monomers at the interface.

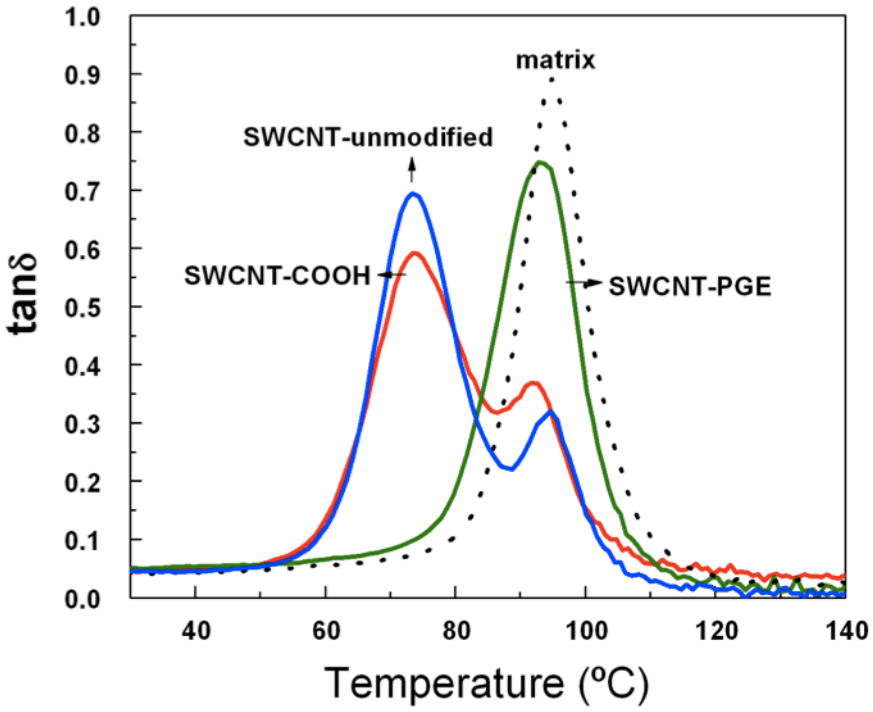

Figure 5.4. Tan δ vs. Temperature for epoxy matrix and unmodified, acidified, and esterified SWCNTs nanocomposites

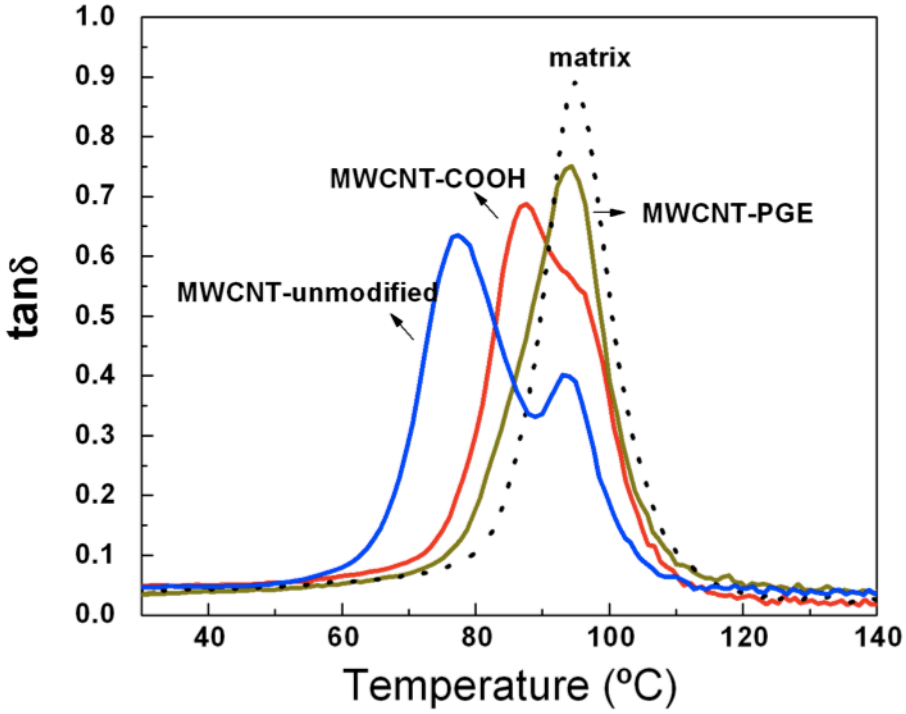

Figure 5.5. Tan δ vs. Temperature for epoxy matrix and unmodified, acidified, and esterified MWCNTs nanocomposites

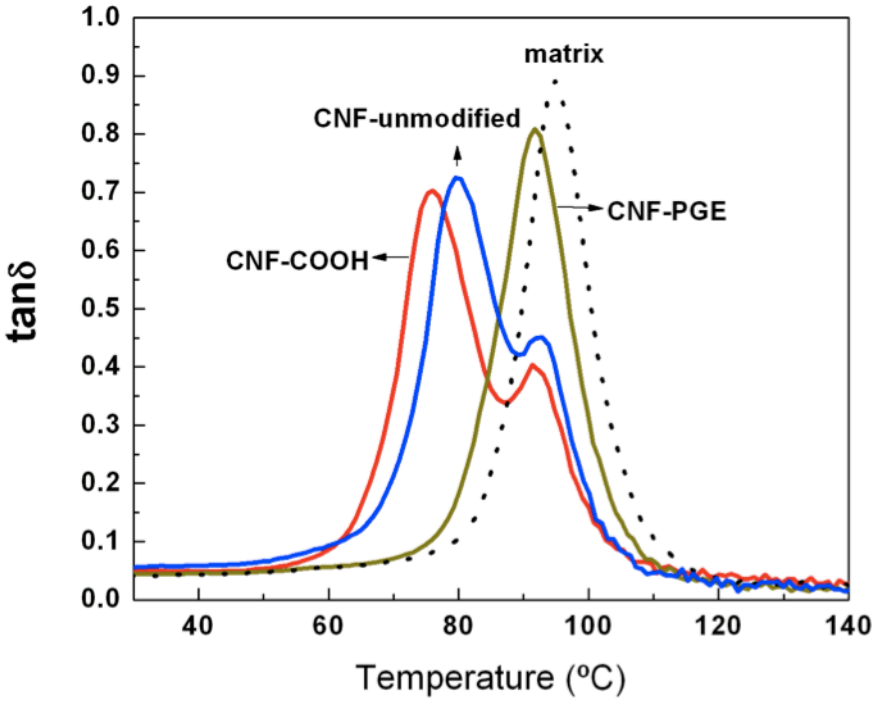

Figure 5.6. Tan δ vs. Temperature for epoxy matrix and unmodified, acidified, and esterified CNFs nanocomposites

5.3.2 Effect of Interphase on Storage Modulus

The bonding between the nanofillers and the matrix is an important mechanism that allows transferring the load efficiently from the matrix to the nanofillers. The mechanism of fiber–matrix bonding includes chemical bonding, inter-diffusion, van der Waals bonds, and mechanical interlocking (Figure 5.7). Chemical bonding gives a relatively larger bonding force, provided by the density of chemical bonds across the fiber–matrix interface. As it is mentioned previously, this can be achieved by the chemical functionalization of the nanotubes. Inter-diffusion at the fiber–matrix interface also results in bonding, though its occurrence requires the interface to be rather clean. Chemical bonding, inter-diffusion and van der Waals bonding require a closer interaction between the fibers and the matrix. In order to do that, the matrix or matrix precursor

must be able to wet the surfaces of the fillers and wetting is governed by the surface energies. Functionalization of nanofillers can enhance wetting through their effects on the surface energies. Among these mechanisms, mechanical interlocking is more useful for the fillers have rough surface. In our case, carbon nanotubes have a smooth surface, thus a small degree of mechanical interlocking takes place. However, mechanical interlocking between the fibers and the matrix is an important contribution to the bonding if the fillers form a three-dimensional network.

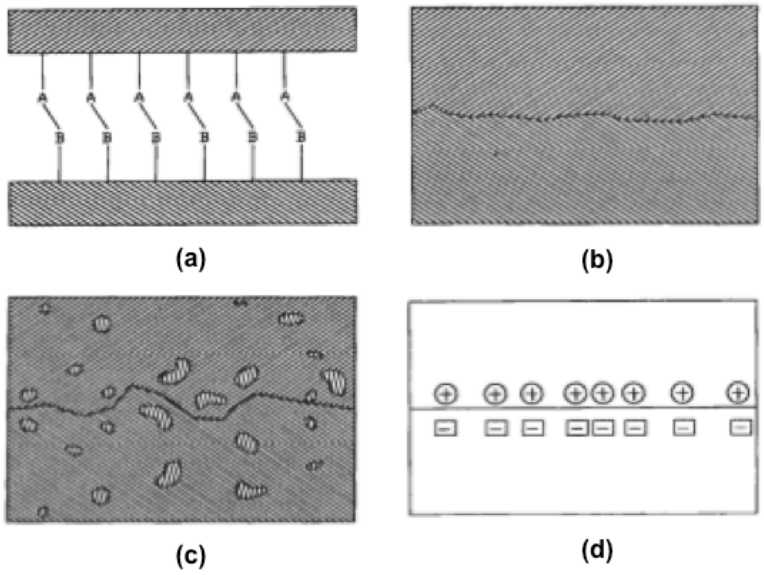

Figure 5.7. Interface bonds formed by (a) chemical bonding, (b) mechanical interlocking, (c) inter-diffusion (d) Van der Waals forces (Hull, 1981)

Figures 5.8, 5.9 and 5.10 show the variation of the storage modulus with temperature for the three nanofillers used as pristine, oxidized and esterified. An increase in the elastic modulus in both rubbery and glassy states with respect to the epoxy/amine matrix produced by the addition of 1 wt % of the corresponding SWCNT, MWCNT and CNF was observed. The increase both in rubbery and glassy state can be related to either the good dispersion of nanofillers or improved adhesion with the epoxy matrix or both. It is also important to mention that SEM images of these

nanocomposites showed that the acidified system has a good dispersion, while the system with PGE does not have a good dispersion (i.e: SEM images were shown in Chapter 3). Based on this knowledge, it can be concluded that the increase in elastic modulus in the acidified system was due to the good dispersion and improved adhesion with Van der Waals interactions. Moreover, the percolation threshold for the acidified SWCNT system was reported around 0.5 wt% which means that at 1 wt% loading in a well dispersed system, SWCNTs can create a three dimensional network. This network can also activate the mechanical interlocking between the epoxy and the nanotubes, even though nanotubes have a smooth surface. However, It needs to be also mentioned that the acid groups do not react with tertiary amines that have been used as cross-linker in this study. Therefore, the enhancement in elastic modulus cannot be related to the chemical bonding between the epoxy and acid groups on nanofillers. In the esterified system, this increase in elastic modulus was because of wetting enhancement with epoxy system. Furthermore, a significant increase in the glass transition temperature for the PGE system was observed at least for the formulation used in the present study. Sue et al. (2007) also studied the effect of SWCNT nanotubes on the storage modulus of epoxy systems. What they observed was an increase in elastic modulus in the glassy region, but a decrease in elastic modulus in the rubbery region with addition of unmodified SWCNTs. They related this effect to the lower cross-link of the epoxy and the poor adhesion between the nanotubes and the epoxy. They also observed that the storage modulus increased in both regions by adding functionalized SWCNTs because of the better dispersion.

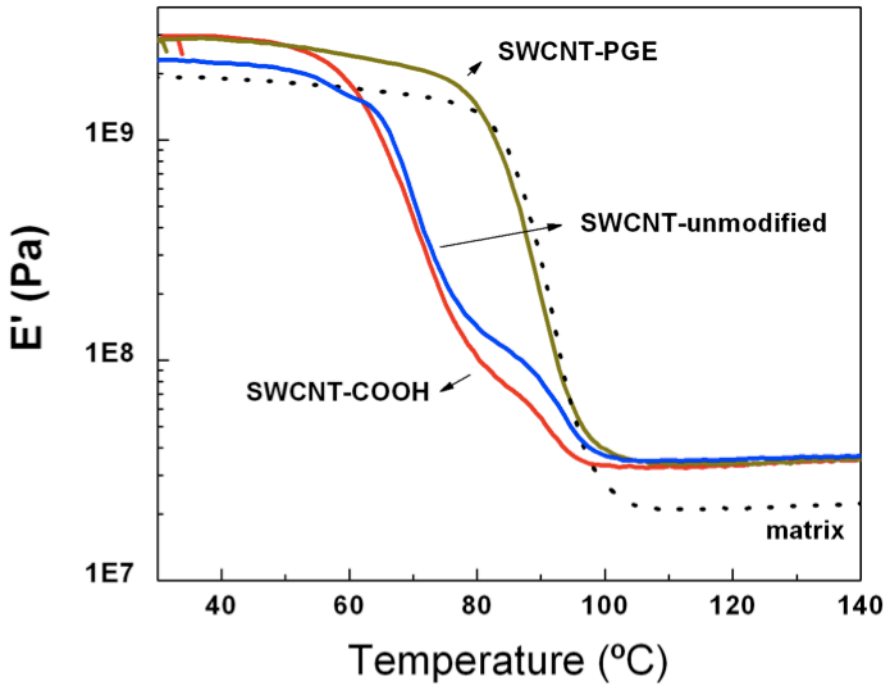

Figure 5.8. Storage modulus (E') vs. Temperature for epoxy matrix and unmodified, acidified, and esterified SWCNTs nanocomposites

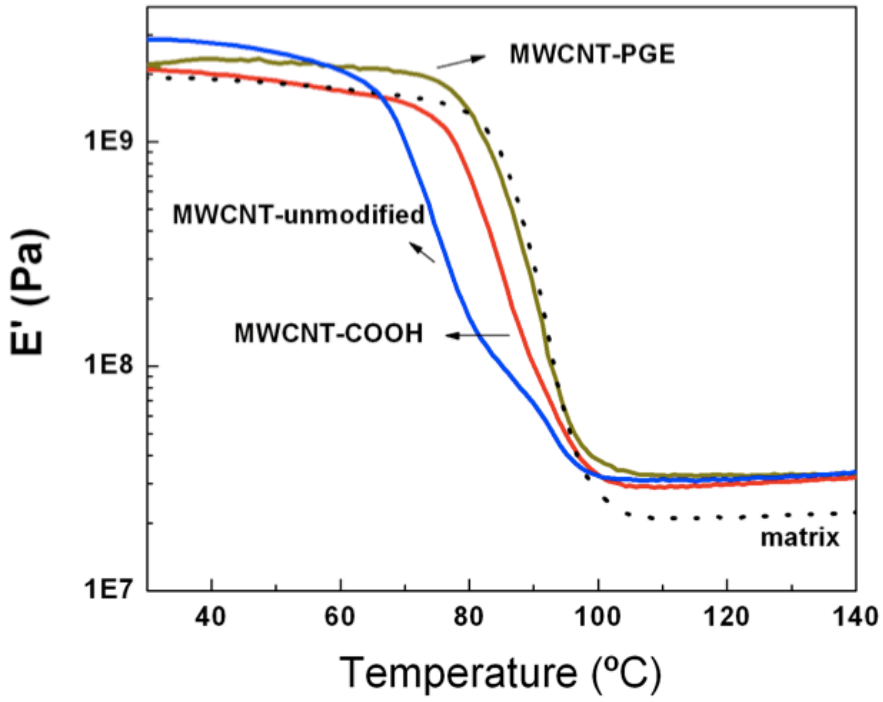

Figure 5.9. Storage modulus (E') vs. Temperature for epoxy matrix and unmodified, acidified, and esterified MWCNTs nanocomposites

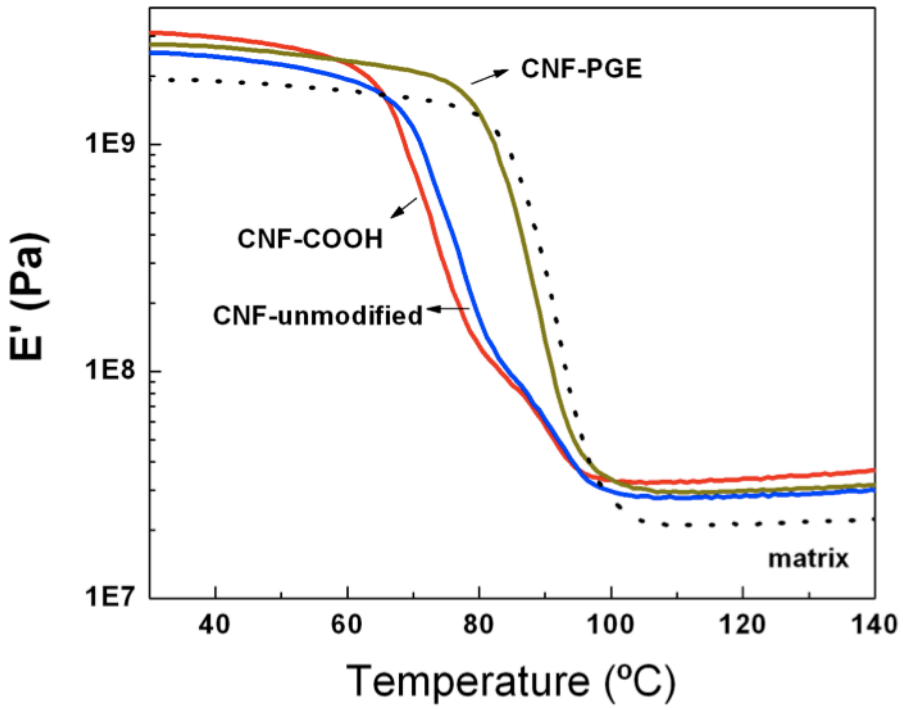

Figure 5.10. Storage modulus (E') vs. Temperature for epoxy matrix and unmodified, acidified, and esterified CNFs nanocomposites

5.3.3 Mechanical Properties

The effects of nanofillers on the mechanical properties of epoxy nanocomposites were studied with dynamic mechanical analysis in a 3-point bending experiment. The flexural modulus of unmodified, acidified and esterified SWCNT, MWCNT and CNF systems are reported in Figures 5.11, 5.12 and 5.13 respectively.

The results showed that incorporation of 1 wt% nanofillers increases the modulus of epoxy matrix. The highest modulus in SWCNT and MWCNT systems was observed for those functionalized with acid groups. The incorporation of acidified SWCNT increased the flexural modulus of epoxy 48% while pure SWCNT and esterified SWCNT increased the flexural

modulus 33 and 28%, respectively. It was also observed through SEM and Raman analysis in Chapter 3 that the best dispersion was obtained with the acidified system followed by unmodified and esterified systems. These results also clarify the effect of the dispersion quality on the mechanical properties of the nanocomposites. The incorporation of acidified MWCNT increased the flexural modulus of epoxy 58% while pure SWCNT and esterified SWCNT increased the flexural modulus 23 and 30%, respectively. However, the system with CNFs did not follow this trend even though the modulus of epoxy increased with the incorporation of CNFs. The pristine CNF system increased the flexural modulus of epoxy 66%, whereas, acidified and esterified system increased the flexural modulus 33 and 46%, respectively. The reason for the decrease in the modulus for acidified and esterified systems compared to the pristine systems can be the destructive effects of functionalization process on the carbon nanofibers.

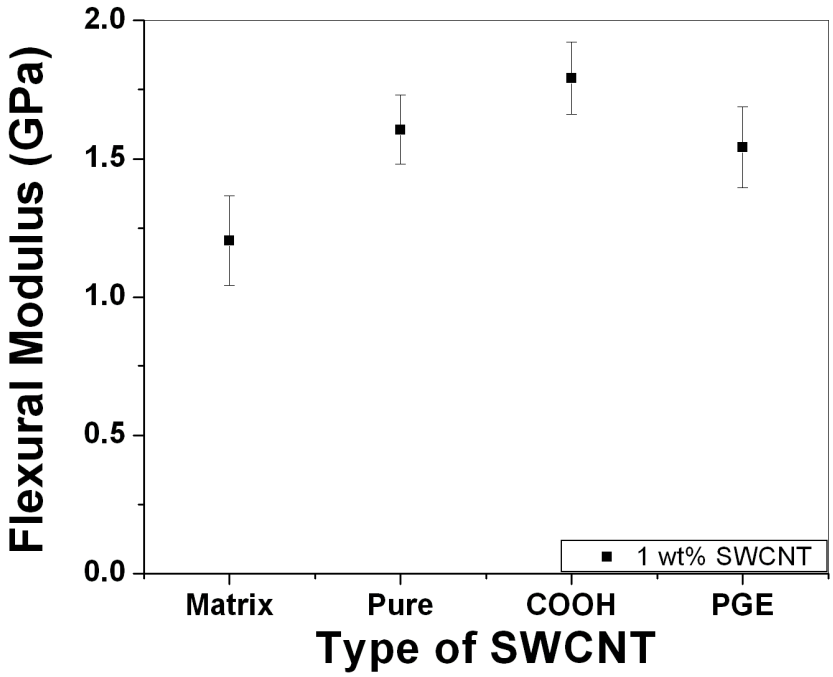

Figure 5.11. Flexural modulus of unmodified, acidified and esterified SWCNT/Epoxy nanocomposites

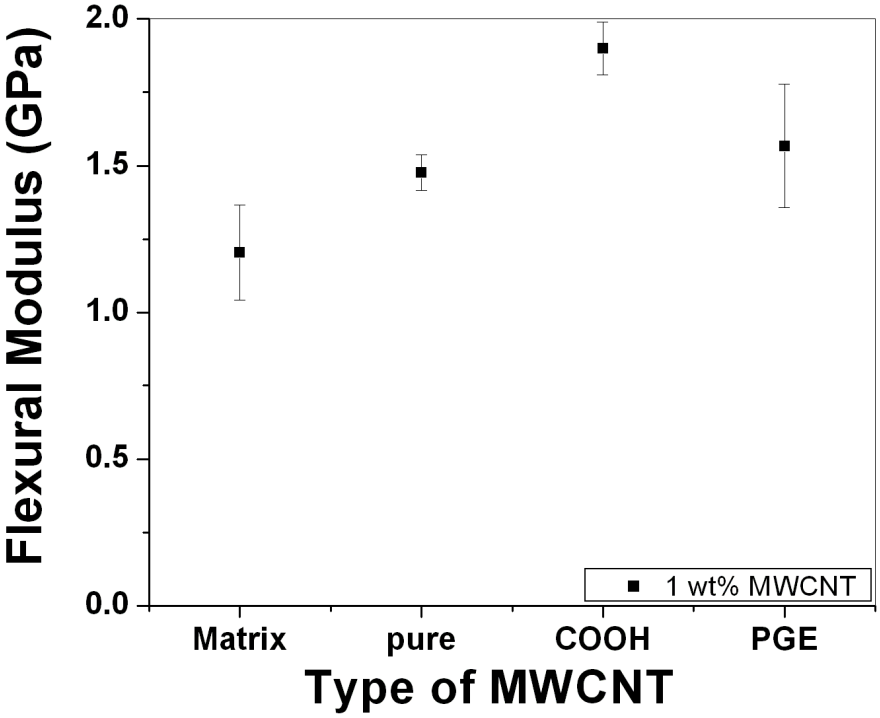

Figure 5.12. Flexural modulus of unmodified, acidified and esterified MWCNT/Epoxy nanocomposites

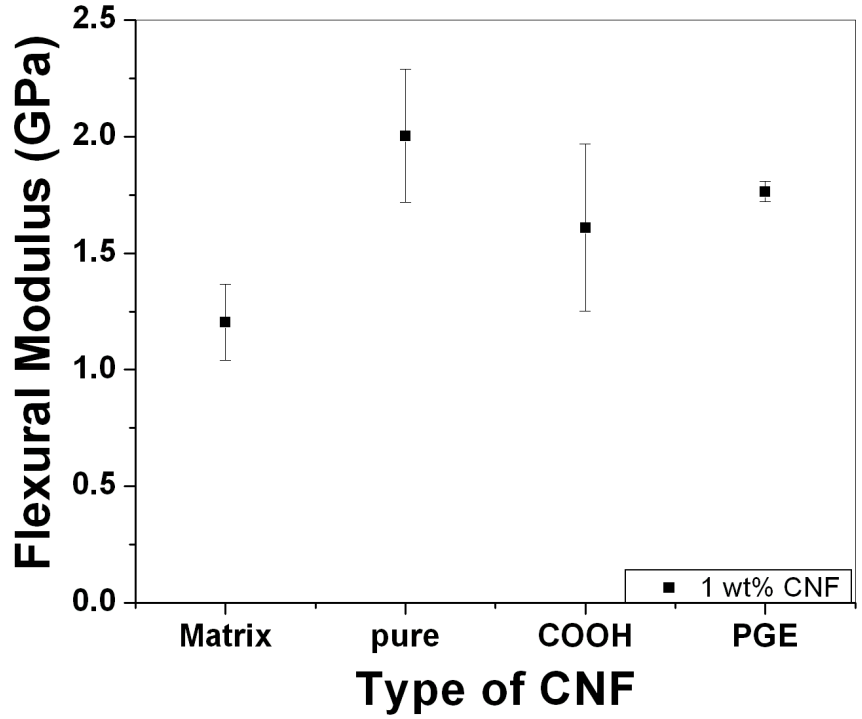

Figure 5.13. Flexural modulus of unmodified, acidified and esterified CNF/Epoxy nanocomposites

Additional to the effect of functionalization on the mechanical properties of the epoxy nanocomposites, the effect of acidified SWCNT with different concentrations was also studied. It is observed that as the concentration of the acidified SWCNT was increased, the flexural modulus also increased. However, as the concentration was reached to 2 wt%, modulus began to decrease because of the lack of good dispersion. In addition, during the sample preparation, a considerable increase of the viscosity was observed.

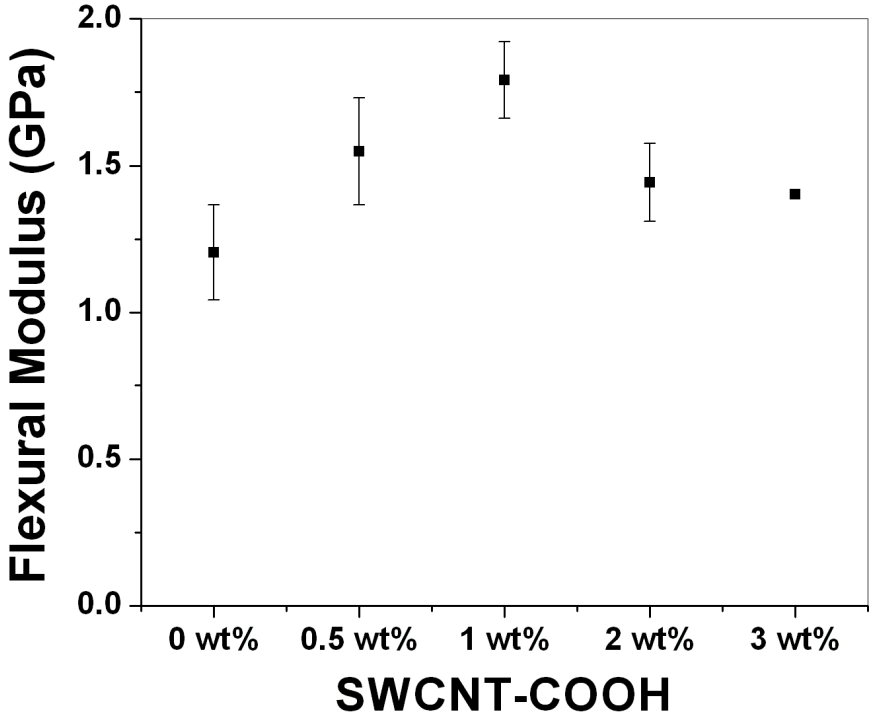

Figure 5.14. Flexural modulus of 0-3 wt% acidified SWCNT/Epoxy nanocomposites

5.4 CONCLUSION

In this chapter, the effects of nanotube/epoxy interphase on the thermo-mechanical and mechanical properties of epoxy nanocomposites were studied. Rigid epoxy nanocomposites were prepared by the reaction of DGEBA with polyethertriamine (Jeffamine T-403) and the incorporation of unmodified, acidified and esterified SWCNTs, MWCNTs and CNFs. The thermo-mechanical properties of these nanocomposites were evaluated through dynamic mechanical analysis by running a temperature ramp experiment. These experiments as well as mechanical experiments were performed with 3-point bending setup.

Dynamic mechanical analysis showed the presence of two relaxation peaks in nanocomposites prepared with unmodified and COOH-modified SWCNT, MWCNT and CNF, assigned to a partitioning of monomers at the carbon interface. This produced a significant decrease of the glass transition temperature. However, esterification with PGE led to a single relaxation peak close to the one of the neat epoxy, for the three types of nanofillers without any penalty in the glassy and rubbery elastic moduli. These behaviors were related to the physical interactions between the matrix and the nanofillers rather than chemical interactions.

Mechanical analysis of these nanocomposites showed that the good dispersion and an adequate adhesion between the matrix and nanofillers affected the modulus of these materials. In SWCNT and MWCNT systems, the highest modulus were observed for the acidified systems, whereas, CNF system had the highest modulus in unmodified system. The reason of this unexpected behavior can be the harmful effects of functionalization process on the structure of carbon

nanofibers. Furthermore, the effect of concentration increase of acidified SWCNTs on the mechanical modulus was evaluated. The flexural modulus increased as the concentration of nanotubes was increased. As the concentration reached 2 wt%, the quality of dispersion dropped down so that the modulus decreased. As a result, all systems with nanofillers showed higher modulus value than epoxy matrix. However, the modulus of these nanocomposites varied based on the dispersion quality of the fillers.

REFERENCES

1. Abdalla M., Dean D., Adibempe D., Nyairo E., Robinson P., and Thompson G., "The effect of interfacial chemistry on molecular mobility and morphology of multiwalled carbon nanotubes epoxy nanocomposite", Polymer, 48, 5662, 2007

2. Drzal L.T., Miyagawa H., "Thermo-physical and impact properties of epoxy nanocomposites reinforced by single-wall carbon nanotubes", Polymer, 45, 15, 5163-5170, 2004

3. Drzal, L.T. and Madhukar, M. "Fiber-matrix adhesion and its relationship to composite mechanical properties", J. Mater. Sci. 28, 569-610

4. Hull, D., "An Introduction to Composite Materials", Cambridge University Press, Cambridge, pp. 3 6, 58. 1981

5. L. S. Schadler, S. C. Giannaris, and P. M. Ajayan, "Load transfer in carbon nanotube epoxy composites", App Physc Letter Vol., 73, 26, 1998

6. Putz K., Krishnamoorti R., Green P.F., "The role of interfacial interactions in the dynamic mechanical response of functionalized SWCNT-PS nanocomposites" , Polymer 48, 3540-3545, 2007

7. R. Andrews, M.C. Weisenberger, "Carbon nanotube polymer composites", Current Opinion in Solid State and Materials Science 8, 31–37, 2004

8. Shen J., Huang W., Wu L., Hu Y., and Ye M., "Thermo-physical properties of epoxy nanocomposites reinforced with amino-functionalized multi-walled carbon nanotubes", Compos. A, 38, 1331, 2007

9. Sun L., Warren G.L., O'Reilly J.Y., Everett W.N., Lee S.M., Davis D., Lagoudas D., and Sue H.J., "Mechanical properties of surface-functionalized SWCNT/epoxy composites", Carbon, 46, 320, 2008.

CHAPTER 6

DAMPING CHARACTERISTIC OF ELASTOMERIC EPOXY NANOCOMPOSITES

6.1 INTRODUCTION

For applications where vibration is an issue, increased damping is necessary in order to decrease the harmful effect of vibration. As a definition, damping can be defined as dissipating some fraction of each increment of energy, which is added to the system by the exciting forces. Metals in general have very low damping capacity whereas polymeric materials and composites will damp vibration much more effectively than metals (David I.G. Jones, 2001). Most polymeric materials exhibit damping behavior, which depends strongly upon temperature and frequency. The internal molecular interactions, which occur during deformation and vibration, induce the macroscopic properties such as stiffness and energy dissipation during cyclic deformation, which is the main mechanism of damping.

The types of polymeric materials that have been used in damping application are very wide and also include commercially available products ranging from natural rubber and adhesives, to stiff plastics, such as polymethylmethacrylate (PMMA), acrylic rubber, high impact polystyrene (HiPS) and silicon rubber. The stiffness and damping characteristics of these polymers can vary widely according to their composition, the crosslink density and the type of fillers. However, these viscoelastic materials can suffer from various limitations such as high weight penalty, low

thermal conductivity, poor reliability and poor performance at elevated temperatures. Recent developments in filling polymeric materials with nanoscale fillers provide a wide opportunity to efficiently and reliably create composite structures that can exhibit high damping capacity. The specific surface area of nanoscale fillers is very large (compared to traditional fillers) providing a mechanism for frictional sliding at the filler-filler and filler-matrix interfaces, which produce a significant impact on the energy dissipation response of the composite. The unique damping properties of carbon nanotube (CNT) based materials have been the subject of several researches. Their unique characteristics such as large surface area, large aspect ratio, high stiffness, low density, and high thermal conductivity make CNTs ideal fillers for high performance damping composites.

In the literature, different studies indicate the high damping capacity of CNT polymer nanocomposites is due to filler-filler and filler matrix frictional sliding or both. For instance, Buldum and Lu (1999) have investigated the sliding of nanotubes and measured the friction force associated with stick-slip motion of the nanotubes using an AFM technique. Recently Zhou et al. (2004) reported a significant increase in the loss factor of a SWCNT/epoxy system. Koratkar et al. reported up to an order of magnitude (>1000%) increase in loss modulus of the polycarbonate system with the addition of 2 wt% of oxidized single-wall nanotubes. They showed that the increase in damping is derived from frictional sliding at the nanotube-polymer interface. In another study, Wang et al. (2004) investigated the dynamic mechanical properties of SWCNT buckypaper/epoxy nanocomposites. In their system, SWCNTs were dispersed in water-based suspension with the aid of surfactant and sonication. Through a filtration process, SWCNTs were fabricated into thin membranes called buckypapers to form networks of SWCNT ropes. A hot

press molding process was used for curing to produce the final nanocomposites of multiple layer buckypapers with high SWCNT loading (up to 39 wt%). The dynamic mechanical analysis showed that the storage modulus increased 429% and damping properties improved significantly compared to the matrix.

The mechanism for the observed damping increase in nanocomposite can be explained by "stick-slip" mechanism (Figure 6.1). In this mechanism, when a tensile stress is applied to a composite, it begins elongating. As a result of the applied stress, the matrix resin starts applying a shear stress (τ_{rz}) on the nanotube fillers; thereby causing the load to be transferred to the nanotubes and normal strain starts to appear in the nanotube fillers. Then, the matrix and filler begin elongating accordingly. When the applied stress is smaller than critical threshold stress ($\tau_{rz} < \tau_c$), the nanotube remains bonded to the matrix (sticking phase) and both the matrix and the nanotubes deform together ($\varepsilon_z^{nt} = \varepsilon_z^{rs}$). As the applied load is increased, the interfacial shear stress on the nanotubes further increases; this results in further elongation of both matrix and the nanotubes. As the critical threshold stress is reached, the nanotubes debond from the matrix resin ($\tau_{rz} > \tau_c$). With further increase in stress, the maximum strain in nanotubes is reached and remains constant ($\varepsilon_z^{nt} = \varepsilon_z^{c}$), while the strain in matrix increases and causes slippage (slipping phase). This results in energy dissipation due to slippage between the matrix and the nanotube that causes the material's structural damping to increase (Zhou et al., 2004, Suhr et al., 2008).

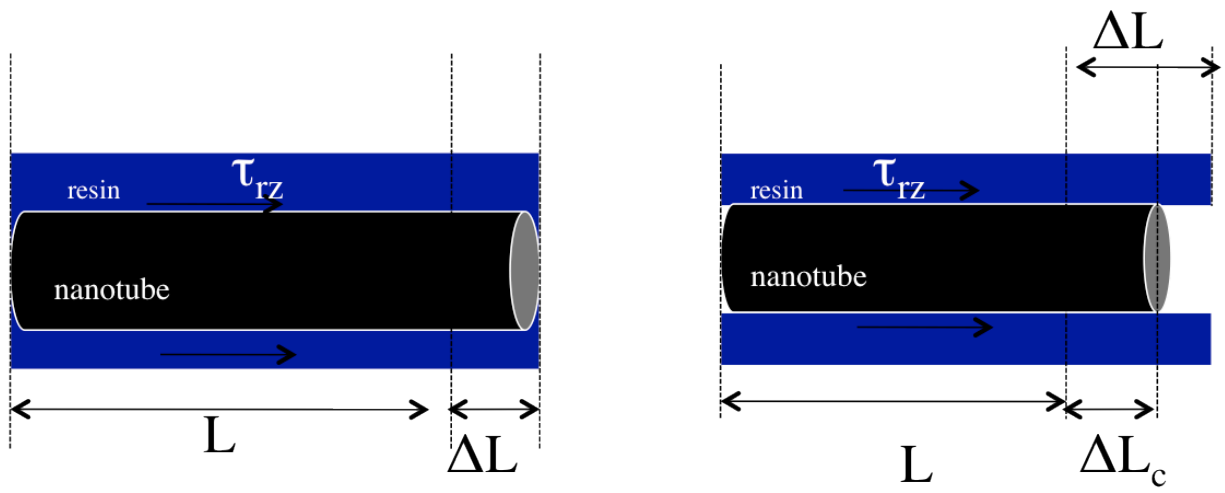

Figure 6.1. Stick-Slip mechanism (Zhou et al., 2004)

The ability of materials to dampen vibrations can be characterized by dynamic mechanical analysis (Figure 6.2). During this experiment, the storage modulus (E') represents the energy stored through elastic behavior and the loss modulus (E'') is the energy lost through conversion to heat via molecular friction. When vibration-damping polymers are formulated, it is desirable to maximize E''. However, maximizing E'' causes a lower elastic response and, therefore, poor physical and mechanical performance may occur.

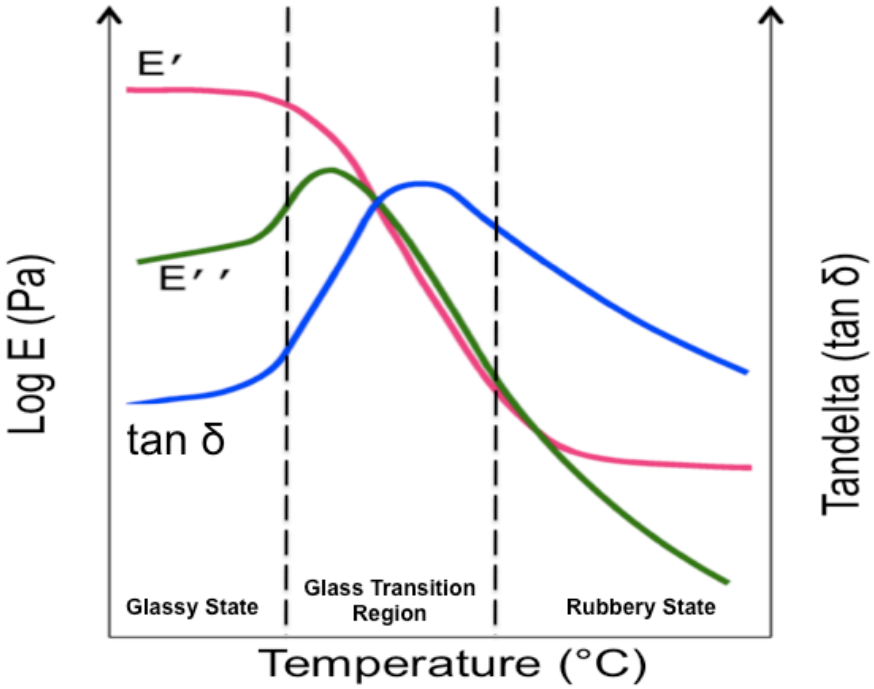

Figure 6.2. Schematic illustration of dynamic mechanical analysis

When a polymer is in its viscoelastic region, at the transition, between the hard glassy state and the soft rubbery state, it exhibits the highest level of damping. At glassy state, damping is low because of the frozen state of chain segments. On the other hand, at rubbery state, molecular sections are quite free to move and there is no resistance to flow. However, in the transition region, damping is high because at this region micro-Brownian motion among the molecular chain segments and their stress relaxation initiates, even though not all the segments will take part in such relaxation together. Thus, in this region a frozen-in segment and also rubbery segment will be observed. The frozen-in segment can store more energy for an applied deformation than a freely mobile rubbery segment. At the transition region, when a stress is applied, frozen-in segments become free to move and thus can make energy dissipated. Furthermore, Micro-Brownian motion takes place with the cooperative diffusion motion of the molecular chain segments and if chain segments take part in this cooperative motion under an

applied stress, maximum damping will occur in that region. In summary, in the transition region, when the material is forced to vibrate, some molecules exhibit viscous flow while the others remain rigid. Thus, the friction among the molecules increases which results in heat build-up and a decreased amount of transmitted energy (Rajoria et al. 2005, Suhr et al. 2006).

This chapter focuses on developing elastomeric epoxy nanocomposites with reinforced with modified and unmodified CNTs and analyzing the damping characteristics of these nanocomposites. The main goal is to observe the damping behavior of these materials in an extended temperature range. To the best of our knowledge, the effect of carbon nanotubes on the damping of elastomeric materials at high temperatures has not been specifically addressed.

6.2 EXPERIMENTAL

6.2.1 Materials

Single-wall carbon nanotubes and MWCNT were purchased from NTP (Nanotech Port, Shenzhen, China). Technical specifications of SWCNT were a diameter < 2 nm, length < 20 μm, purity of CNTs >90%, amorphous carbon < 5%. For MWCNT, the diameter range was 40– 60 nm, the length range was 5–15 μm, and the purity was 95%.

The elastomeric epoxy/amine matrix was formulated using stoichiometric amounts of an epoxy monomer based on diglycidylether of bisphenol A (DGEBA, Epon 828, Miller-Stephenson), and a polyoxypropylene with average molar mass of 2000, end-capped with primary amine groups (Jeffamine D-2000, Huntsman) (Figure 6.3), as hardener. The cured product had a glass transition temperature located below room temperature (T_g = -45°C) implying that the matrix behaved as a cross-linked elastomer at room temperature.

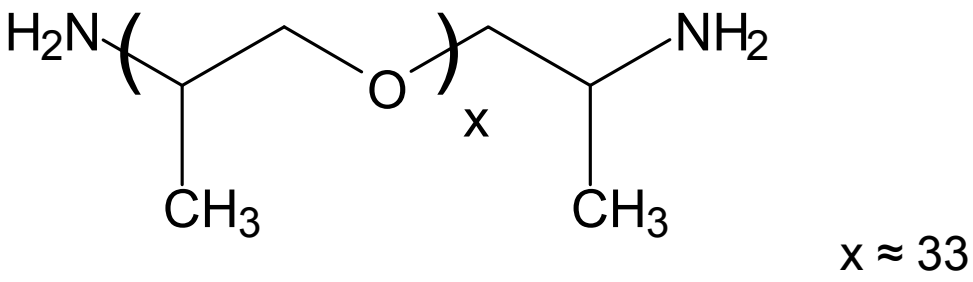

Figure 6.3. Structure of polyether triamine (Jeffamine D-2000, Huntsman)

6.2.2 Sample Preparation

Epoxy nanocomposites were synthesized employing 1 wt% pristine SWCNT and MWCNT or 0.5–3 wt% of SWCNT-COOH and MWCNT-COOH (the weight refers to the neat mass of carbon nanotubes discounting the mass of organic material lost at 600 °C under nitrogen, calculated from thermal gravimetric analysis). THF was selected as an intermediate solvent for the dispersion of SWCNT because it is a good solvent for DGEBA (the final solvent) and it can be easily eliminated at 50 °C under vacuum. Direct dispersion in DGEBA was not performed because of its high viscosity. SWCNT were dispersed in THF and then sonicated for 5 min. Following DGEBA addition, the dispersion was sonicated for 20 min. and placed overnight in a vacuum oven at 50°C to allow solvent evaporation. Finally, a stoichiometric amount of hardener was added, followed by further mixing (2 min) and degasification (10 min). The solution was cast into a PTFE mold and cure was performed at 75°C for 3 hr., with a subsequent step at 125°C for 3hr.

6.2.3 Characterization

The glass transition temperature of the neat epoxy matrix was determined by differential scanning calorimetry (DSC Q2000, TA Instruments). Samples were heated from −80 °C to 100 °C at 5 °C/min under nitrogen atmosphere.

Dynamic mechanical analysis was performed with a RSA III device (TA Instruments), using a film-testing tool. Samples were subjected to sinusoidal displacement of 1% strain at a frequency of 1 Hz, from 25 °C to 200 °C at a heating rate of 5 °C/min.

6.3 RESULTS AND DISCUSSION

The damping behavior of epoxy nanocomposites was evaluated via dynamic mechanical analysis at an extended temperature range. All the experiments were done in the linear viscoelastic region. In order to find the strain and frequency values that take place in the viscoelastic region, a strain sweep and a frequency sweep experiments were performed (Figure 6.4, Figure 6.5, respectively). Based on these experiments, 1% strain and frequency of 1 Hz were used.

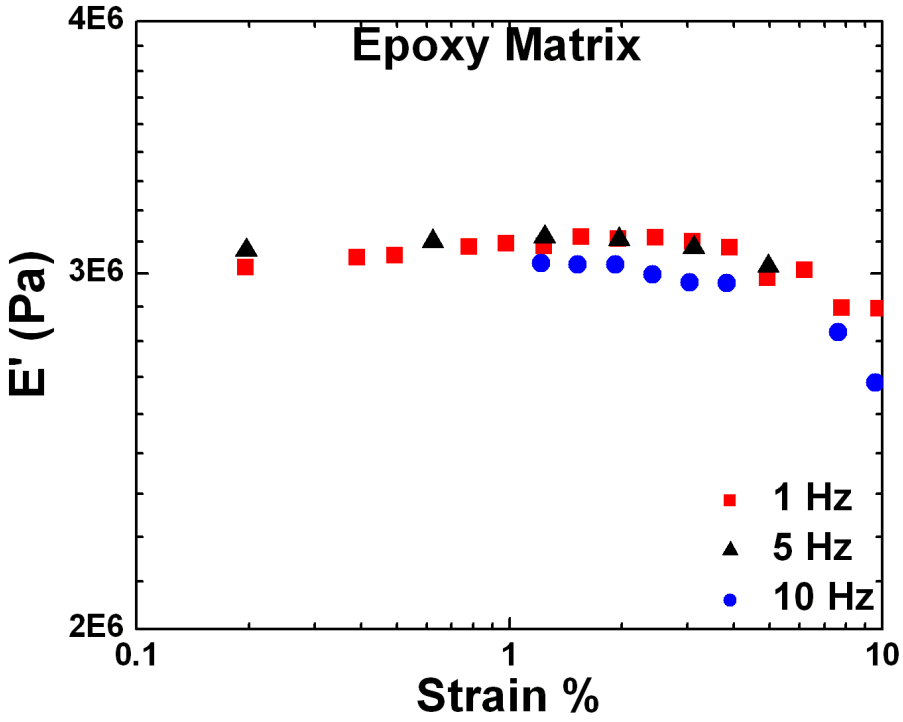

Figure 6.4. Strain sweep test for elastomeric epoxy

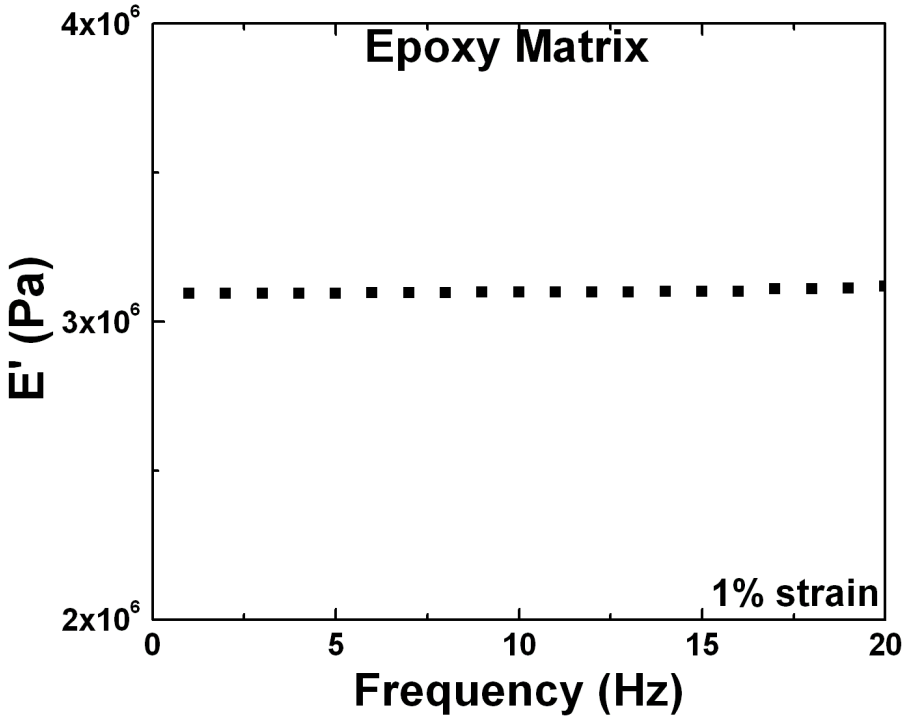

Figure 6.5. Frequency sweep test for elastomeric epoxy

Figure 6.6 shows the behavior of acidified SWCNT/epoxy nanocomposites and the epoxy matrix at the room temperature. The storage modulus (or stiffness) of the epoxy nanocomposites reinforced with acidified SWCNT showed a gradual decrease with increasing strain amplitude. As the strain was increased, filler-matrix debonding (sliding) was initiated resulting in a decrease in the nanocomposite's stiffness. However, the storage modulus of the epoxy matrix did not show a considerable decrease rather than it showed almost constant storage modulus because of its homogenous structure.

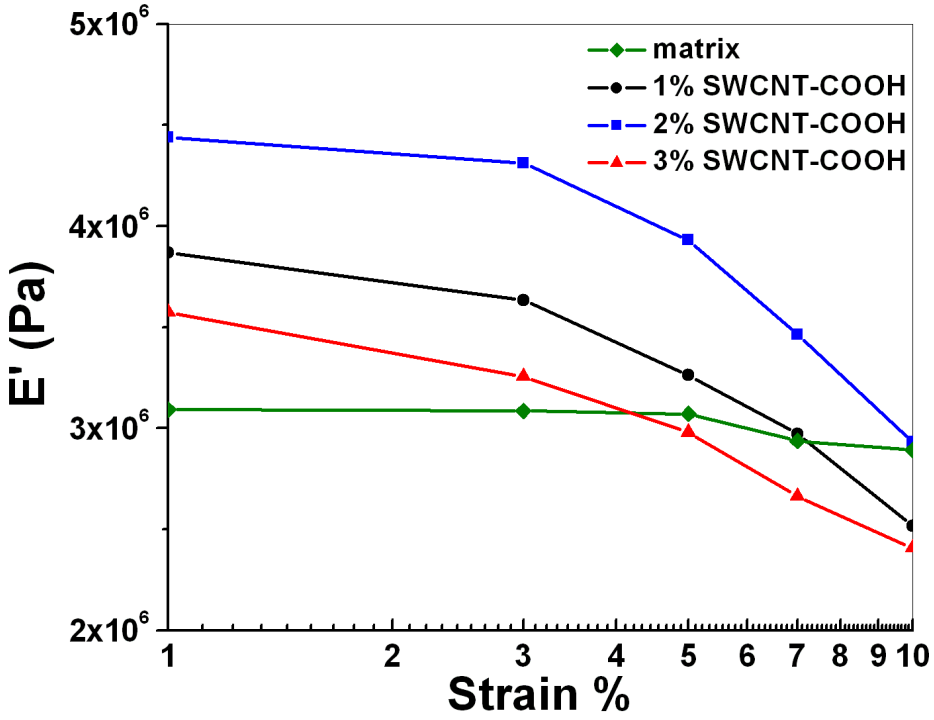

Figure 6.6. Storage modulus as a function of strain

The damping capacity of the nanocomposites can be measured by the increase in the loss modulus with respect to the one of the matrix. In Figure 6.7 an increase in the loss modulus (damping) of the nanocomposites was observed, as frictional sliding at the tube-polymer interfaces was activated. At higher strain values, the loss modulus of the nanocomposites leveled off due to fully activated interfacial slip that was occurred for a majority of nanotubes within the composite.

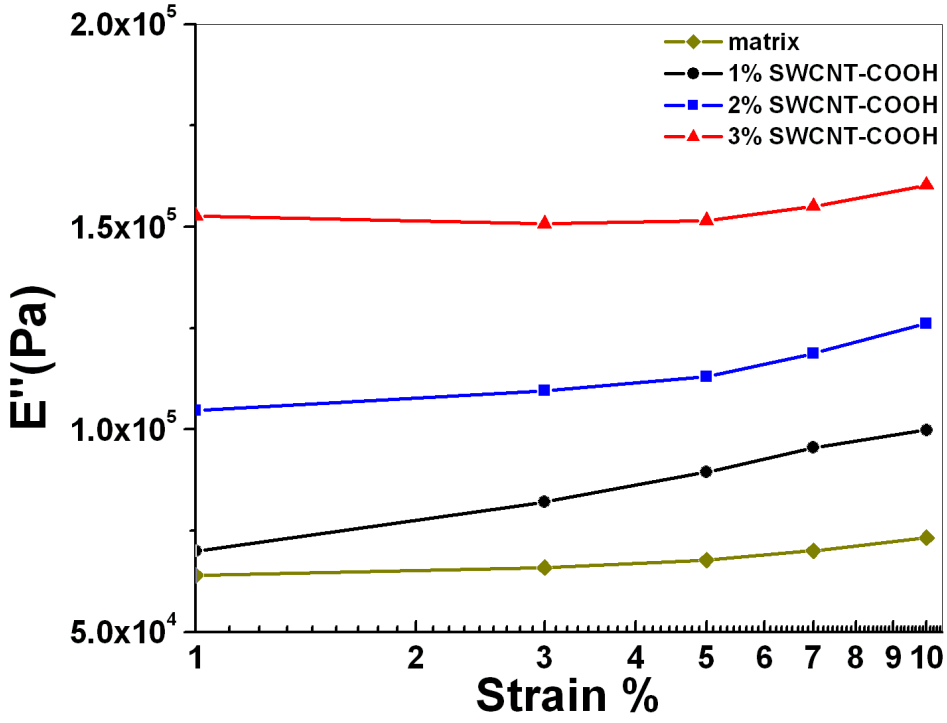

Figure 6.7. Loss modulus as a function of strain

At the room temperature damping response of the nanocomposites is sensitive to the strain amplitude. This is because to activate interfacial sliding of nanotubes the interfacial shear stress at the tube-polymer interfaces must exceed a threshold value. In practice, large strain values are unlikely to be faced, and so it is important to investigate whether interfacial slip in nanotube composites can be activated at lower strain levels. By using the temperature nanotube-matrix slip can be facilitated at low strain values.

Figure 6.8 shows the storage modulus as a function temperature for the neat epoxy elastomer (matrix) and nanocomposites containing 1 wt% unmodified and modified SWCNTs. For the four samples, the elastic modulus increased with temperature because of the entropic contribution to the elastic behavior. Modification of SWCNTs with functional group (-COOH) and surfactant

(TritonX-100) led to an increase in the elastic modulus. The increase in modulus was larger for modified SWCNTs (both surfactants and –COOH) (about %30 at room temperature), possibly reflecting the better quality of the dispersion in the final material.

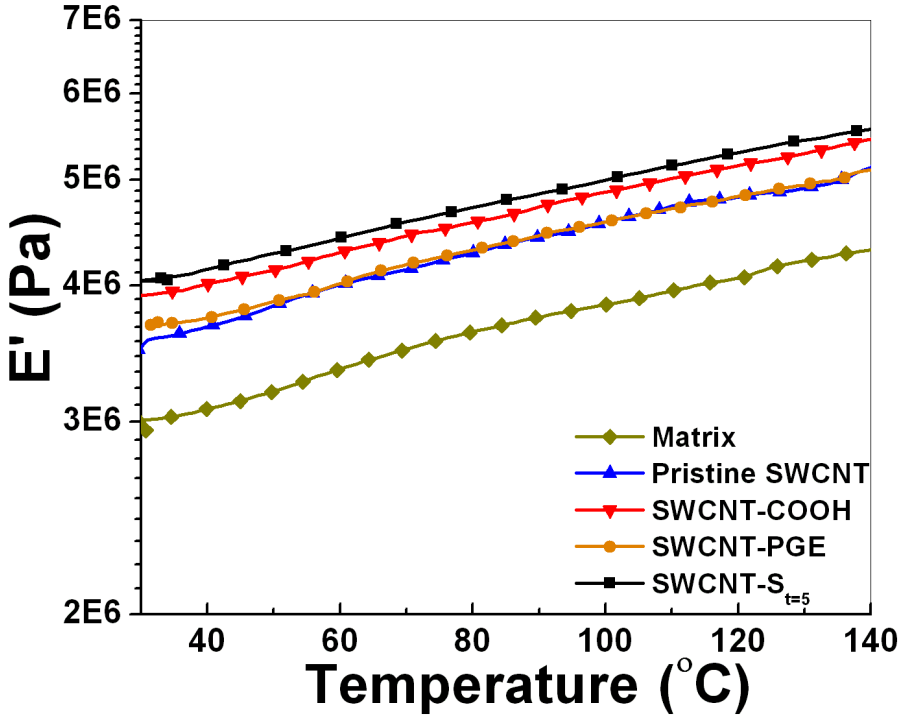

Figure 6.8. Storage modulus as a function of temperature

Figure 6.9 shows the loss modulus as a function of temperature for the neat epoxy elastomer (matrix) and nanocomposites containing 1wt% unmodified and modified SWCNTs. After adding carbon nanotubes into the system, the loss modulus (damping capacity) increased significantly. The relative increase is higher at high temperatures where the loss modulus value of the matrix is very low. It is also important that the better dispersion of acidified SWCNTs did not improve the loss modulus at room temperature compared to the pristine SWCNTs whereas the storage modulus exhibited higher value at room temperature. Considering the mechanism of energy dissipation derived from frictional sliding between the filler and matrix, adhesion of nanotubes to

the polymer matrix should produce a significant effect on the damping capacity. Functionalization of carbon nanotubes with acid groups might produce covalent bonding to the matrix by reaction with epoxy groups. H-bonding between the COOH groups attached to carbon nanotubes and hydroxyl, ether or tertiary amine groups of the cross-linked network can increase the adhesion with a corresponding decrease of the damping capacity. Furthermore, the filler-filler sliding in bundles can also led increase to the overall energy dissipation.

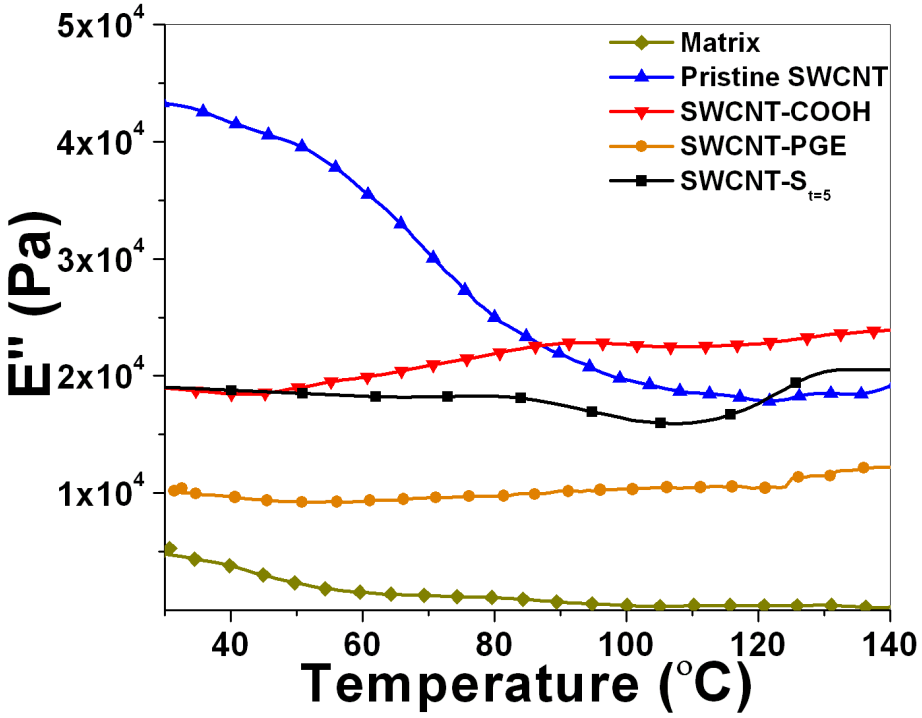

Figure 6.9. Loss modulus as a function of temperature

Table 6.1 shows the improvement in storage and loss modulus of epoxy nanocomposites unmodified and modified SWCNTs and MWCNTs compared to the epoxy matrix. The MWCNTs showed considerable increase in loss modulus at higher temperatures similar to the systems with SWCNTs. However, it needs to be noted that pristine MWCNTs showed higher increment in loss modulus than acidified and esterified systems. The reason might be the higher

amount of MWCNT bundles in unmodified system that activates tube-tube sliding. It is also notable that addition of 5 minute sonicated MWCNTs with surfactant into the system did not increase the storage modulus at room temperature. In this system, sonication might have a harmful effect on the mechanical structure of MWCNTs. Also, the incorporation of surfactant might now improve the dispersion of the system.

Table 6. 1 Increment in storage modulus and loss modulus values of MWCNT/Epoxy systems (E'_m and E''_m refers to storage modulus and loss modulus of epoxy matrix, respectively)

Sample MWCNT (1 wt%)	30° C		140° C	
	E'/E'_m (%)	E''/E''_m (%)	E'/E'_m (%)	E''/E''_m (%)
Pristine MWCNT	29	122	35	1,900
MWCNT-COOH	44	63	43	1,025
MWCNT-PGE	30	212	27	1,040
MWCNT-$S_{t=5}$	-	166	19	2,860
Pristine SWCNT	17	334	20	6,400
SWCNT-COOH	28	250	26.7	9,000
SWCNT-PGE	22	92	18.5	4,500
SWCNT-$S_{t=5}$	33	268	29	8,500

Figure 6.10 shows the effect of the increase in concentration of SWCNT-COOH on the storage modulus of the epoxy nanocomposites. Increasing the concentration of SWCNT-COOH in the cross-linked elastomer increases the storage modulus. However, in the range of 2-3 wt% no variation of the storage modulus was observed. The reason is that the quality of dispersion decreased because of the increase in bundling of nanotubes when increasing the concentration. This result was also supported the tensile experiments (Figure 6.11).

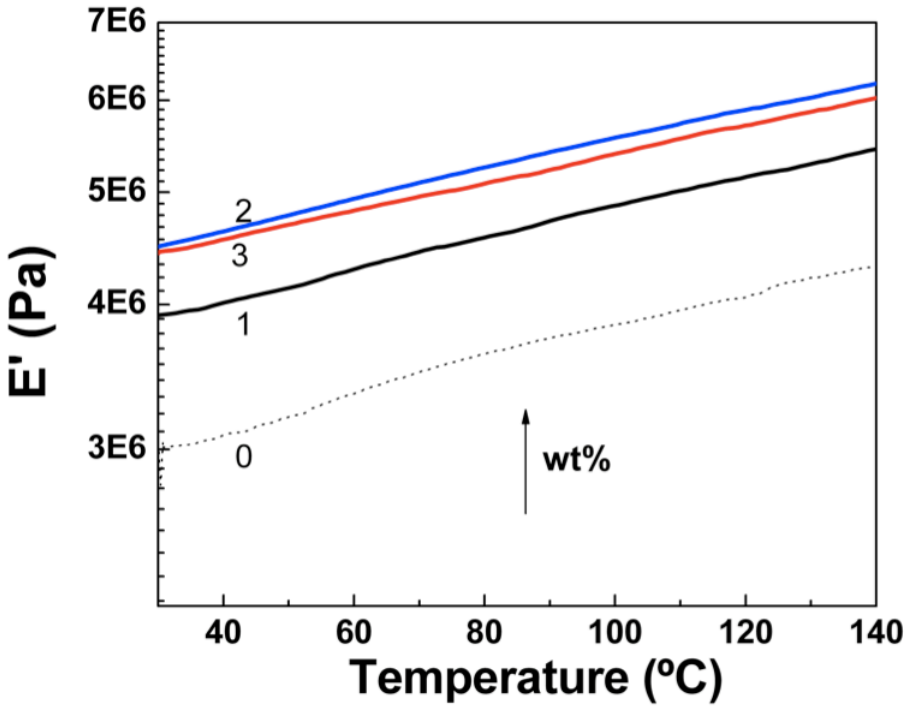

Figure 6.10. Storage modulus as a function temperature for nanocomposites containing 0-3 wt% SWCNT-COOH

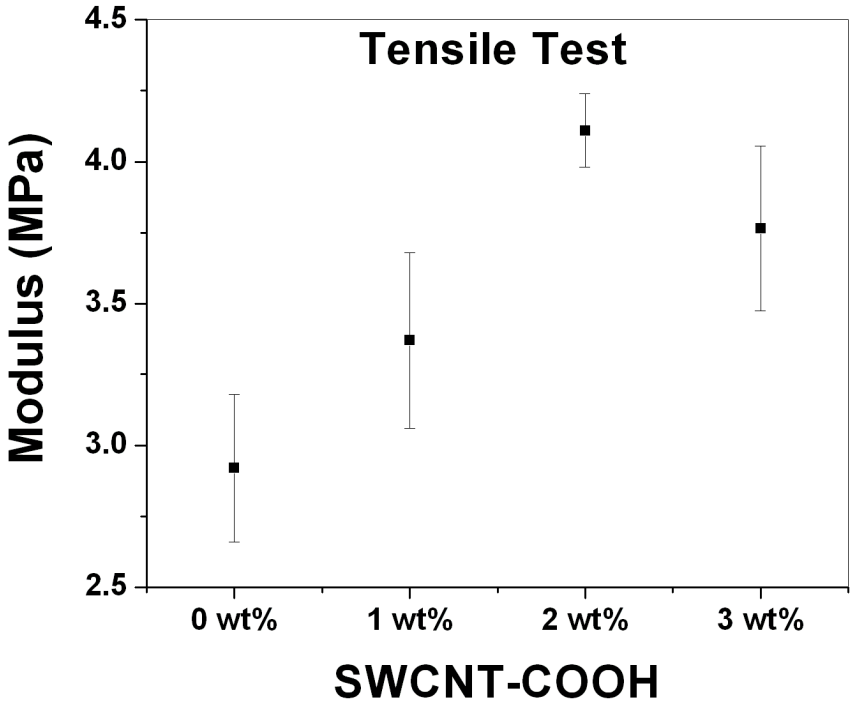

Figure 6.11. Tensile modulus for nanocomposites containing 0-3 wt% SWCNT-COOH

On the other hand, Figure 6.12 shows the effect of the increase in concentration on the loss modulus of nanocomposites. Although the storage modulus decreased in the range of 2-3 wt%, this effect was not observed in the loss modulus. A 12-times increase in the loss modulus at room temperature was calculated for the nanocomposites containing 3 wt% SWCNT-COOH, compared with a 5 times increase for the nanocomposite with 2 wt% SWCNT-COOH. It can be indicated that the nanotube-nanotube sliding mechanism was more significant than nanotube-polymer sliding mechanism for the loss modulus of the nanocomposite with 3 wt% SWCNT-COOH.

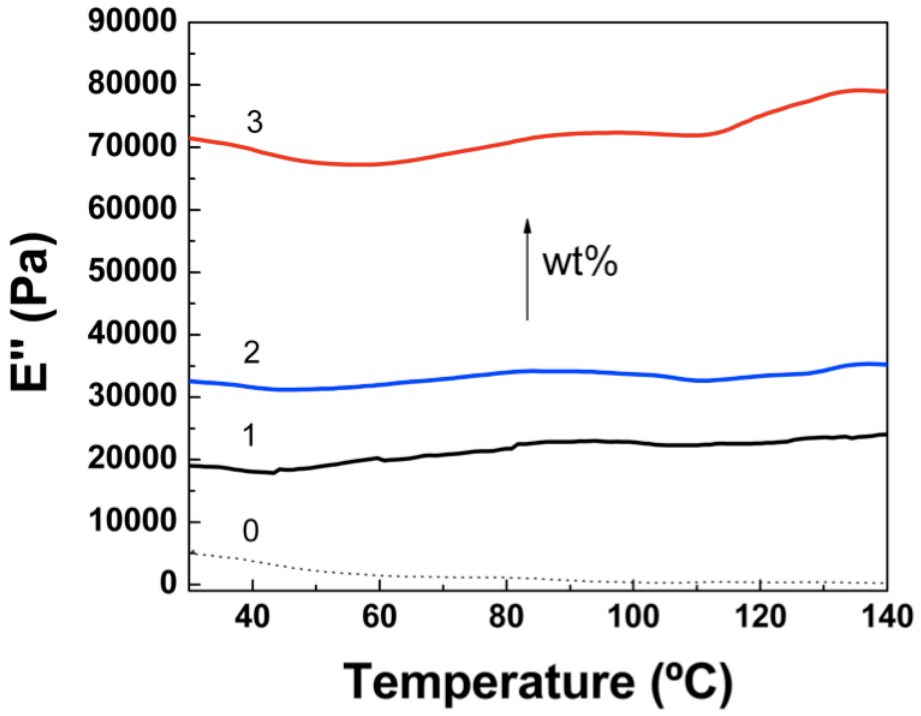

Figure 6.12. Loss modulus as a function temperature for nanocomposites containing 0-3 wt% SWCNT-COOH

Mathematical Model for Damping Capacity

The energy dissipation of a material can be also evaluated by the ratio of the dissipated work by the material (ΔW) to the maximum elastic energy stored in the cyclic loading process (W). The ratio between those is shown as Ψ.

$$\Psi = \frac{\Delta W}{W} \qquad \text{Equation 1}$$

Where ΔW can be written as;

$$\Delta W = \oint \sigma d\varepsilon \quad \text{Equation 2}$$

which is the area surrounded by cyclic stress-strain curve. W can be defined as;

$$W = \int_0^x \sigma d\varepsilon \quad \text{Equation 3}$$

where x is the maximum strain during the loading process while σ and ε represent the macroscopic average stress and strain of the model (Zinoviev and Ermakov, 1994).

In order to reach these values, a stress-strain experiment was performed for different SWCNTs. During loading, the area under the stress-strain curve is the strain energy per unit volume absorbed by the material. Conversely, the area under the unloading curve is the energy released by the material. In the elastic range, these areas are equal and no net energy is absorbed. However, if the material is loaded into the plastic range as shown in Figure 6.13, the energy absorbed exceeds the energy released and the difference is dissipated as heat.

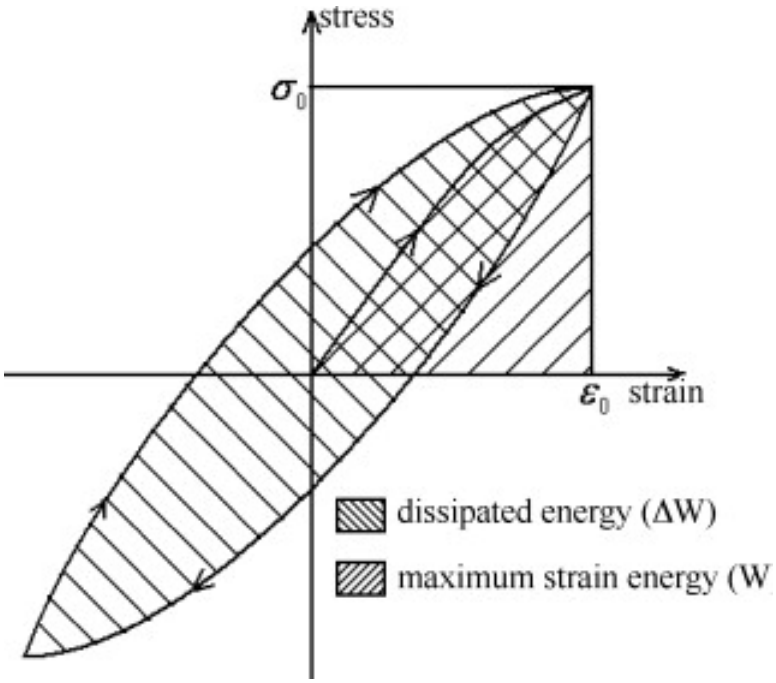

Figure 6.13. Technique used for calculation of W and ΔW

The inverse quality factor Q^{-1} is widely used to measure the damping capacity of the materials, which has relationship with Ψ as,

$$Q^{-1} = \frac{\Psi}{2\pi} \qquad \text{Equation 4}$$

With the conception of the energy dissipation and the equations above, it is possible to simulate the damping capacity of a material by calculating the area of the hysteresis loop.

Figure 6.14 and 6.15 show the performance of the pristine and acidified SWCNTs and the epoxy matrix under the cyclic load. Epoxy nanocomposite with pristine SWCNTs and functionalized SWCNTs showed higher energy loss compared to the epoxy matrix. The highest energy lost was observed for the acidified SWCNT system.

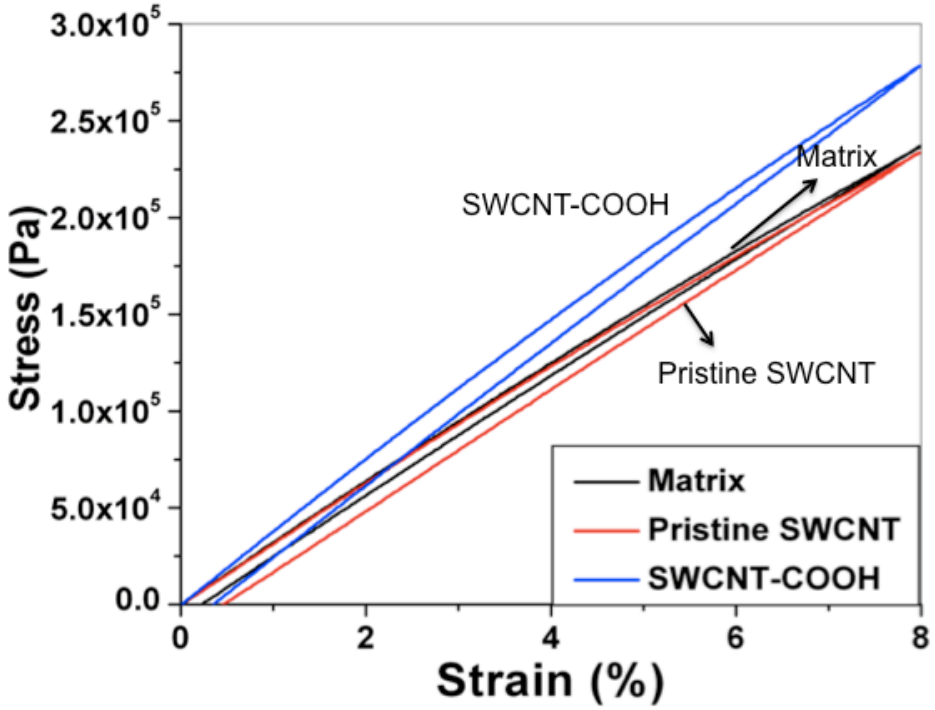

Figure 6.14. Cyclic loading process for epoxy matrix, pristine and acidified SWCNTs epoxy nanocomposites

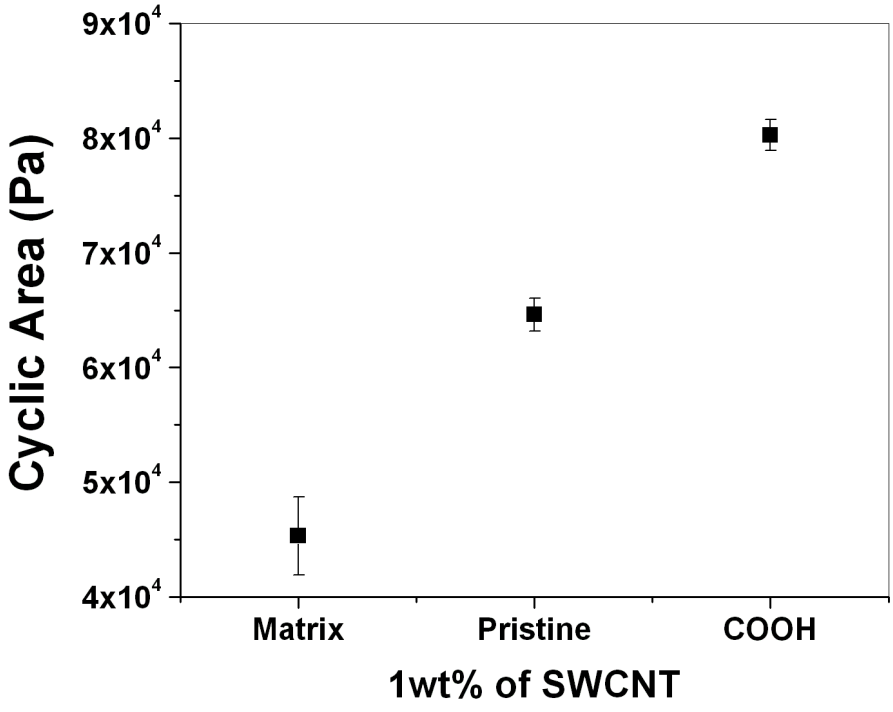

Figure 6.15. Cyclic area of epoxy matrix, pristine and acidified SWCNT epoxy nanocomposites

Figure 6.16 and 6.17 show the performance of 0-3 wt% of acidified SWCNTs under cyclic load. Similar to the tensile experiment, the cyclic area increased with the increase in concentration. However, as the concentration reaches 3 wt%, the cyclic area decreased. Cyclic area increased 68% compared to the matrix at 1 wt% loading compared to the matrix. As the concentration was increased to 2 wt%, the cyclic area increased 204% and as the concentration reached the 3 wt%, the cyclic area increased 89% compared to the matrix.

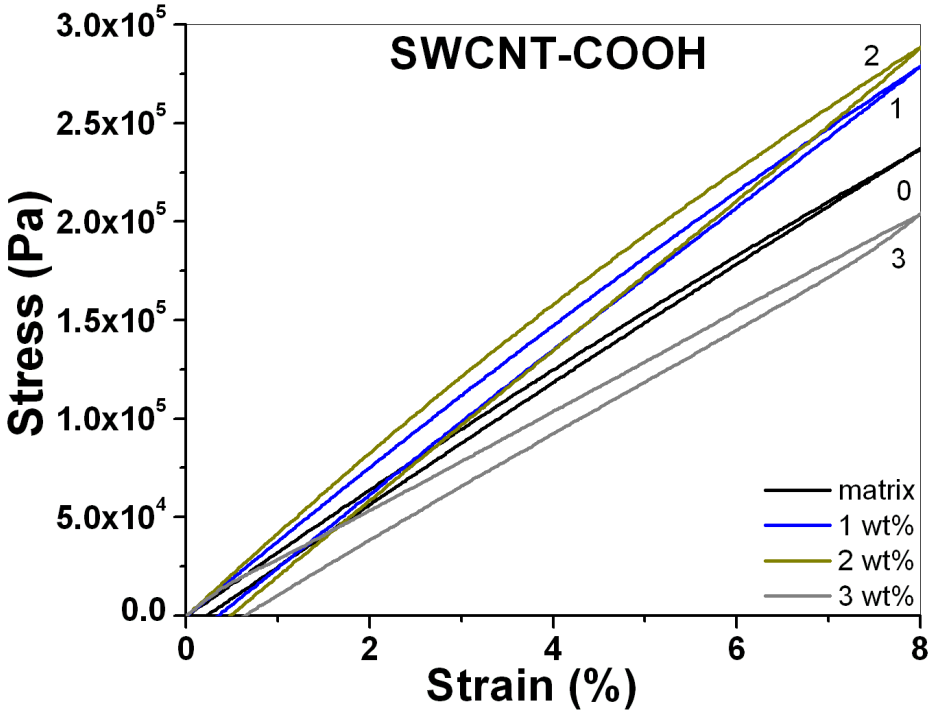

Figure 6.16. Cyclic loading process for nanocomposites containing 0-3 wt% SWCNT-COOH

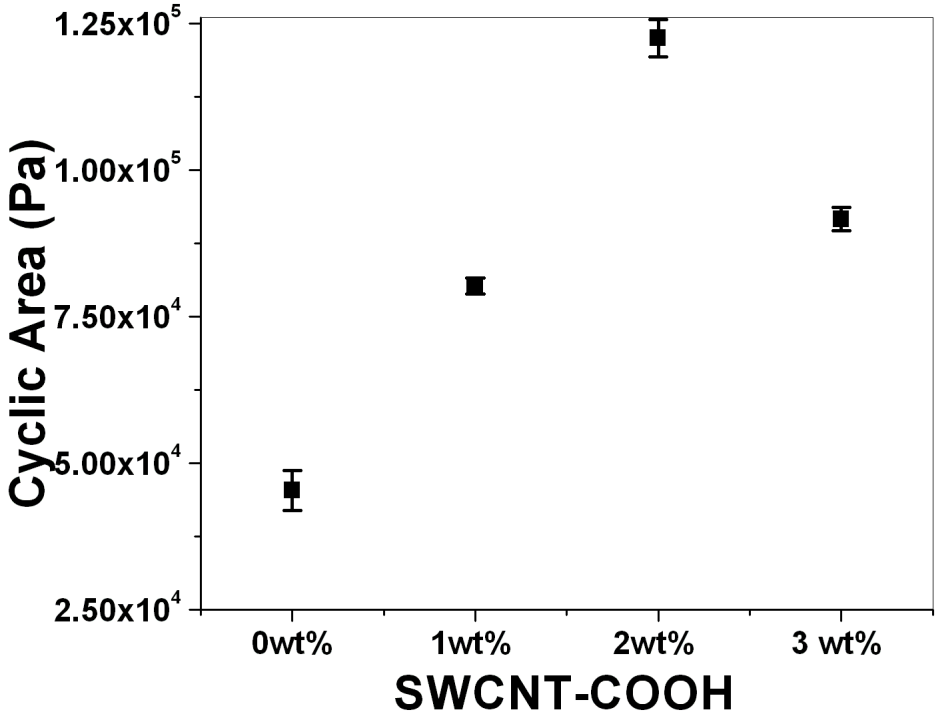

Figure 6.17. Cyclic area of nanocomposites containing 0-3 wt% SWCNT-COOH

Based on the equation 4 that is used to calculate the inverse quality factor or damping capacity, the values for matrix, pristine and acidified SWCNT systems were calculated and plotted in Figure 6.18. This theoretical approach showed that the highest damping capacity was obtained for the system with acidified SWCNTs. The same calculation also took place for nanocomposites containing 0-3 wt% acidified SWCNTs (Figure 6.19). It was found that the damping capacity increased until the concentration reached 2 wt%. When the concentration reached 3 wt%, damping capacity decreased. However, the highest loss modulus (E'') value during dynamic temperature ramp and dynamic strain sweep experiments was observed at 3 wt% loading at room temperature. It also needs to be pointed that the pristine SWCNT system showed higher loss modulus value than acidified SWCNT system during dynamic experiments, whereas the acidified system showed the highest damping capacity during the tensile cyclic experiments.

However, the calculations from the damping capacity showed similar trend with the storage modulus values. This shows that damping capacity increased as the quality of dispersion increased in the systems after the tensile experiments.

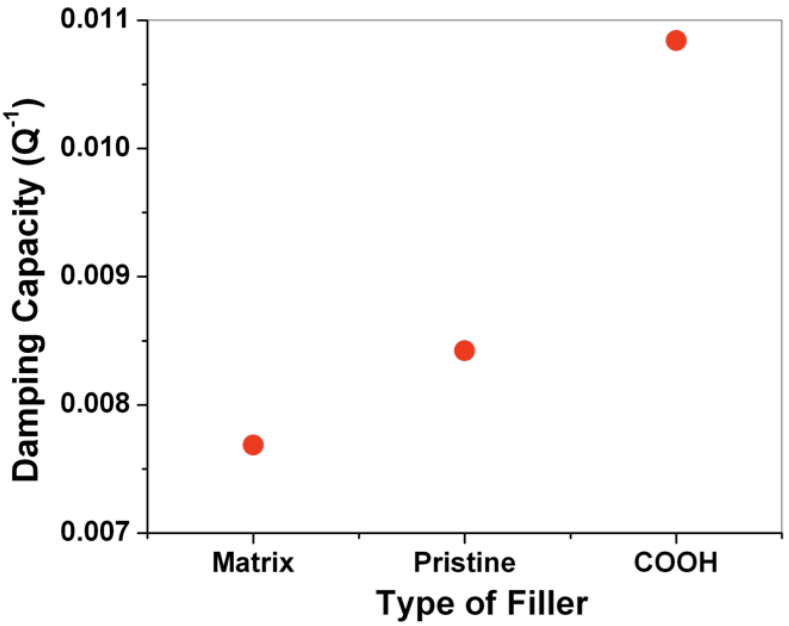

Figure 6.18. Damping capacity of epoxy matrix, pristine and acidified SWCNT epoxy nanocomposites

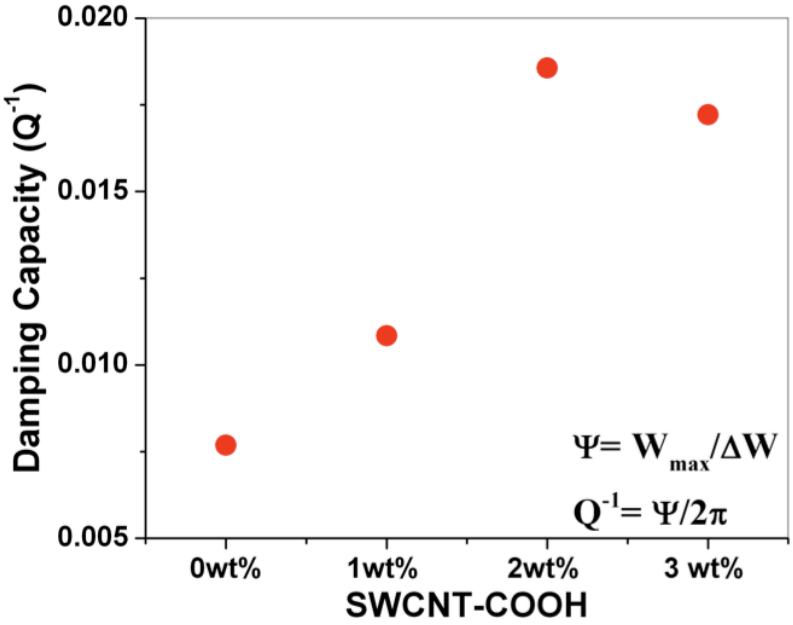

Figure 6.19. Damping capacity of nanocomposites containing 0-3 wt% SWCNT-COOH

6.4 CONCLUSION

In this chapter, the damping characteristics of carbon nanotube/epoxy nanocomposites were discussed. Nanocomposites were prepared by using an elastomeric epoxy/amine matrix. The glass transition temperature for these nanocomposites was under the room temperature implying that the matrix behaved as a cross-linked elastomer at room temperature.

Firstly, the effects of nanotube concentration on the storage and loss modulus during a strain sweep experiment were discussed. It was observed that the storage modulus of the nanotubes showed a gradual decrease with increasing strain value. As the strain value was increased and the critical threshold stress was reached, the nanotube-polymer interfacial slip was activated and filler-matrix debonding occurred resulting in a decrease in the storage modulus of nanocomposites. On the other hand, this slippage at the nanotube-polymer interfaces created a frictional energy that increases the loss modulus value. The highest loss modulus value was observed at 3 wt% loading.

Secondly, the effect of nanotube functionalization and concentration on the mechanical and damping properties at elevated temperatures were evaluated. It was observed that the incorporation of carbon nanotubes increased the storage modulus moderately. On the other hand, this increase was considerable at the values for loss modulus, especially at higher temperatures. Even though an enormous increase was observed for loss modulus at higher temperatures, the storage modulus value did not decrease. This shows that the system has reached our goal, which was to produce ultimate nanocomposites that show high damping capacity at elevated

temperatures without sacrificing mechanical properties and structural integrity. Another important finding was that nanocomposites with 3 wt% loading did not improve the storage modulus, however, the loss modulus of this system showed a considerable increase. This result shows that as the quality of dispersion decreased at higher concentrations, the storage modulus decreased. However, this high concentration created the friction energy due to slippage between the tube bundles that causes high loss modulus value.

All these results from dynamic experiments were compared with a mathematical model that calculates the area between the stress-strain curves during a cyclic load. The damping capacity of the nanocomposite films was calculated by using the inverse quality factor. It was observed that the highest damping capacity was obtained for the systems with acidified SWCNTs at 2 wt%. These results did not follow the same trend with the results obtained from dynamic experiments. However, it needs to be noted that the damping capacity calculated with this mathematical model showed an agreement with the quality of nanotube dispersion in the system.

REFERENCES

1. Ajayan P.M., Schadler L.S., Giannaris C., Rubio A., “Single-Walled Carbon Nanotube-Polymer Composites: Strength and Weakness”, Adv Matter, 12, 10, 2000

2. Auad M.L, Mosiewicki M.A., Uzunpinar C., Williams R.J.J., ”Single-wall carbon nanotubes/epoxy elastomers exhibiting high damping capacity in an extended temperature range”, Composites Science and Technology, 69, 1088–1092, 2009

3. Buldum A., Lu J.P., Phys. Rev. Lett. 83, 5050, 1999

4. David I.G. Jones, “Handbook of Viscoelastic Vibration Damping”, WILEY, New York, 2001

5. Rajoria H., Jalili N., “Passive Vibration Damping Enhancement Using Carbon Nanotube-Epoxy Reinforced Composites”, Composites Sciences and Technology, 65, 2079-2093, 2005

6. Suhr J., Zhang W., Ajayan P.M., Koratkar N.A., “Temperature activated interfacial friction damping in carbon nanotube polymer composites”, Nano Lett., 6 (2), pp 219–223, 2006

7. Wang X., Liu H. and Ouyang S., “Damping properties of flexible epoxy resin”, Journal of Wuhan University of Technology-Mater. Sci. Ed. Volume 23, Number 3, 411-414, 2008

8. Zhou X., Wang K.W., Bakis C.E., ”Interfacial damping characteristics of carbon nanotube-based composites, Compos. Sci. Technol. 64, 2425, 2004

9. Zinoviev A.P., Ermakov Y.A, “Energy dissipation in composite materials”, 1994

CHAPTER 7

CONCLUSIONS

During this work, the main focus was to study the effect of modification of carbon nanofillers on the final properties of the epoxy nanocomposites. Additionally, the dispersion of carbon nanofillers was studied as a route to create a uniform system. Particular focus was to analyze the covalent functionalization on the dispersion and thus the final properties such as thermal, mechanical and damping behaviors.

Early in the research, defect functionalization of SWCNTs, MWCNTs and CNFs was used in order to graft organic functional groups. Acid groups, ester groups and epoxy groups were attached on CNTs defect sites in order to increase the compatibility with epoxy polymer. In addition, glycidyloxypropyl-heptaisobutyl polyhedral oligomeric silsesquioxane (iBu-Gly-POSS) molecules were attached on CNTs defects sides, which have been studied first time by our group. Furthermore, surfactant adsorption was also used in order to distinguish the effects of covalent and non-covalent functionalization methods. The effectiveness of these functionalization methods was discussed through thermal gravimetric analysis (TGA), Raman spectroscopy and FTIR analysis. TGA analysis showed that 8.6 wt% acid groups were attached onto SWCNTs. The amounts of acid groups attached onto MWCNTs and CNFs were 4.9 and 4.7 wt%, respectively. Raman analysis showed that functionalization process increased the defects on the

structure of SWCNTs that proves the existence of functional groups. Furthermore, the existence of ester groups and POSS molecules was shown at FTIR analysis.

Following the functionalization of nanofillers, the dispersion quality of these systems was evaluated. Several dispersion techniques were chosen such as covalent and non-covalent functionalization, and ultra-sonication. The quality of the dispersion was evaluated through rheological studies. The highest storage modulus (G') value, which implies better dispersion, was observed for SWCNTs with surfactants after 5 min. sonication.

The effect of carbon nanotubes concentration on the final dispersion was also studied. It was observed that as the carbon nanotube concentration increased, the suspension showed a noticeable transition between a liquid-like to solid-like behavior (percolation concentration). The percolated threshold concentration was found to be approximately 0.41 wt% for acidified SWCNTs. Moreover, the sonication time produced considerable effect on the final dispersion of the fillers. The G' value increased as the sonication time increased indicating a better disentanglement of the SWCNTs bundles. However at longer sonication time storage modulus (G') decreased because of the weaker interconnection between the carbon nanotubes and possible degradation of the final structures. The effect of the orientation on the storage modulus was also discussed. The orientation of SWCNTs in the suspension decreased the resistance to flow and thus decreased the storage modulus of the suspensions.

The dispersion of nanotubes after curing was also discussed through Raman spectrum and SEM images. It was found that the dispersion of carbon nanotubes after acidification improved as it was mentioned through rheological analysis. However, esterified SWCNTs showed a decrease in the quality of dispersion.

Beside evaluating dispersion of nanofillers by modifying them, phase separation process during the polymerization was discussed. The epoxy network (DGEBA/MDEA) was modified by monofunctional POSS units as well as unmodified, acidified, esterified and POSS functionalized SWCNTs. It was discussed whether phase separation process occurred in these systems. The curing analysis was studied through rheology, DSC and visual observations. The time where gel point was reached and the conversion at that time were calculated. It was observed that adding POSS molecules slowed down the polymerization process, however they did not have any effect on the conversion. On the other hand, incorporation of SWCNTs accelerated the polymerization because of the high thermal conductivity of nanotubes. The main finding of this research was that all these systems with fillers showed a plateau at G' before the gel point that refers to phase separation.

By using these results and confirming that phase separation may take place in DGEBA/MDEA system with incorporation of POSS and SWCNTs, POSS functionalized SWCNTs were prepared and tested. After rheological experiences, it was observed that this system also showed phase separation and accelerated the polymerization. After confirming the existence of phase

separation, whether this phase separation process could help the dispersion of SWCNTs and created an effective percolation was discussed with SEM images and DMA analysis.

SEM images of these system showed that adding POSS molecules into the system created spherical domains that were result of phase separation process. Moreover, these systems showed rougher surface compared to the epoxy matrix. It is notable that pure SWCNT system and POSS functionalized SWCNTs showed phase separation process. During DMA experiments, it was expected to observe a higher storage modulus value compared to the matrix for the systems with acidified SWCNTs and POSS functionalized SWCNTs. However, both systems showed decrease in storage modulus at both glassy and rubbery regions. It is notable that incorporation of only POSS molecules decreased the glass transition temperature while the incorporation of nanotubes did not have any harmful effect on the glass transition temperature. This shows that POSS molecules acted like a plasticizer in the system and it also confirms the results obtained from rheological analysis and DSC.

Following steps were to study of the final properties such as mechanical, thermal and thermo-mechanical properties of epoxy nanocomposites. Therefore, two different systems were prepared. First system was produced using epoxy matrix (DGEBA) with triamine (Jeffamine T-403) hardener and the second system was epoxy matrix (DGEBA) with diamine (Jeffamine D2000). First system had a glass transition temperature around 95°C and the second system was an elastomeric epoxy with a glass transition temperature of - 45°C.

At the first system, the changes at interface of epoxy/nanofiller were also discussed. The characterization was made through dynamic mechanical analysis by using 3-point bending setup. Dynamic mechanical analysis showed the presence of two relaxation peaks in nanocomposites prepared with unmodified and COOH-modified SWCNT, MWCNT and CNF, assigned to a partitioning of monomers at the carbon interface. This produced a significant decrease of the glass transition temperature. However, esterification with PGE led to a single relaxation peak close to the one of the neat epoxy, for the three types of nanofillers without any penalty in the glassy and rubbery elastic moduli. These behaviors were related to the physical interactions between the matrix and the nanofillers rather than chemical interactions.

Furthermore, mechanical analysis of these nanocomposites showed that the good dispersion and an adequate adhesion between the matrix and nanofillers affected the modulus of these materials. In SWCNT and MWCNT systems, the highest modulus were observed for the acidified systems, whereas, CNF system had the highest modulus in unmodified system. In addition, the effect of concentration increase of acidified SWCNTs on the mechanical modulus was evaluated. The flexural modulus increased as the concentration of nanotubes was increased. As the concentration reached 2 wt%, the quality of dispersion dropped down so that the modulus decreased.

The second system, which was an elastomeric epoxy system, was analyzed to observe how carbon nanofillers and their functionalization affect the damping behavior at high temperatures. It was observed that the incorporation of carbon nanotubes increased the storage modulus

moderately. On the other hand, this increase was considerable at the values for loss modulus, especially at higher temperatures. Even though an enormous increase was observed for loss modulus at higher temperatures, the storage modulus value did not decrease. This shows that the system has reached our goal, which was to produce ultimate nanocomposites that show high damping capacity at elevated temperatures without sacrificing mechanical properties and structural integrity. Another important finding was that nanocomposites with 3 wt% loading did not improve the storage modulus, however, the loss modulus of this system showed a considerable increase. This result shows that as the quality of dispersion decreased at higher concentrations, the storage modulus decreased. However, this high concentration created the friction energy due to slippage between the tube bundles that causes high loss modulus value.

All these results from dynamic experiments were compared with a mathematical model that calculates the area between the stress-strain curves during a cyclic load. The damping capacity of the nanocomposite films was calculated by using the inverse quality factor. It was observed that the highest damping capacity was obtained for the systems with acidified SWCNTs at 2 wt%. These results did not follow the same trend with the results obtained from dynamic experiments. However, it needs to be noted that the damping capacity calculated with this mathematical model showed an agreement with the quality of nanotube dispersion in the system.